

## **APPENDIX III: VOLUNTEER-PLANT CONTAINMENT POOL COMPUTATIONAL-FLUID-DYNAMICS ANALYSIS**

### **III.1 INTRODUCTION**

A three dimensional computational fluid dynamics (CFD) model was developed to analyze the flow patterns developed in the Nuclear Regulatory Commission's (NRC's) volunteer-plant reactor containment during loss-of-coolant accidents (LOCAs). The purpose of the CFD modeling was to assess the water velocities and flow patterns developed during sump pump operation to support estimates of subsequent LOCA-generated sump pool debris transport. Water sources to the sump pool included effluents from the LOCA break and containment spray drainage. The locations and flow rates of each of these water sources and the recirculation pumping rates determined the characteristics of the sump pool that subsequently determined whether, and what fraction of, the debris deposited into the pool could transport to the recirculation sump screens. Threshold transport velocities were determined by experiments conducted at the University of New Mexico (UNM) for debris from pressurized-water-reactor (PWR) insulating materials [NUREG/CR-6772]; therefore, these threshold velocities were used to set the velocity contours of the CFD flow diagrams to facilitate the determination of whether debris would likely transport. The CFD simulations are discussed in Section III.2.

A logic chart debris-transport model was developed to supplement the CFD analyses so that information from the CFD simulations could be used with the blowdown/washdown transport analyses documented in Appendix VI to determine estimates of debris transport to the recirculation sump screens. The pool velocity and turbulence characteristics determine areas of the pool where debris entrapment may occur. The flow streamlines can be used to determine whether debris entering the pool at a discrete location would likely pass through one of the potential entrapment locations. The debris transport process was decomposed using a logic chart approach to facilitate the individual transport steps—steps that could be determined analytically, experimentally, or simply judged. The subsequent quantification of the chart then provided an estimate of the overall sump pool debris transport. The debris transport estimates are discussed in Section III.3.

### **III.2 ANALYSIS OF THE CFD SIMULATION**

#### **III.2.1 Modeling Methodology, Assumptions, and Conditions Simulated**

The commercial CFD program Fluent™ was used to compute the volunteer-plant containment pool flows for large and small LOCA breaks. The containment geometry was available in Autocad™ format and was imported into the Fluent™ preprocessor and grid generator. As shown in Figure III.2-1, all of the structures, stairwells, and sumps were included in the model geometry, but the containment pool was modeled only to a depth of 6 ft. This is the maximum anticipated depth of water during steady-state operation of the spray system and sump pump operating in the recirculation mode.

The splash locations are shown in Figure III.2-2 and can be seen as the extruded volumes above the containment pool in Figure III.2-1. The splash locations and flow rates shown in Figure III.2-2 are explained in detail in Appendix VI. A few modifications to the splash locations and flow rates were made in the CFD model.

1. One of the four “yellow“ floor drains from Level 832, with a total flow rate of 397 gpm in Figure III.2-2, is located on top of a wall. Thus, the adjacent yellow splash located in the corridor had double the individual flow rate. (Note: for all the Level 832 floor drains, the total mass flow was evenly distributed to all locations, with the exceptions noted here.)
2. The uniformly distributed “liner film flow“ of 700 gpm and
3. The “Level 808 sprays“ of 1080 gpm were neglected entirely.

Thirteen LOCA break conditions were simulated: eight large LOCA conditions (four break locations each considered with and without the spray flows) and five small LOCA conditions (four break locations without spray flows and one location with spray flows). Both large and small LOCA breaks were considered because each can cause the sump screens to become clogged in a different way. The large LOCA break and spray flows will result in a large pool depth and all of the screen surface area to be come wetted. The large LOCA break will likely generate more debris that can migrate to the sump screens causing an unacceptable head loss due to the amount of debris collected. The small LOCA break may not cause the spray systems to be activated, and could result in a water depth wetting only the lower portion of the sump screens. This has the potential of forming a thin bed debris mat over a small portion of the screen area resulting in an unacceptable head loss. If the spray flow systems are not activated, depending on break location, a larger portion of the pool flows do not have velocities in excess of the debris threshold velocities and do not participate in the recirculation flow. Therefore the debris generated in those regions does not migrate to the sump screens and provide information on areas to divert debris into during the break and pool fill up.

The four break locations considered correspond to a break occurring in one of the four quadrants [steam generator (SG) compartments] in Figure III.2-2. The total break flow was assumed to be 7400 and 1611 gpm for the large and small LOCA break flows, respectively. It was assumed that the upper two SG compartments were physically separate from the lower two compartments; thus, if the break were postulated to occur in the upper left quadrant, 75% of the break flow would be partitioned to the upper left and 25% to the upper right quadrants; none of the break flow was considered in the lower two quadrants. The 75%/25% partitioning was determined arbitrarily, but it seemed to be a realistic assumption. Additionally, a transient pool fill-up simulation was initiated for a large LOCA break in the upper-left quadrant. Only the break flows were simulated in the upper half of the SG compartments with the break flow partitioned as described above. It should be noted that the above apportionment of the flow represents an estimate of the volunteer plant break due to the steam generator compartment configuration. The steam generators are raised above the pool floor level and do not participate in the recirculation flow, thus the break flow enters the pool by flowing down the steam generator stairwells and thus the water sheets across the steam generator compartment and does not pool to any significant depth. Thus the 75/25% apportionment was assumed, but a thorough analysis of how the break flow would enter the pool would be required. These analyses would be required by each plant, using their expert knowledge of the containment configuration, thus the above apportionment is illustrative of the types of flows that would enter the pool.

Three boundary condition types were used in the simulation. All hard surfaces (walls, floors, etc.) were specified to be a no-slip wall condition. The spray system splash and LOCA break flows were specified as a mass flow inlet condition, and the sumps were set to a pressure outflow boundary condition. Because the break flow sheeting described

previously was not included, the break and spray flows present in the SG compartment were applied as a mass inflow boundary on a vertical surface at the exit of the SG entrance steps of each quadrant (i.e., a mass flow boundary condition located at the “door” of the SG entrance steps, for instance). The spray/splash mass flow boundary conditions were placed on the “top” of each extruded spray location, as shown in Figure III.2-1. This extruded volume was found to be easier to handle in Fluent™ than trying to set the boundary condition on the “top” of the pool surface.

The combination of mass inflow and pressure outflow satisfies the mass continuity condition without unnecessary complications due to numeric and other boundary condition errors. In theory, a mass outflow condition at the bottom of the sump could be specified, but there are numerical instabilities when that condition is prescribed. By using a pressure outflow condition at the sumps, the pressure is allowed to “float” to satisfy the incompressible continuity equation. In other words, the pressure at the bottom of the sump is adjusted by the code to balance the mass flow entering and exiting the pool. In this way the introduction of artificial pressure waves in the solution that can be created by specifying mass inflow and outflow conditions were avoided.

A second-order-accurate numerical method was used to solve the incompressible Navier-Stokes equations, in conjunction with a renormalized group-theory turbulent-kinetic-energy and dissipation (RNG  $\kappa$ - $\varepsilon$ ) turbulence closure. This closure was chosen because of its ability to treat swirling flows, but in practice, little difference was found between the RNG  $\kappa$ - $\varepsilon$  and the more traditional  $\kappa$ - $\varepsilon$  closure for these simulations. The pressure equation was solved using a PISO method, as described in the Fluent™ documentation. For the steady state pool flow analyses, the pool volume was assumed to be completely full of liquid water and initialized to zero velocity. The inflow boundary conditions were flowing from the start, and the solution was allowed to proceed until a steady-state condition was achieved. The normalized residuals of the continuity, momentum, and  $\kappa$  and  $\varepsilon$  equations were monitored until convergence was achieved, typically about 400 iterations. For the steady state pool flow analysis, an additional convergence criterion was to integrate the mass flow rate at the two sump pressure outflow boundaries and compare it with the mass inflow. A mass balance had to be achieved, in addition to a drop in the normalized residuals, for the simulation to be deemed converged.

## III.2.2 Results and Discussion

This section contains the results of the CFD simulations. These simulations illustrate what can be achieved with a CFD analysis of the containment pool flows. For application to a particular plant containment, a more rigorous set of simulations should be performed, including grid convergence tests (e.g., does doubling the number of grid points change the results significantly).

One figure of merit was to determine the fraction of the pool flow volume that produced velocities in excess of the debris migration threshold velocities. Based on the experimental measurements reported in NUREG/CR-6772, the RMI and fiber flock transport threshold velocities were determined to be 0.085 and 0.037 m/s, respectively. Note that only one debris transport threshold velocity for fiber and one for small RMI were used for the following analyses.

### III.2.2.1 Transient Containment Pool Fill-Up

For this simulation, a volume-of-fluid (VOF) method was used. The containment pool was initially filled with air, and water was allowed to enter the pool from the SG entrance stairs. Only the break flows for a large LOCA break, located in the upper-left quadrant, were included. As noted in Section III.2.1, the break flow is partitioned such that 75% of the water leaves the upper-left SG compartment stairwell and 25% leaves the upper-right SG compartment stairwell. This condition corresponds to the time immediately after a break occurs and before the spray system is activated. All walls were treated as no-slip surfaces, and because the fill-up phase is being simulated, the sumps were also treated with no-slip surfaces instead of pressure outflow boundary conditions. The top boundary of the simulated pool was prescribed as a pressure outflow boundary condition instead of as a no-slip wall. This treatment allows the air to leave the domain as the water displaces it. The containment pressurization that occurs during a LOCA was not modeled because it has minimal effect on pool transport.

Figures III.2-4 through III.2-12 show the volume fraction of water, at a height of 0.01 m above the containment floor, as the containment pool fills at 0.34, 0.94, 11.4, 21.4, 31.4, 41.4, 51.4, 71.4, and 111.4 seconds after the water leaves the SG compartment stairwells. The color scheme shown corresponds to a red color for 100% water in the computational cell and blue for 100% air in the cell. Other colors indicate that the computational cell has both air and water partially filling the cell. From Figures III.2-4 to III.2-12, the areas that are first swept by the water can be seen, as well as how the containment pool fills. This simulation shows the areas that fill first and thus provides information needed to design systems to divert debris to areas of the pool that do not participate in recirculation flow. In general, the water leaves the SG compartment, flows out the doorway, and hits the circular outer wall. Then the water flows circumferentially around the containment until the two water streams meet near the sumps. Then the water starts to enter the areas between the upper and lower SG compartments. For this plant configuration, these two areas between the upper and lower SG compartments are the only “quiet” zones (i.e. flow velocities much lower than the debris threshold) in the pool when all break locations are considered in the subsequent steady-state pool flow analysis.

Figures III.2-13 through III.2-21 show the fluid velocity during the fill-up at the same set of time increments previously discussed for volume fractions. Note that when the water volume fraction and fluid velocity plots are compared, there is motion ahead of the water. This motion is the air moving in response to the approaching front of water. During fill-up, the water velocity near the front is in the range of 2–3 m/s, well in excess of the debris transport threshold velocities of 0.037 and 0.085 m/s for fiber and RMI, respectively.

#### III.2.2.2 Steady-State-Flow Analysis

To study the containment pool’s steady-state-flow dynamics, the simulated volume was considered to be completely full of water. In the case of a small LOCA break, the spray flows were not included; however, for the large LOCA break, spray flows were included in the simulations. With the simulated pool full of water, the break and spray flows were introduced as mass inflow boundary conditions and the sumps were set to a pressure outflow boundary condition. These simulations produced a simulated steady-state-flow condition for further debris transport analysis, which will be discussed in Section III.3.

Figures III.2-22 through III.2-29 show the steady-state-flow pattern developed for a small LOCA break condition, without spray flows, and Figures III.2-30 to III.2-37 show large LOCA break conditions, including spray flows. These figures show contours of water velocity at a height of 0.01 m above the containment floor and show a velocity range from 0 m/s up to the threshold velocity for fiber or RMI, 0.037 and 0.085 m/s, respectively. From these plots, the area enclosed by the threshold velocity contour can be computed, and by dividing by the entire available flow area in the containment, a percentage of area in excess of the threshold velocity may be computed. These percentages, or fractional areas in excess of the threshold velocity, are summarized in Table III.2-1 for both large and small LOCA break conditions.

Figures III.2-38 through III.2-47 show streamlines for origins near the splash locations for a large LOCA break at two different locations: an upper-left break and a lower-right break. A rake of particles was released from  $(-15 < X < -5, Y=10)$ , and also from  $(0 < X < 5, Y=15)$  and allowed to follow the flow. From these streamlines, debris trajectories can be determined and their fate postulated. Figures III.2-38 and III.2-39 show the streamlines superimposed on the background velocity map that were color coded using the fiber (0.037 m/s) and RMI (0.085 m/s) threshold velocity, respectively. An oblique view showing the three-dimensionality of the streamlines is shown in Figures III.2-41 and III.2-42, color coded according to the flow speed, using the fiber and RMI threshold velocity, respectively. Thus, it could be deduced that if the velocity (speed) along a particular streamline became smaller than the debris type threshold velocity, it would not be so likely to migrate to the sump screen. By using rakes and streamline analysis at potential debris entry locations, a method for determining whether the debris will transport to the sump screens could be developed.

A similar set of plots are shown in Figures III.2-42 through III.2-45 for the large LOCA break located in the lower-right quadrant. Notice that the streamline patterns are quite different for the lower-right break location when compared to the upper-left break location.

Shown in Figure III.2-46 is a vortex induced by the splash located in the upper-right quadrant in Figure III.2-42. Here the streamlines are color coded by velocity using the fiber velocity threshold. Because the water enters the pool from above and penetrates to the containment floor, a vortex with significant vertical motion is created. Figure III.2-47 shows the streamlines color coded by turbulent kinetic energy (TKE). This type of information would be useful in determining debris degradation mechanisms, particularly for fibrous debris. In Figures III.2-46 to III.2-47, the streamlines show the type of rotation that debris can encounter near the entry of a splash into the pool. The water flow produces vortices around the splash entry and could potentially shred debris into finer particles/pieces than those generated by the break itself. No attempt was made in this document to quantify the debris shredding mechanisms; rather, this document simply illustrates what can be gleaned from a CFD analysis of the pool dynamics.

**Table III.2-1 Percentage of Containment Pool Flow Area in Excess of the Debris Transport Threshold Velocity. Total Pool Area = 767.7 m<sup>2</sup>**

Break Location	Break Size	RMI (%)	Fiber Flocks (%)
Upper Right	Large	35	60
Upper Left	Large	30	54
Lower Left	Large	22	43

Break Location	Break Size	RMI (%)	Fiber Flocks (%)
Lower Right	Large	22	41
Upper Right	Small	5	31
Upper Left	Small	2	25
Lower Left	Small	5	14
Lower Right	Small	5	19

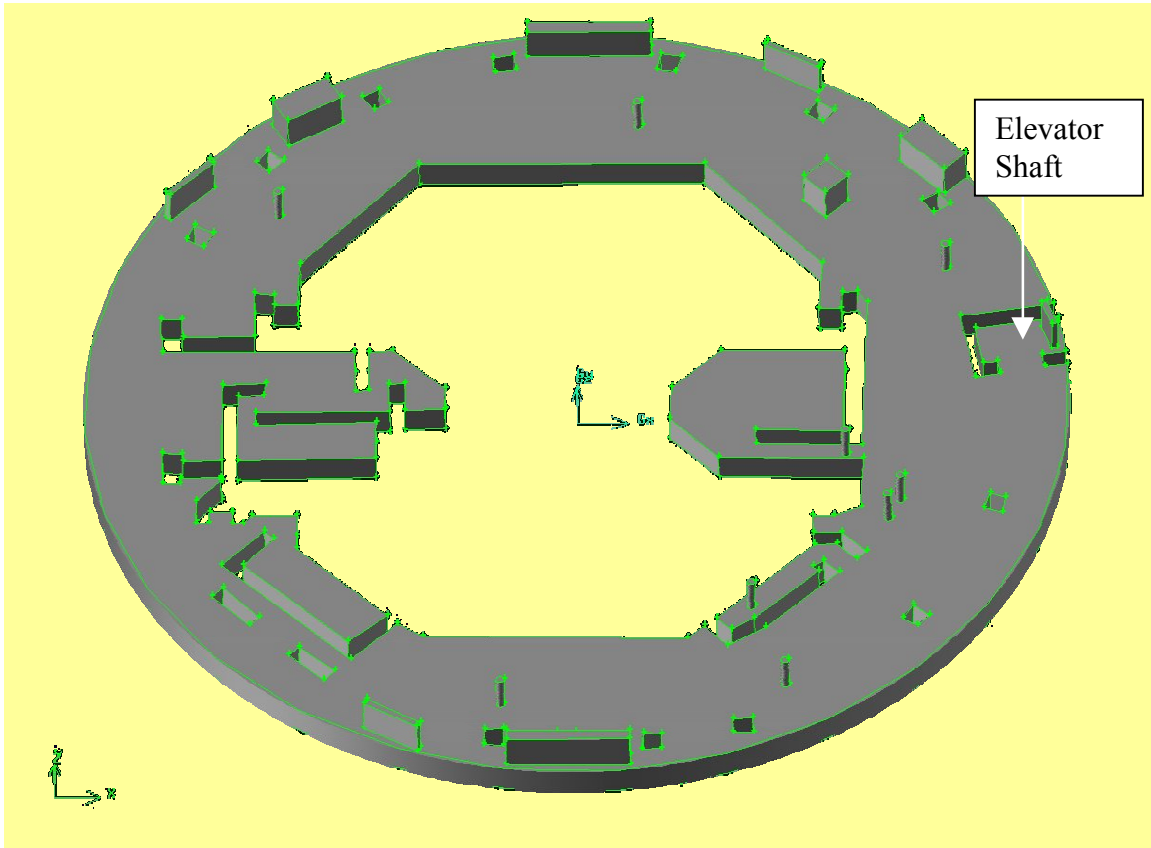


**Figure III.2-1. Volunteer plant geometry and flow region modeled. (Note: Splash Locations Are Shown Extruded above the Nominal Pool Depth.)**

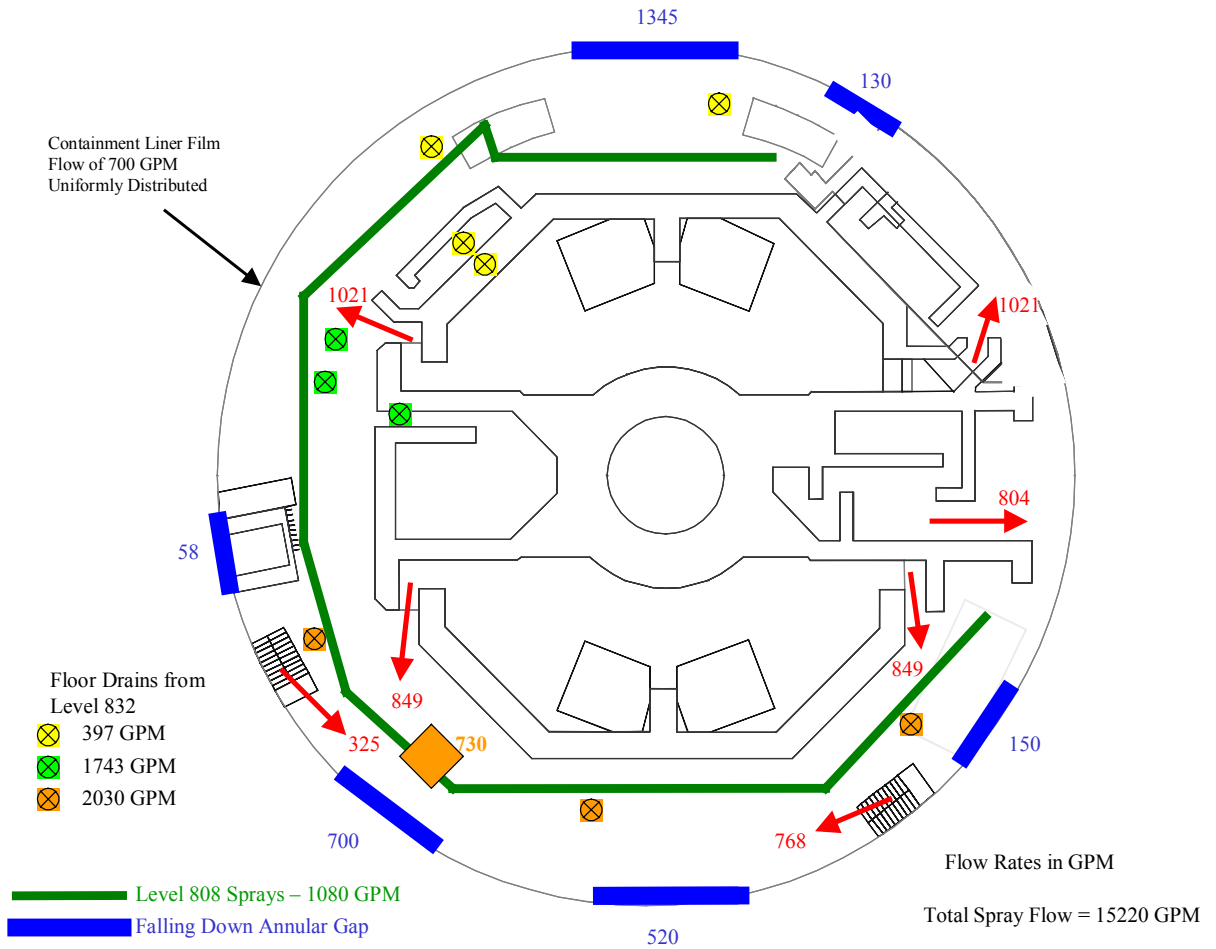


**Figure III.2-2. Spray Flow Rates (gpm) and Locations for the Volunteer-Plant Pool Flow Calculations.**

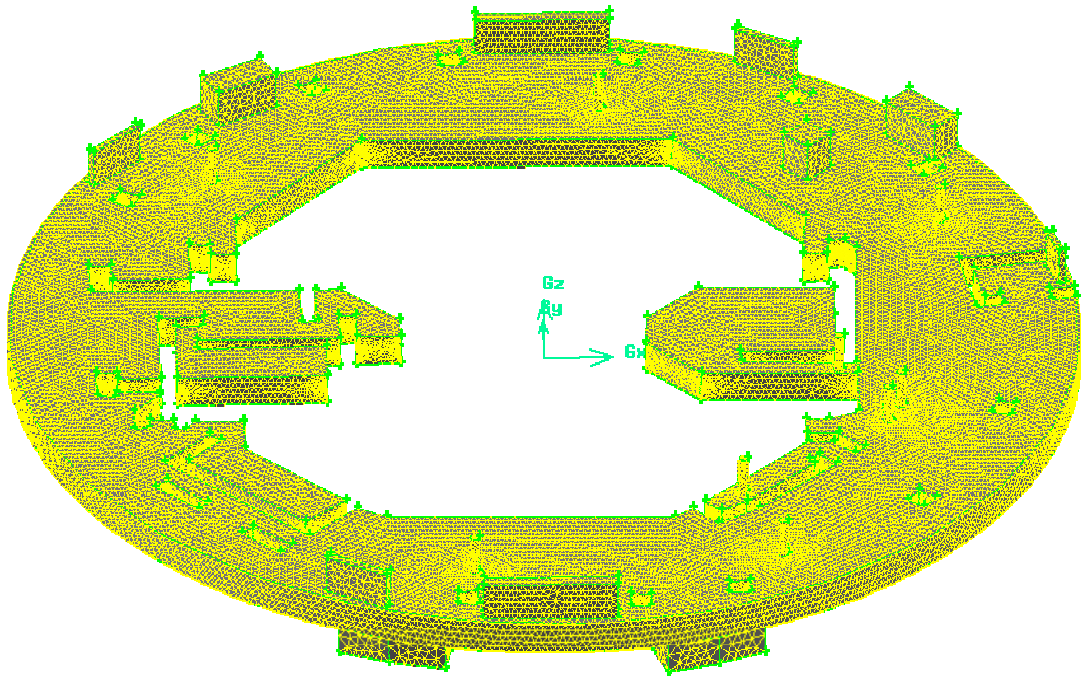


**Figure III.2-3. Unstructured Mesh Created for Containment Pool Flow Calculations.**

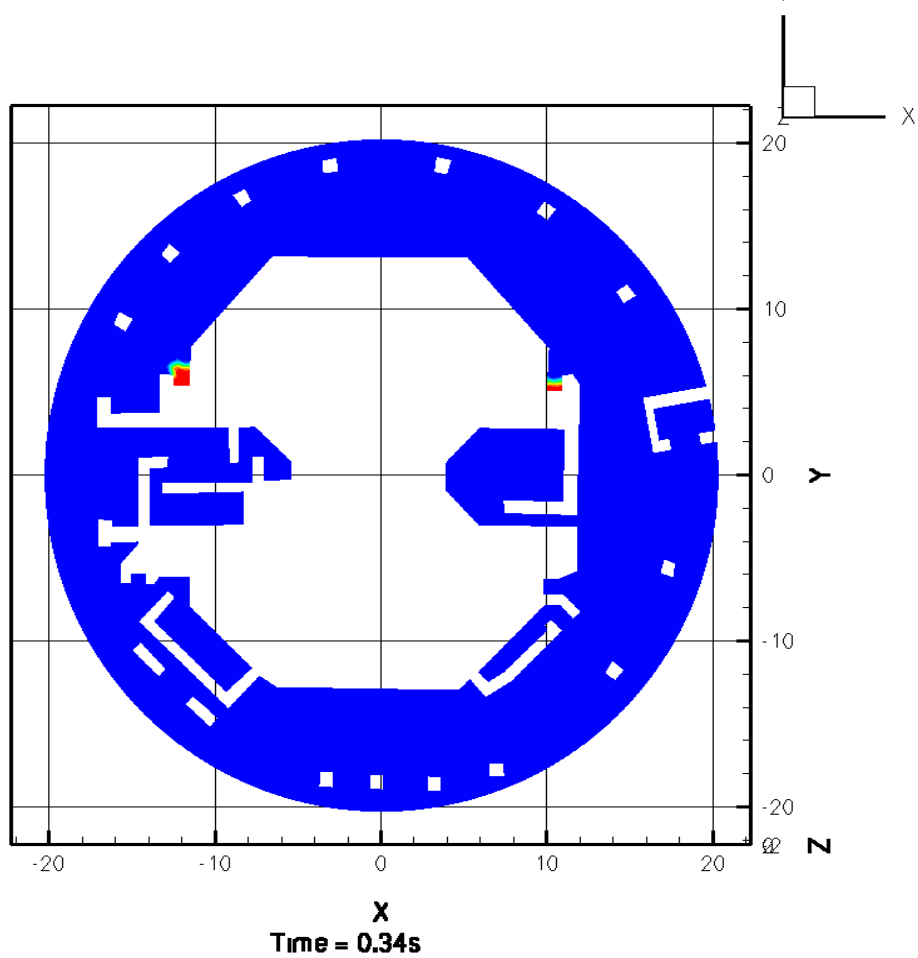


Figure III.2-4. Transient volume of fluid during the simulation of containment pool fill up. Computational cell volume fraction of water is shown at a height of 0.01m above the containment floor. Red is 100% water (0% air), blue 0% water (100% air). Time of the snapshot in seconds after the break flow is initiated is shown in the bottom of the figure.

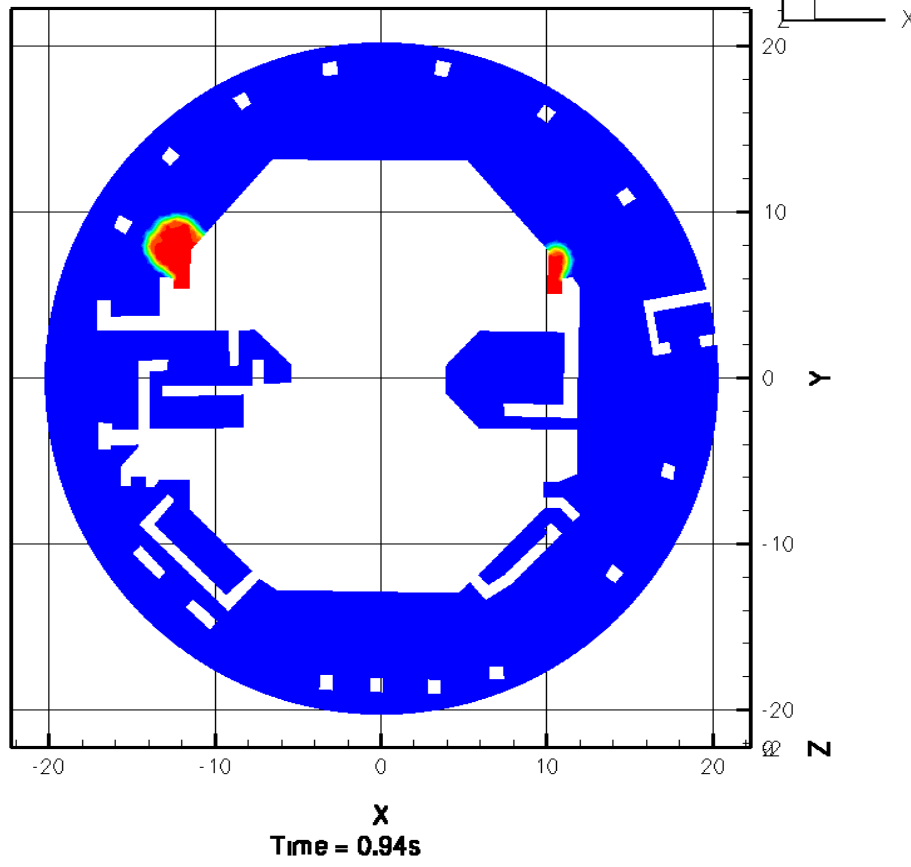


Figure III.2-5. Same as Figure III.2-4 for  $t = 0.94$  Seconds.

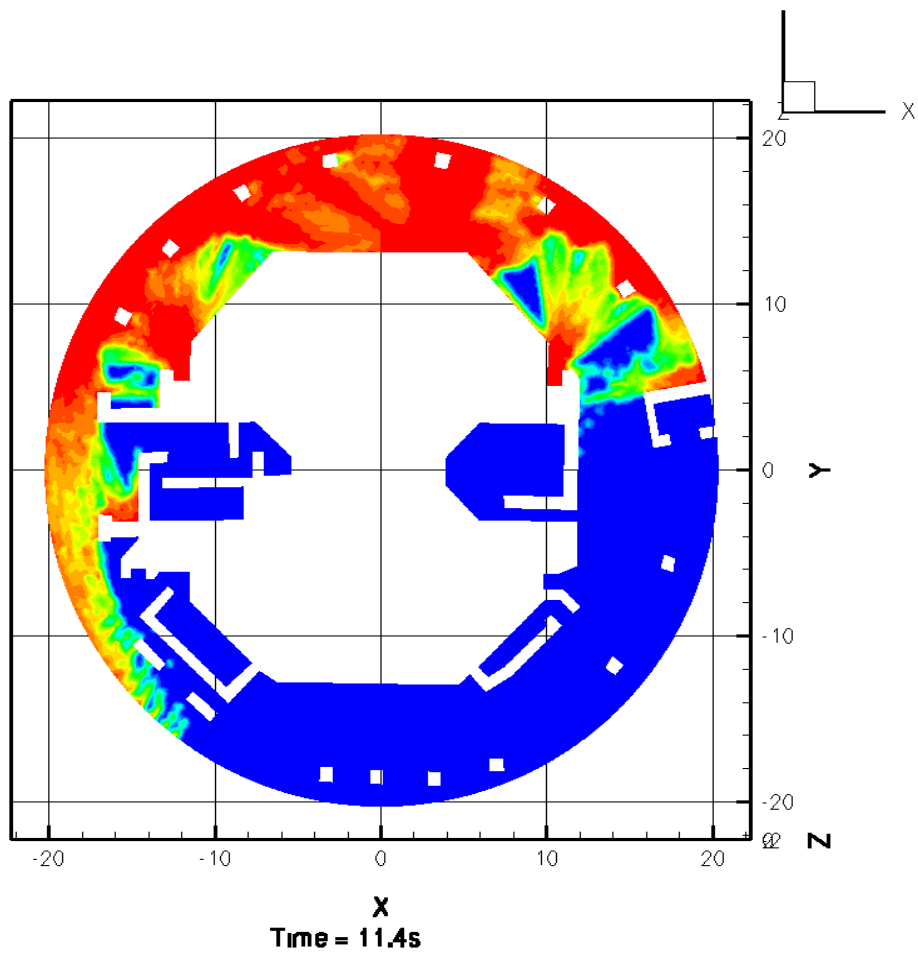


Figure III.2-6. Same as Figure III.2-4 for  $t = 11.4$  Seconds.

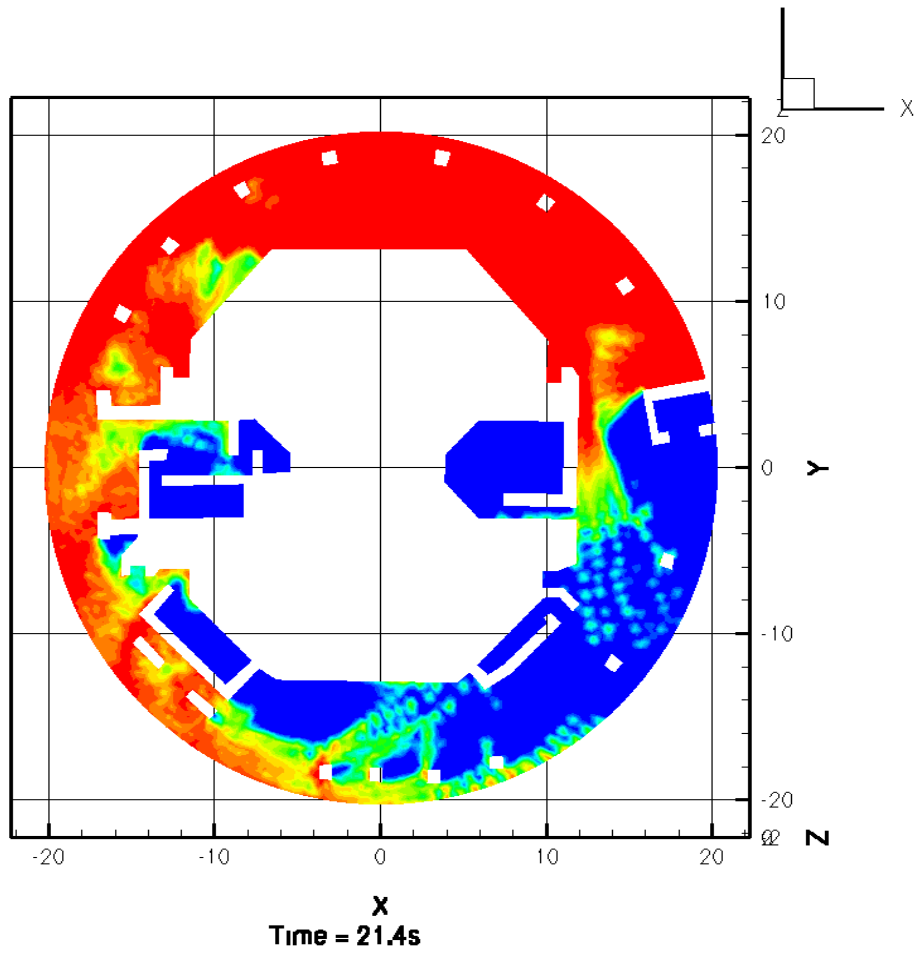


Figure III.2-7. Same as Figure III.2-4 for  $t = 21.4$  Seconds.

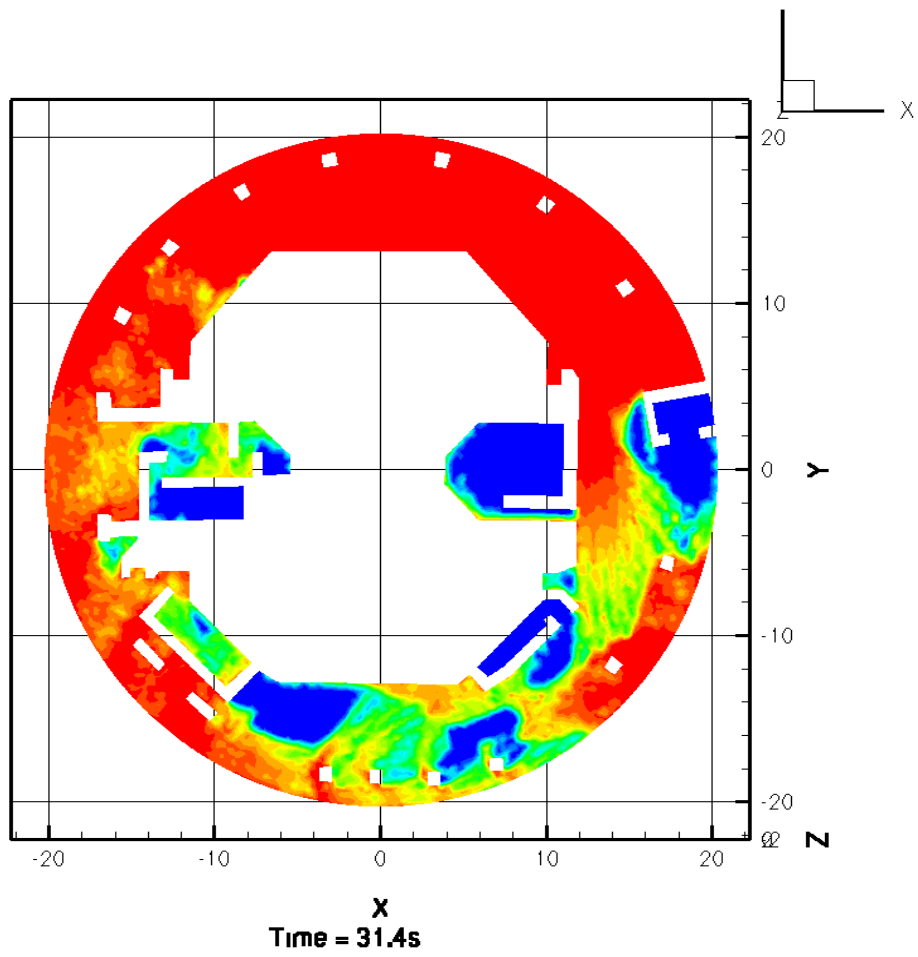


Figure III.2-8. Same as Figure III.2-4 for  $t = 31.4$  Seconds.

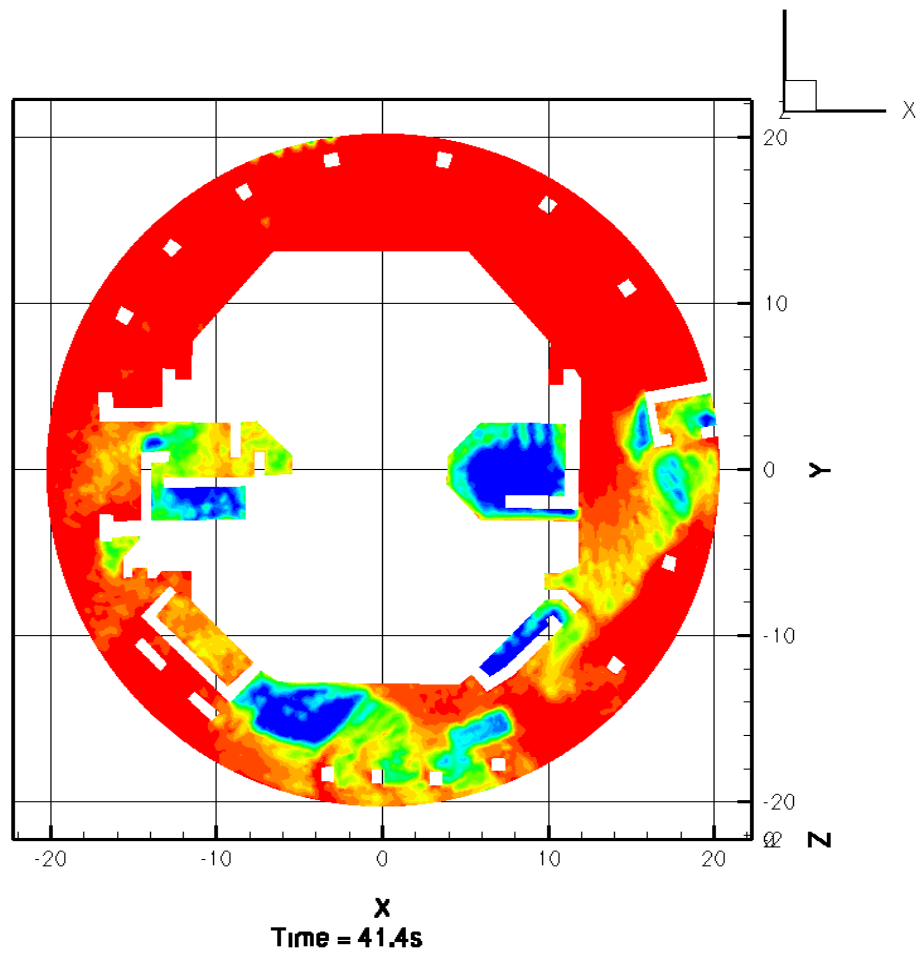


Figure III.2-9. Same as Figure III.2-4 for  $t = 41.4$  Seconds.

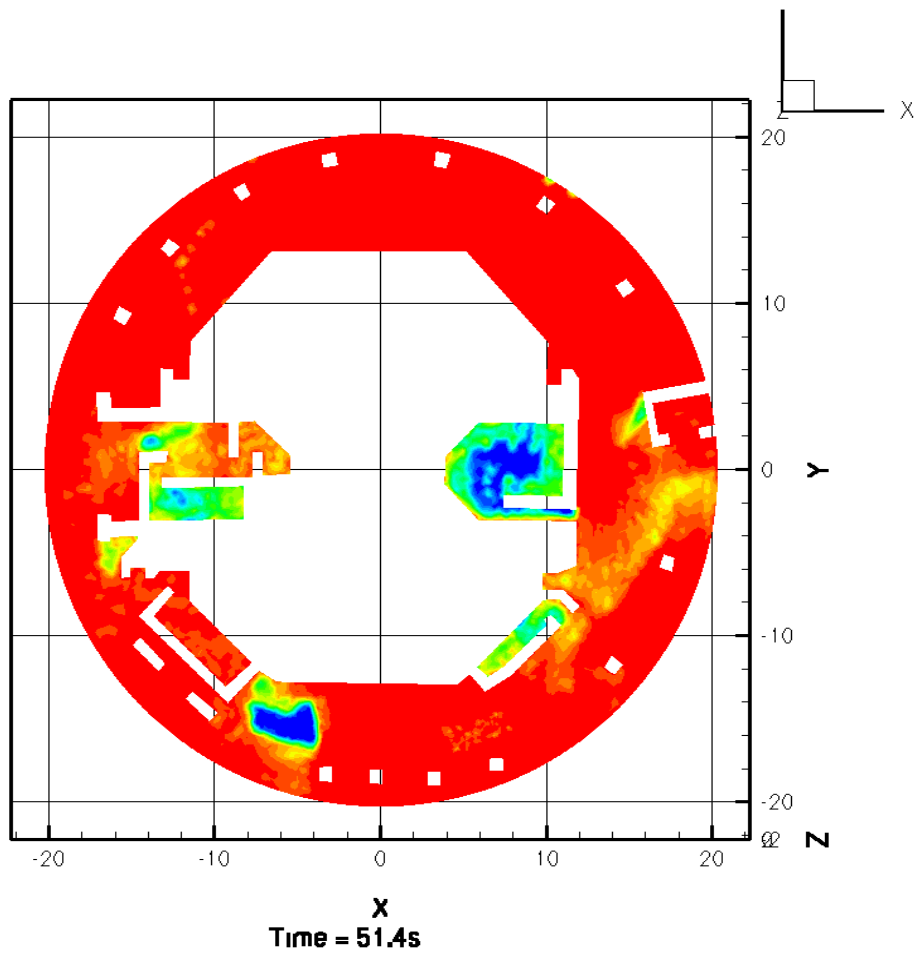


Figure III.2-10. Same as Figure III.2-4 for  $t = 51.4$  Seconds.

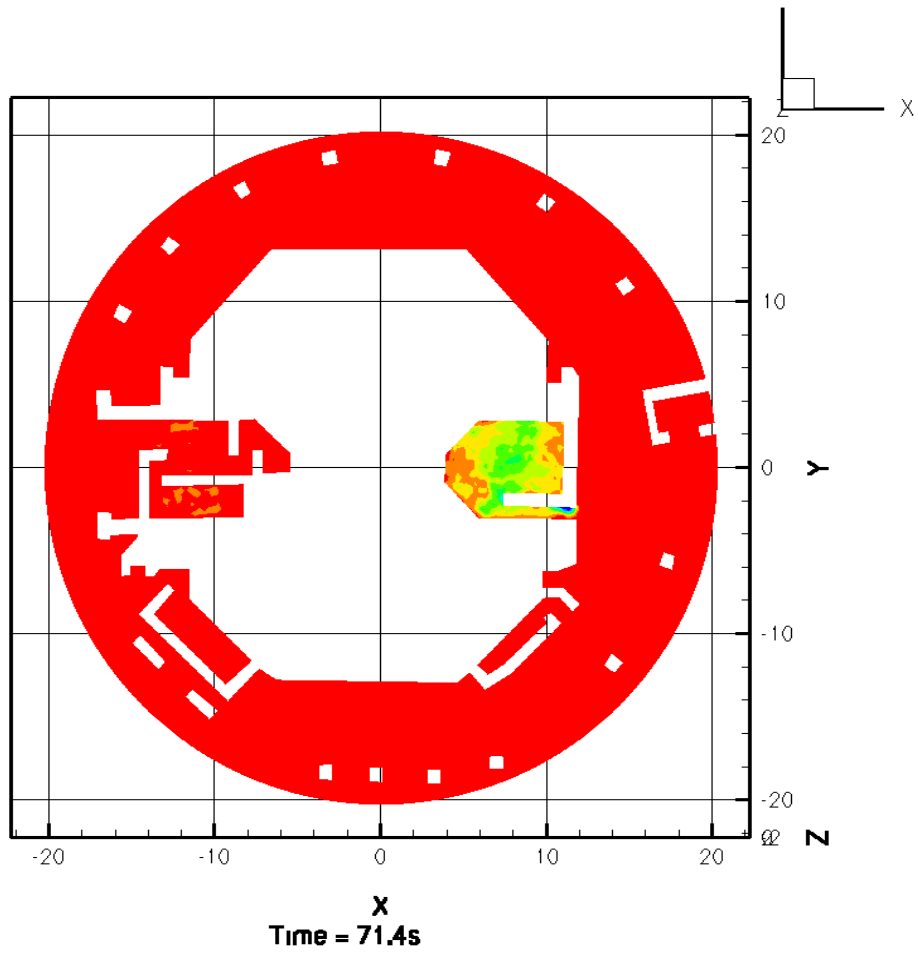


Figure III.2-11. Same as Figure III.2-4 for t = 71.4 Seconds.

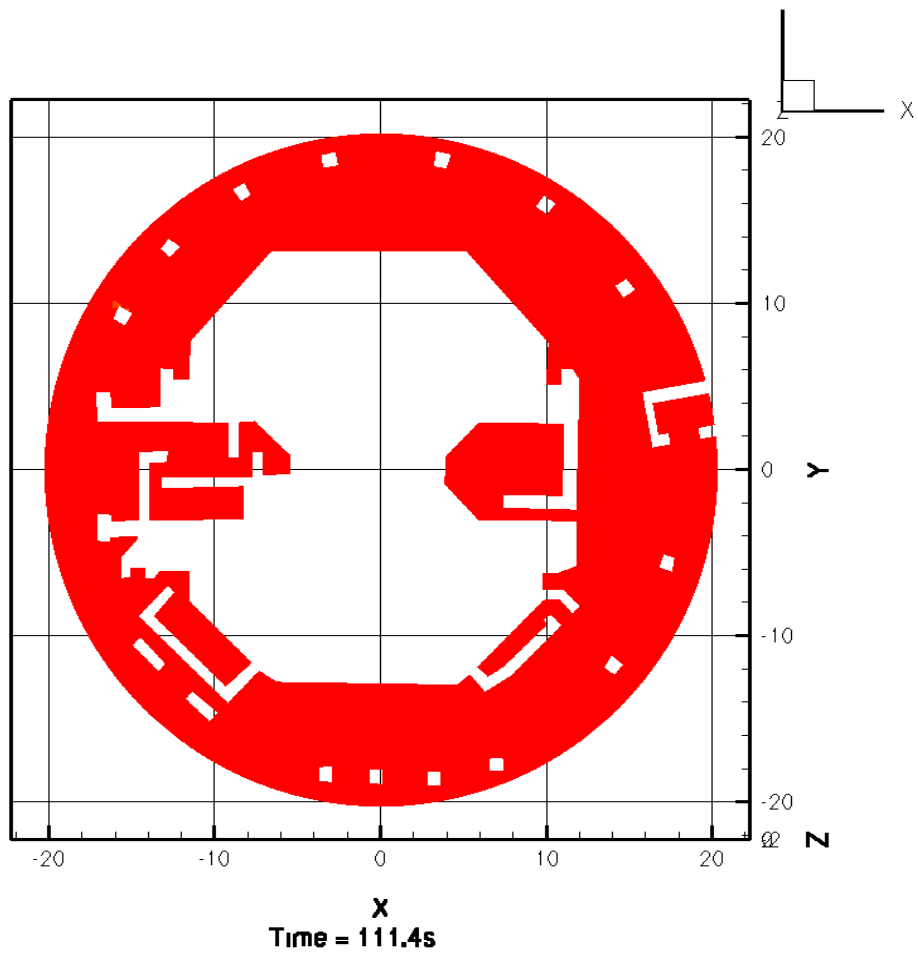
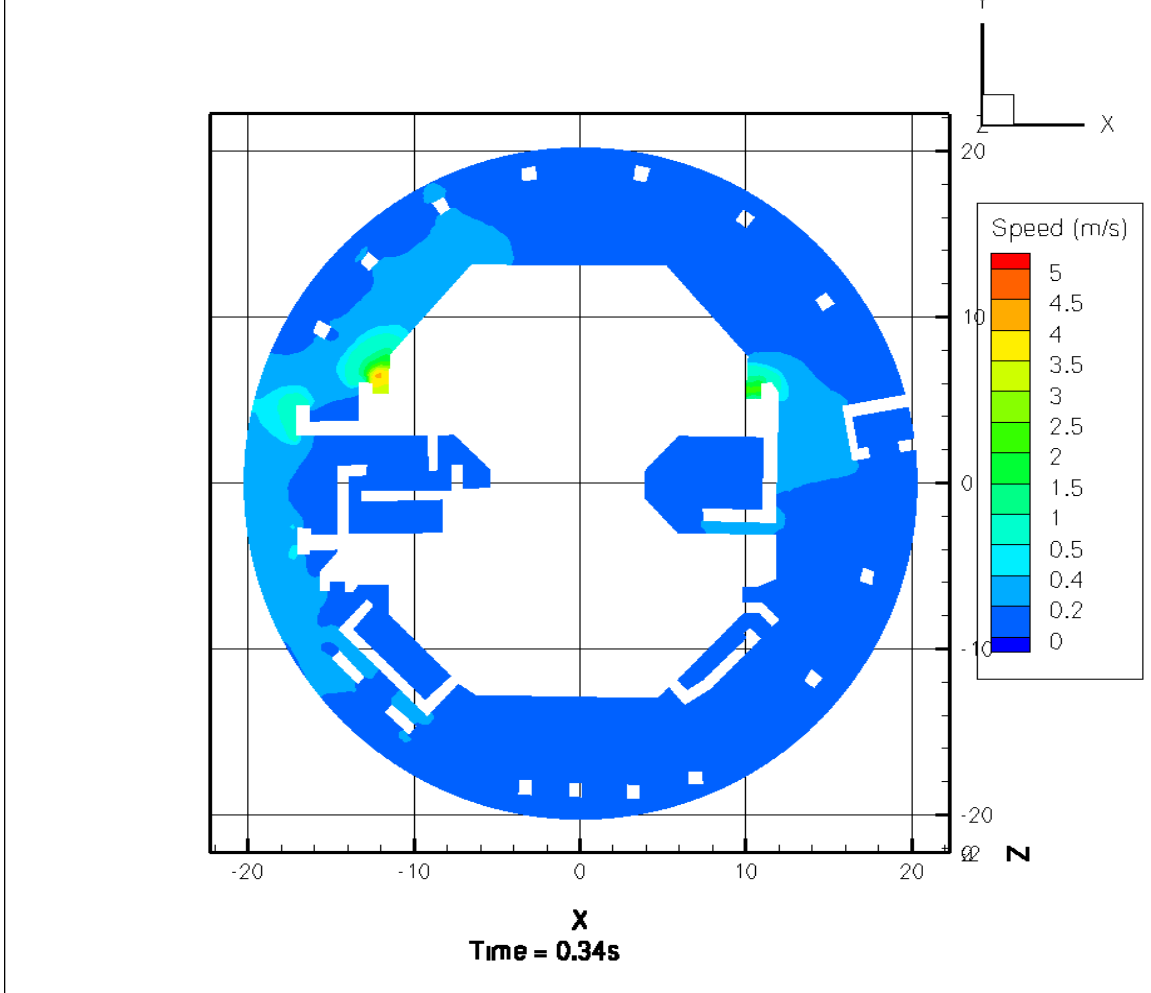


Figure III.2-12. Same as Figure III.2-4 for  $t = 111.4$  Seconds. Note That the Solid Red Color Indicates That the Cells Adjacent to the Floor Are Full of Water, Not That the Entire Pool Is Full of Water.



**Figure III.2-13. Transient VOF Simulation of Containment Pool Fill-Up. Contours of Fluid Velocity Are Shown. Time Snapshot Shown in the Figure Is Seconds after the Break Flow Is Initiated. Note That the Fluid Velocity May Be Water or Air; Figures Showing the Volume Fraction of Water (Figures III.2-4 to III.2-12) Should Be Used to Determine the Actual Water Velocity.**

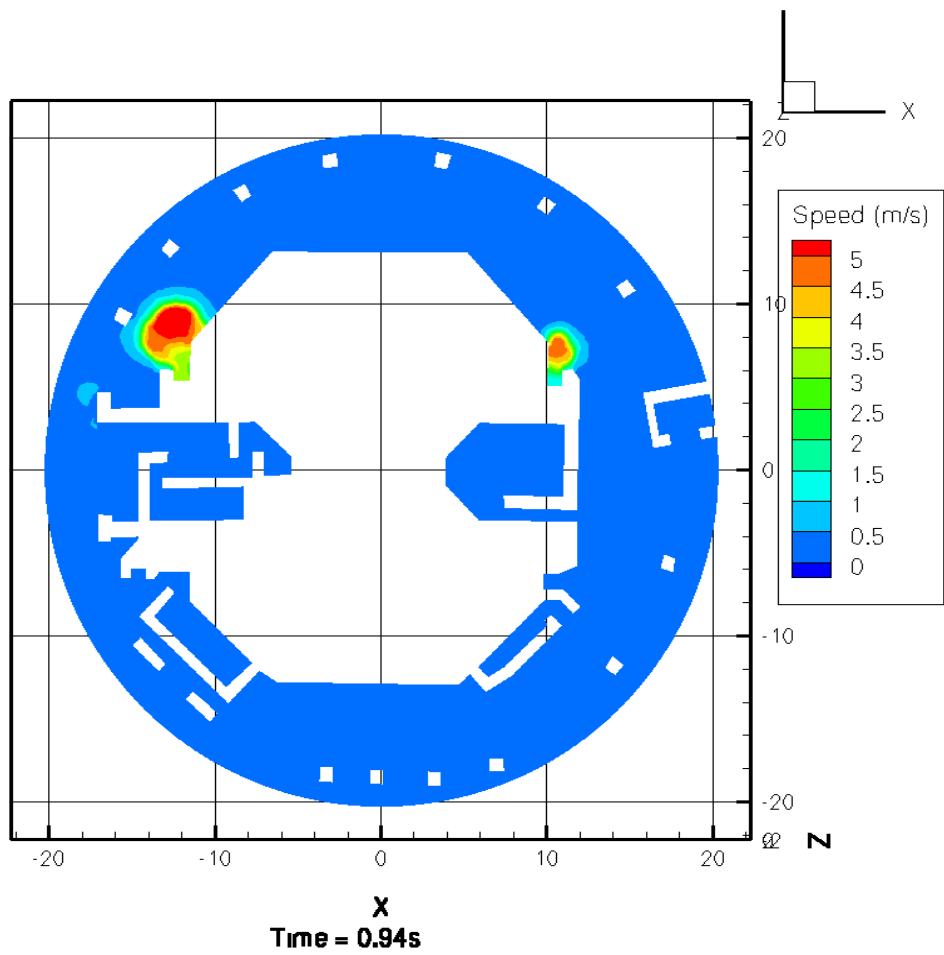


Figure III.2-14. Same as Figure III.2-13 for  $t = 0.94$  Seconds.

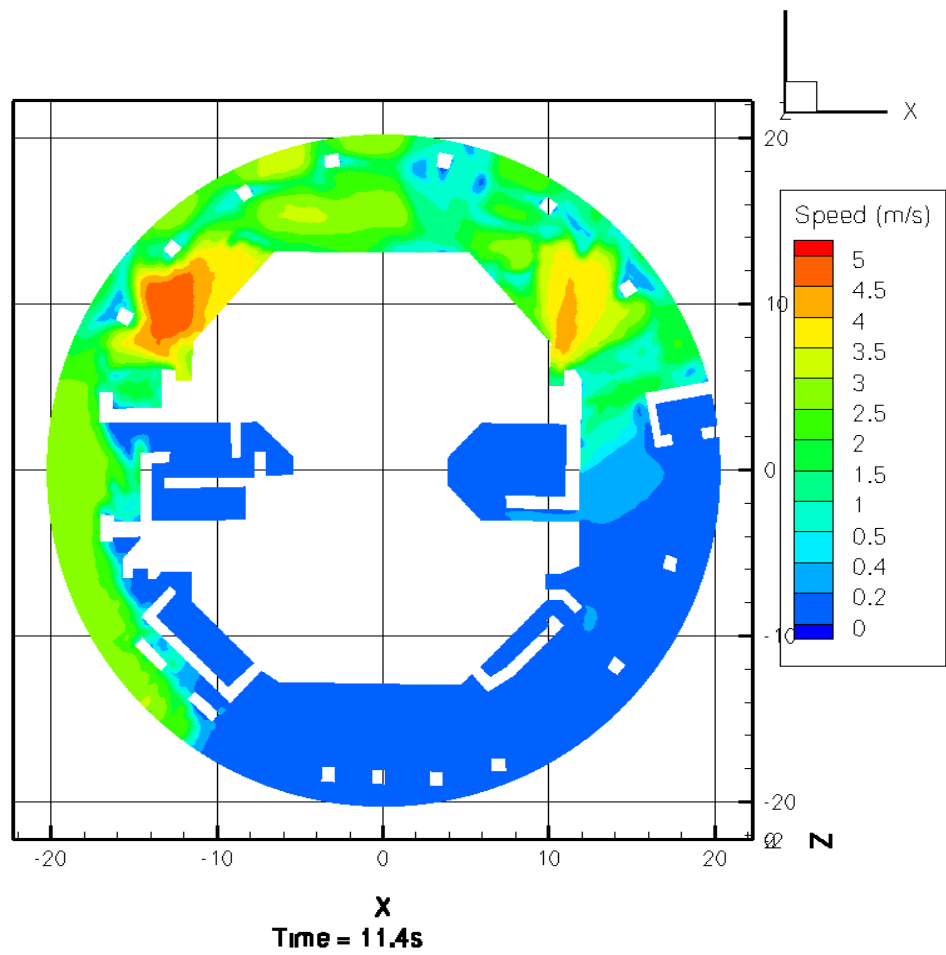


Figure III.2-15. Same as Figure III.2-13 for  $t = 11.4$  Seconds.

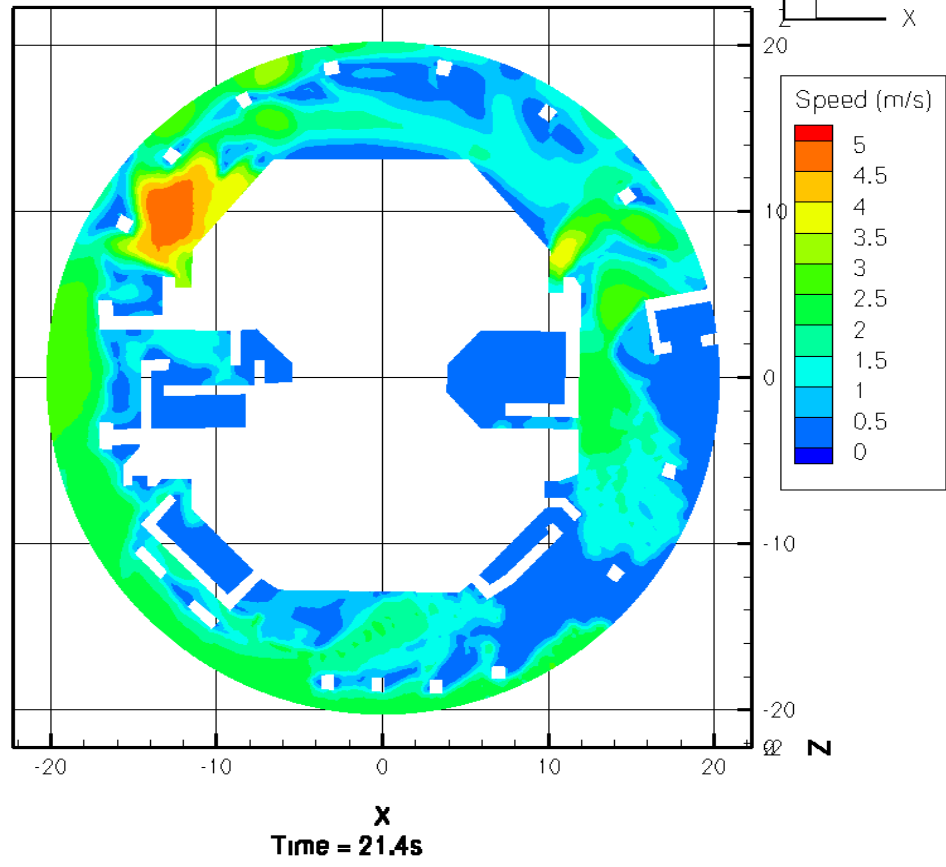


Figure III.2-16. Same as Figure III.2-13 for  $t = 21.4$  Seconds.

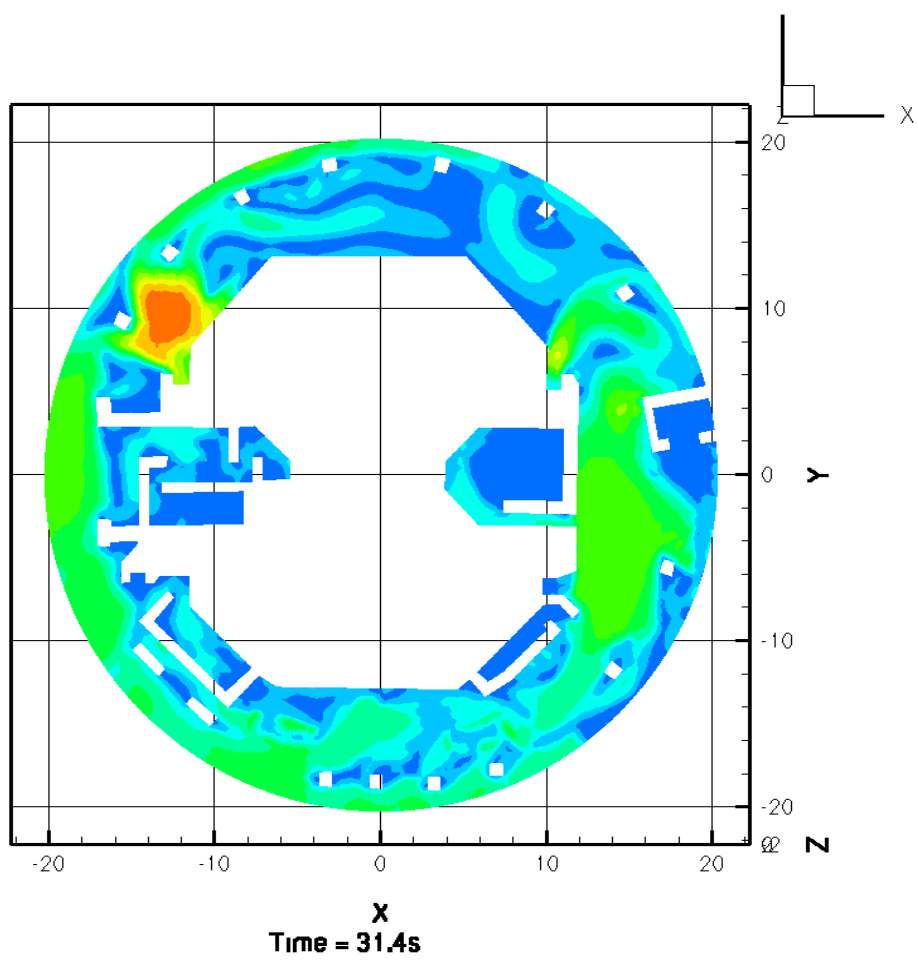


Figure III.2-17. Same as Figure III.2-13 for  $t = 31.4$  Seconds.

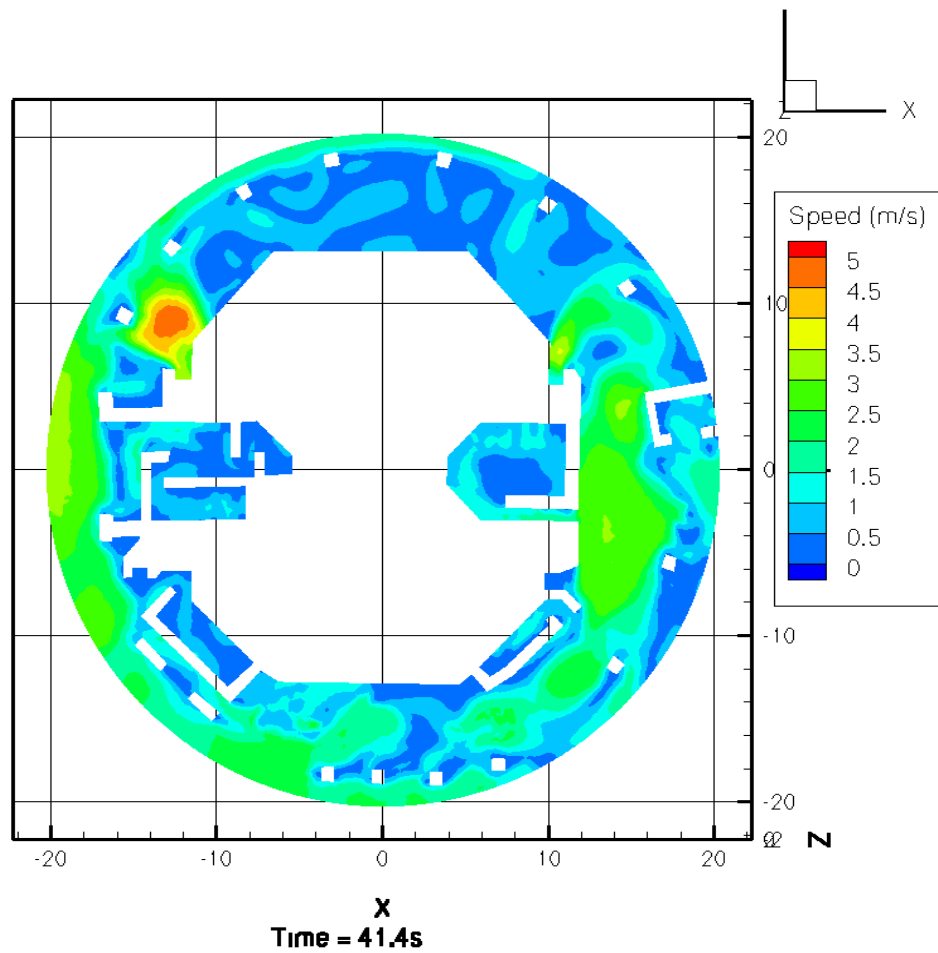


Figure III.2-18. Same as Figure III.2-13 for  $t = 41.4$  Seconds.

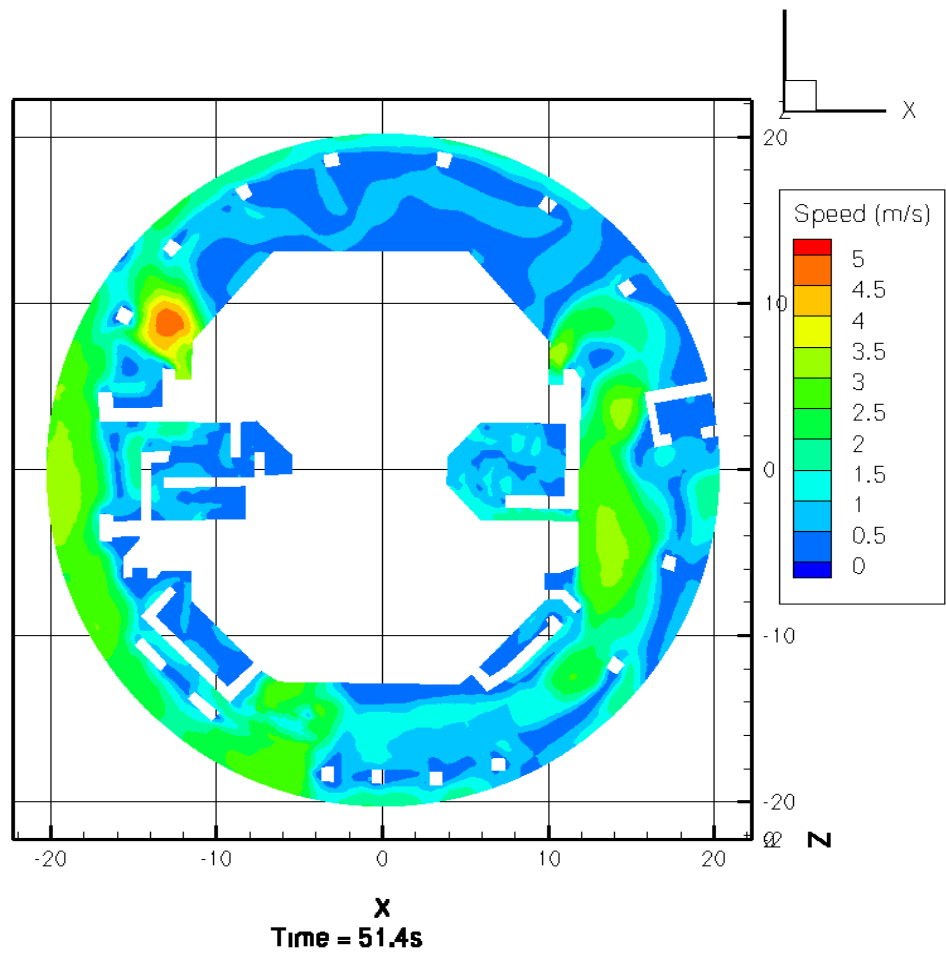


Figure III.2-19. Same as Figure III.2-13 for  $t = 51.4$  Seconds.

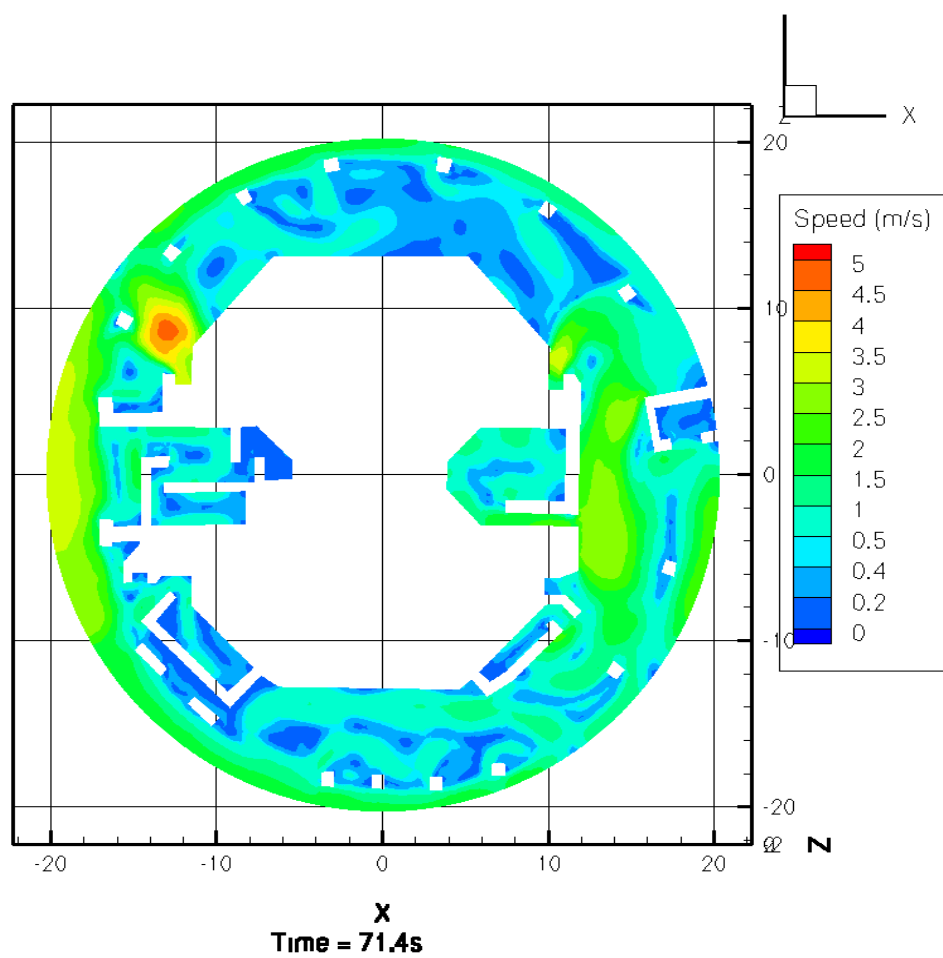


Figure III.2-20. Same as Figure III.2-13 for  $t = 71.4$  Seconds.

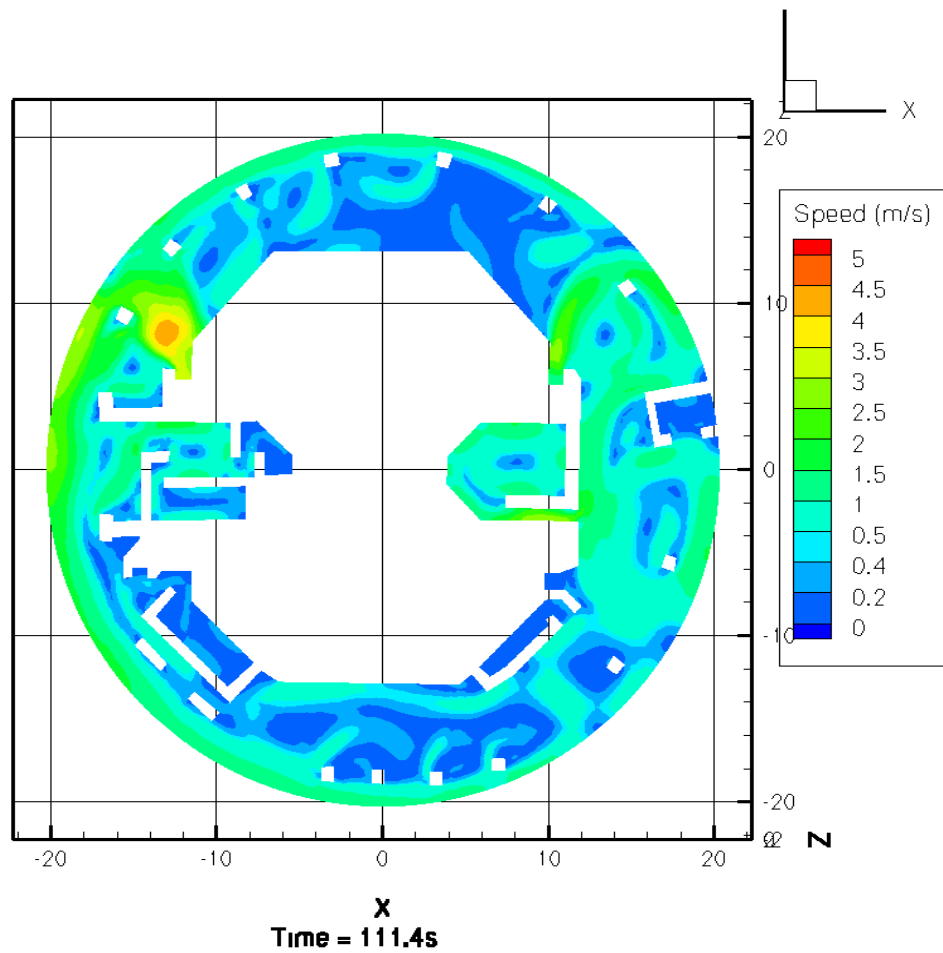
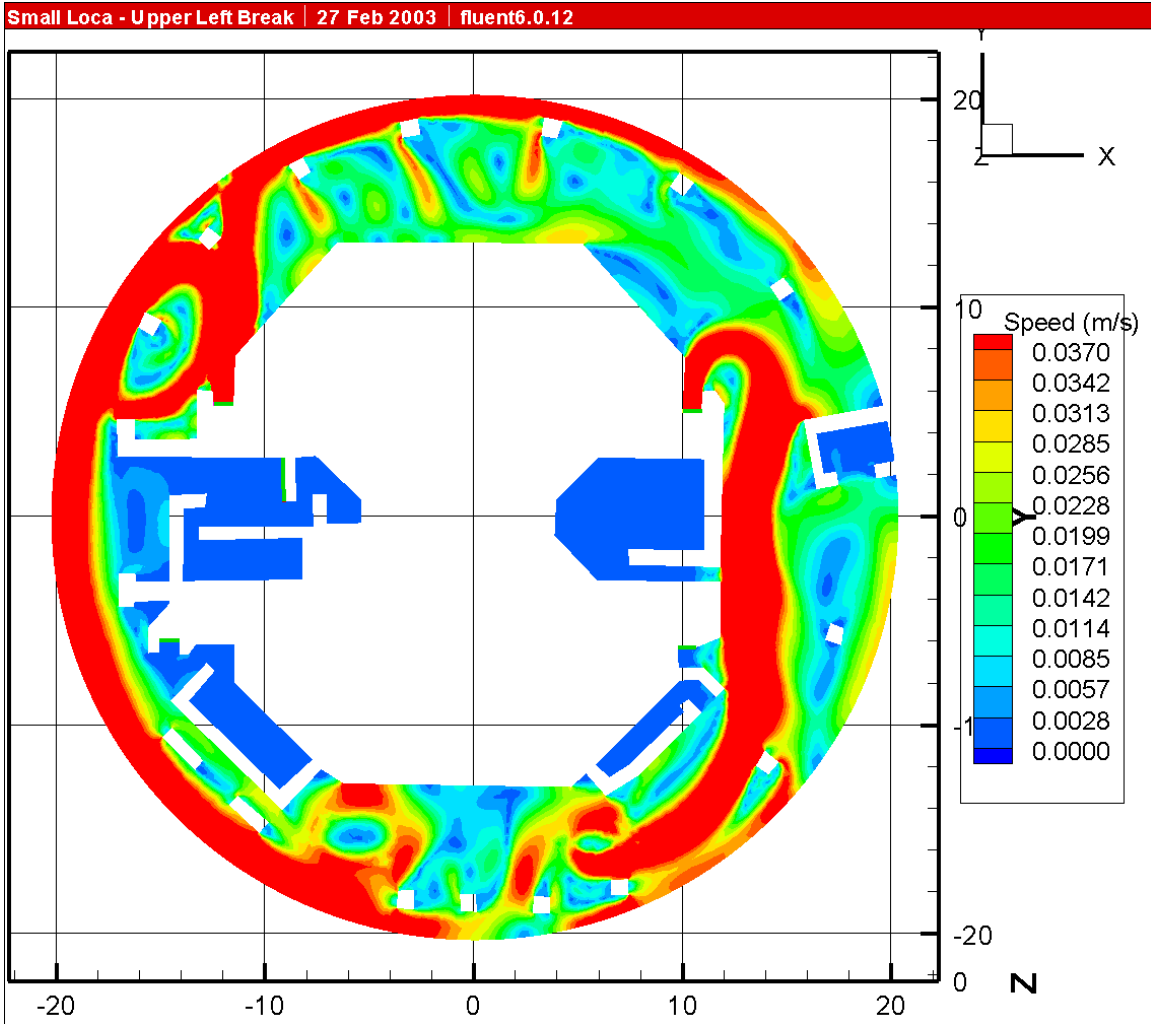
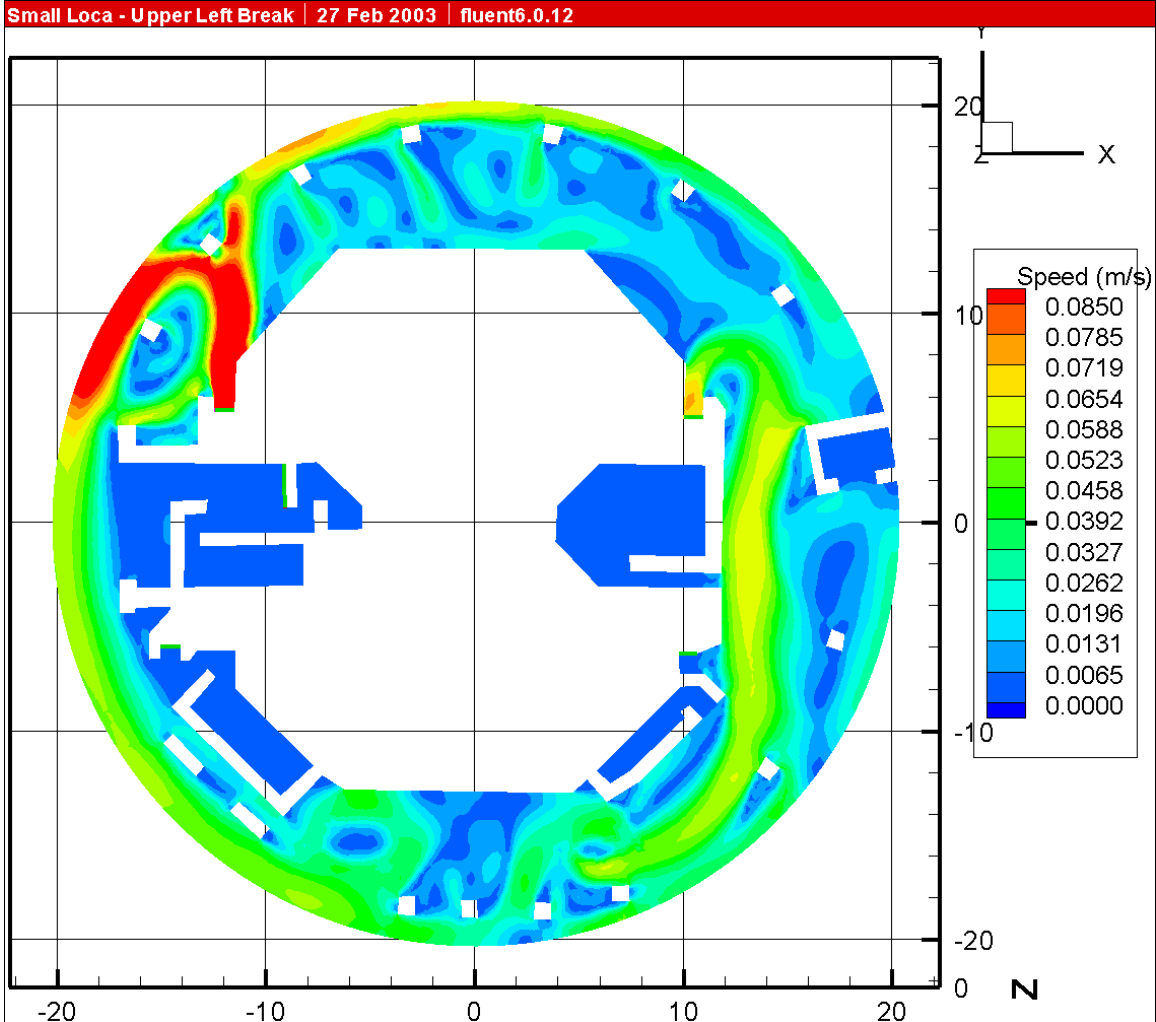


Figure III.2-21. Same as Figure III.2-13 for  $t = 111.4$  Seconds.



**Figure III.2-22. Small LOCA Break Located in the Upper-Left Quadrant. Speeds Greater Than or Equal to the Fiber Threshold (0.037 m/s) Are Colored RED.**



**Figure III.2-23. Small LOCA Break Located in the Upper-Left Quadrant. Speeds Greater Than or Equal to the RMI Threshold (0.085 m/s) Are Colored RED.**

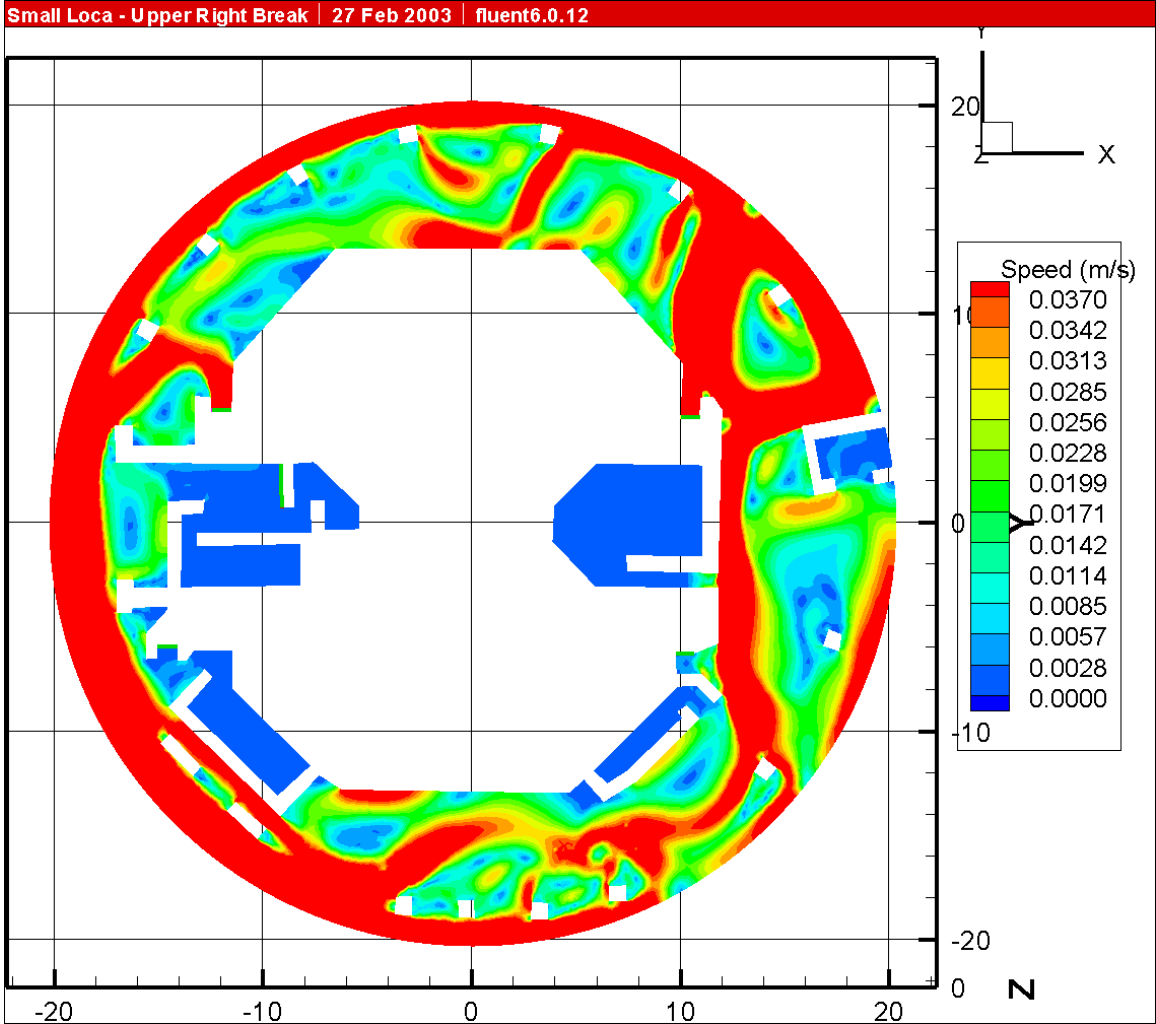


**Figure III.2-24. Small LOCA Break Located in the Upper-Right Quadrant. Speeds Greater Than or Equal to the Fiber Threshold (0.037 m/s) Are Colored RED.**

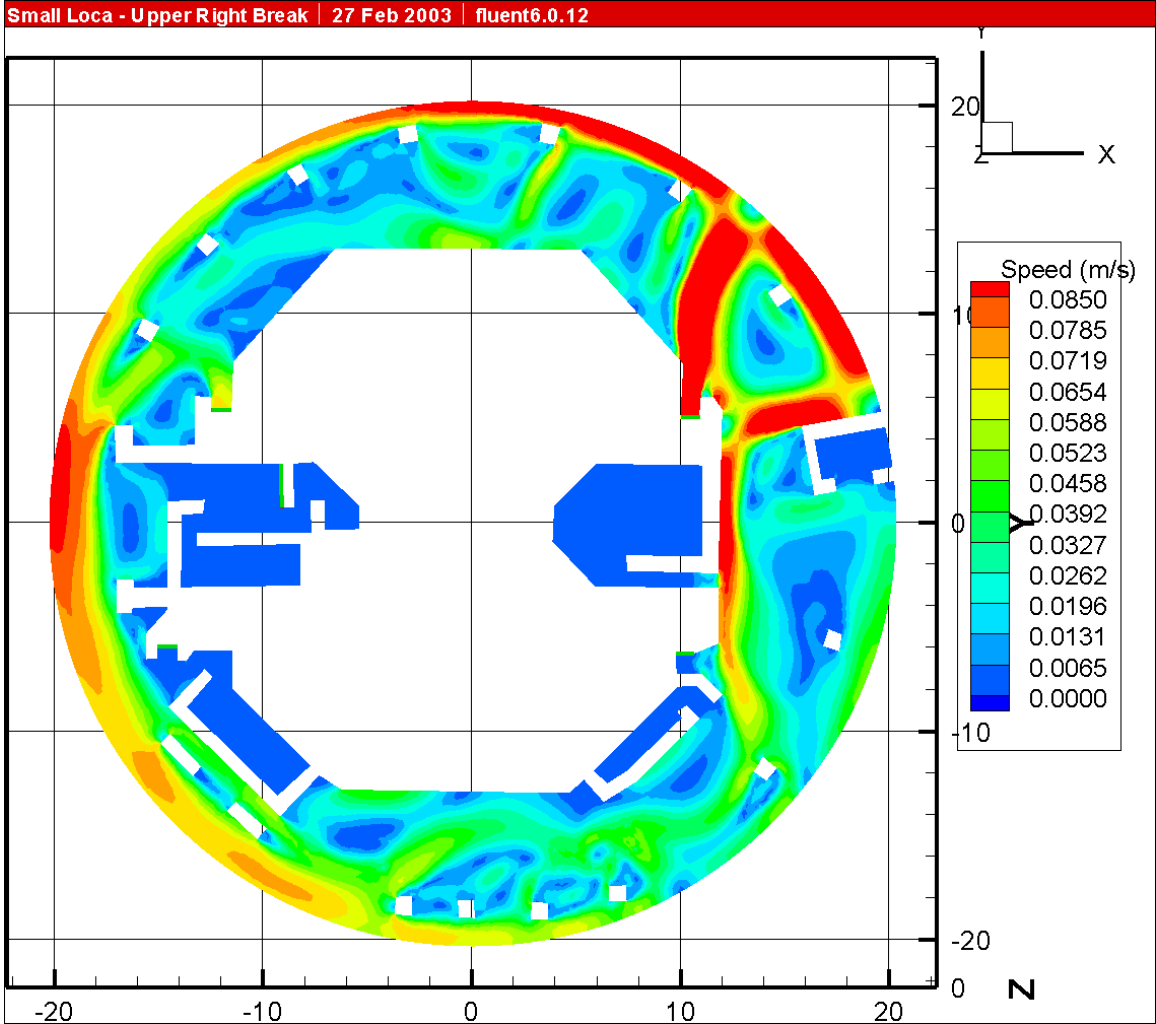


**Figure III.2-25. Small LOCA Break Located in the Upper-Right Quadrant. Speeds Greater Than or Equal to the RMI Threshold (0.085 m/s) Are Colored RED.**

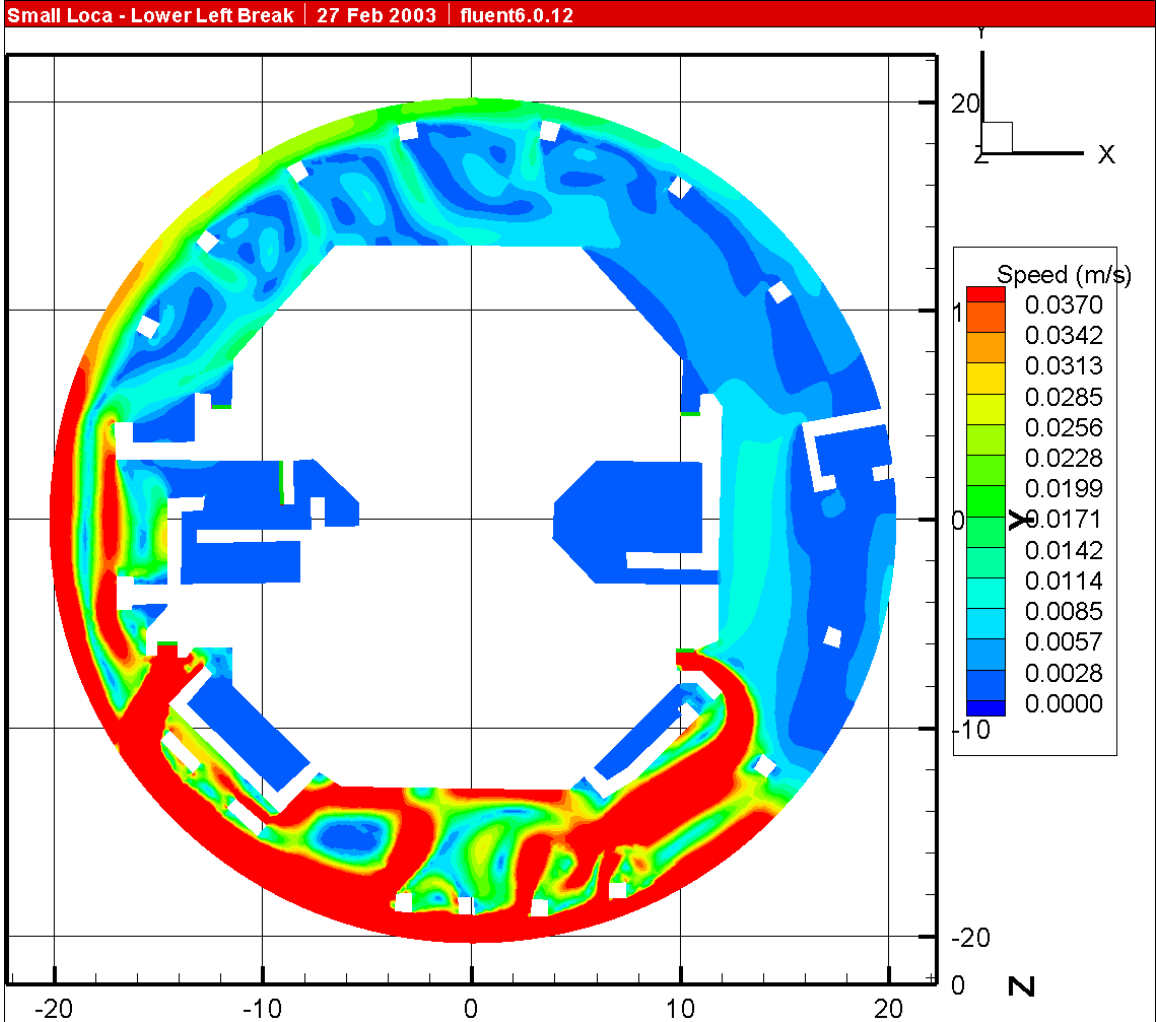
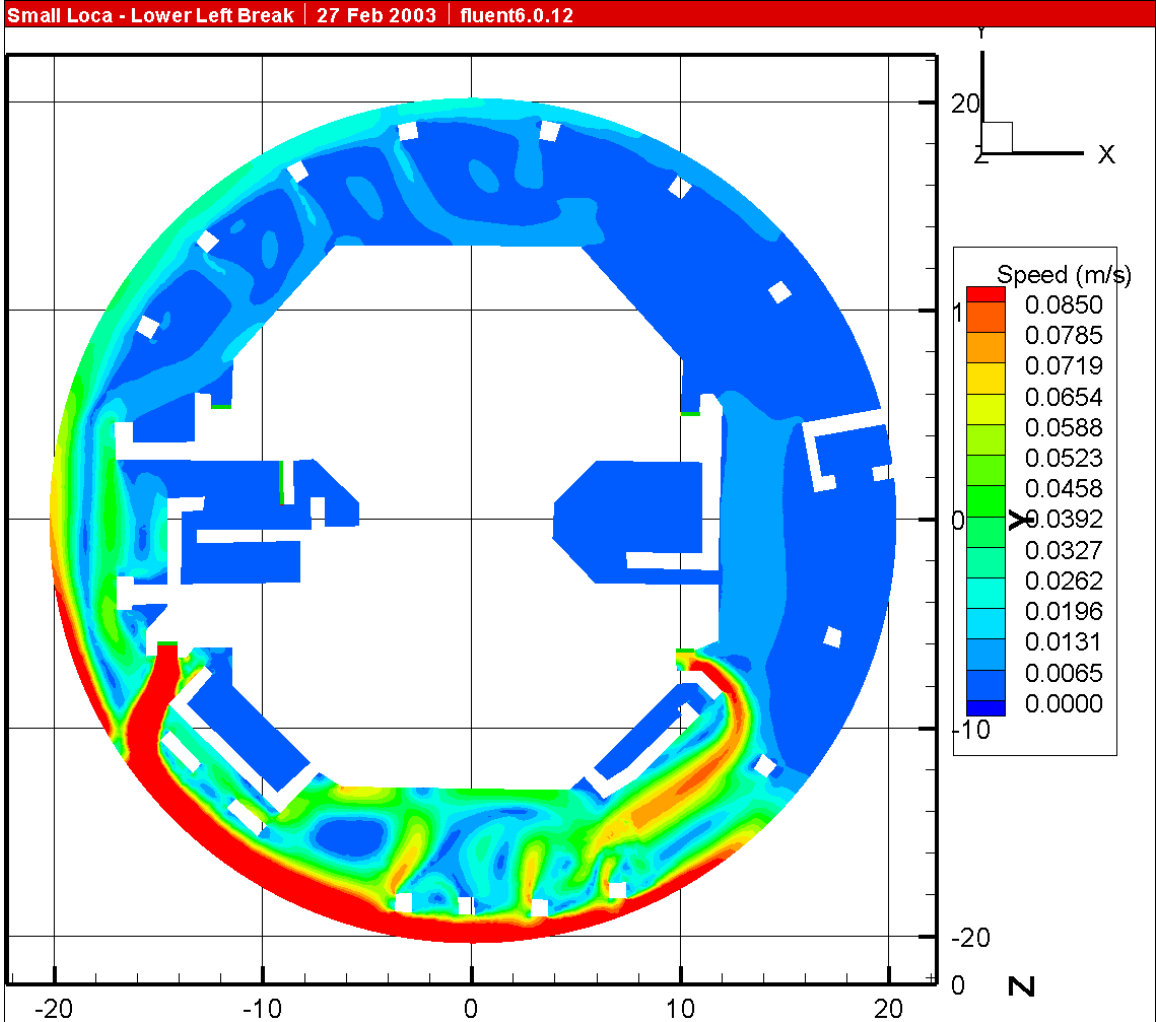


Figure III.2-26. Small LOCA Break Located in the Lower-Left Quadrant. Speeds Greater Than or Equal to the Fiber Threshold (0.037 m/s) Are Colored RED.



**Figure III.2-27. Small LOCA Break Located in the Lower-Left Quadrant. Speeds Greater Than or Equal to the RMI Threshold (0.085 m/s) Are Colored RED.**

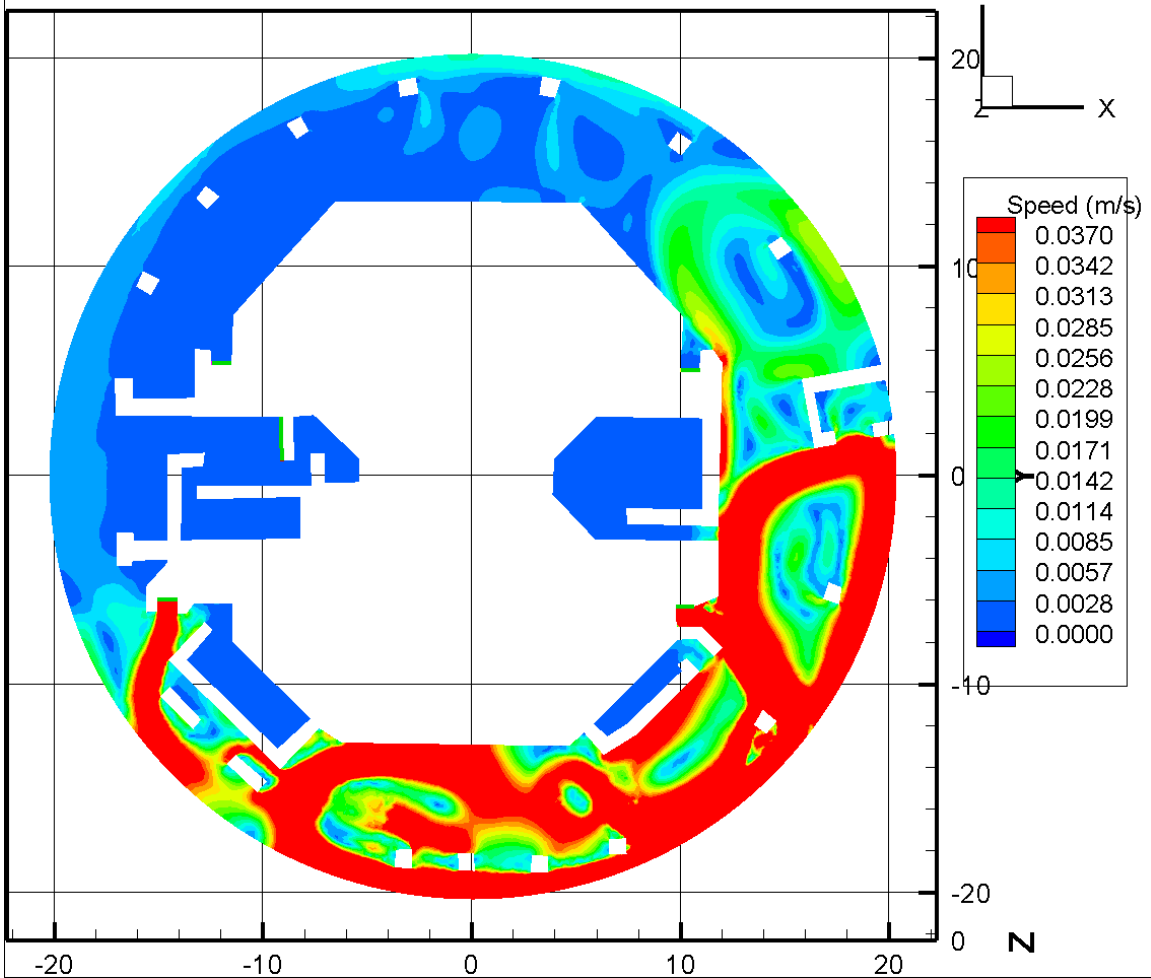
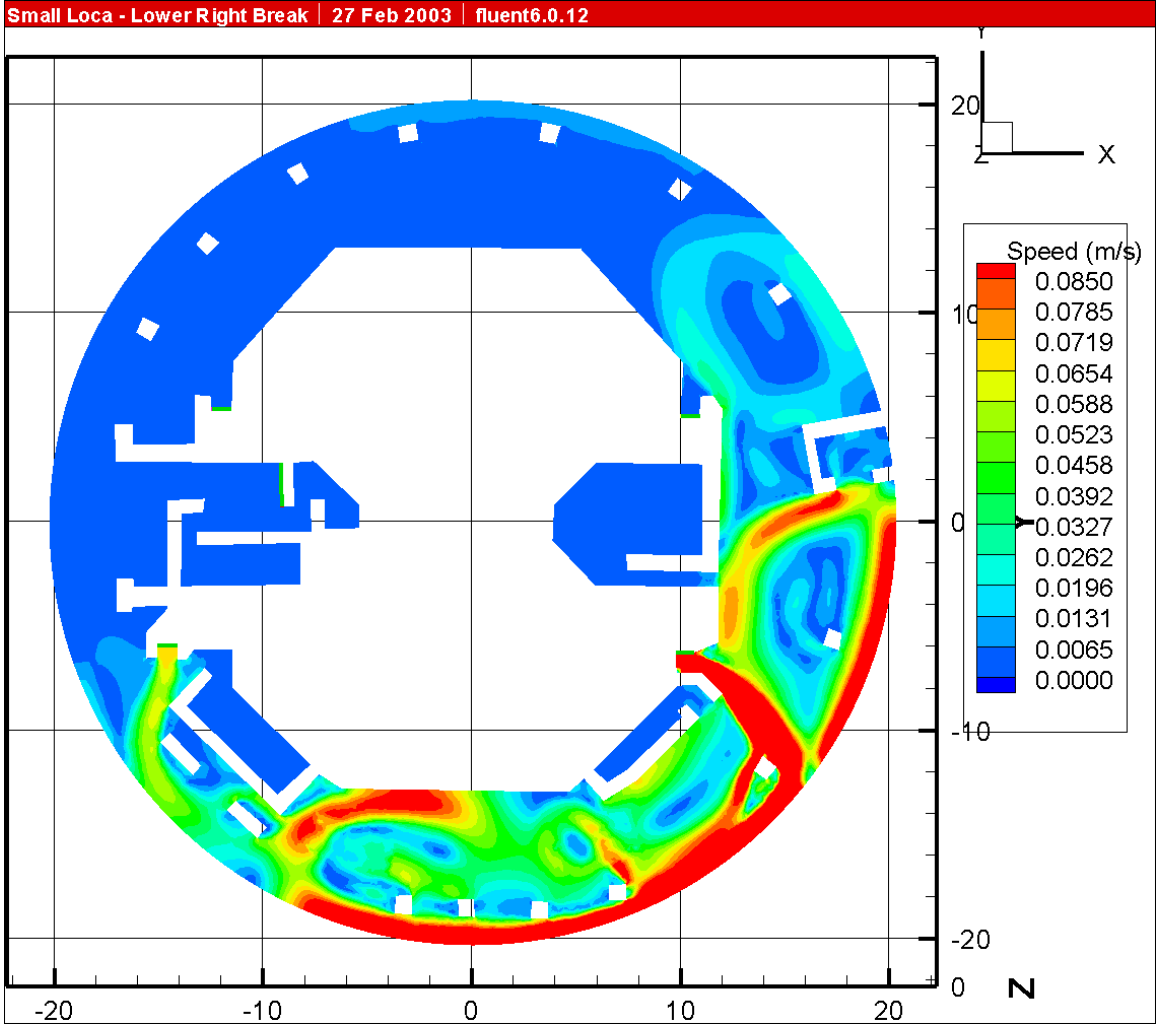
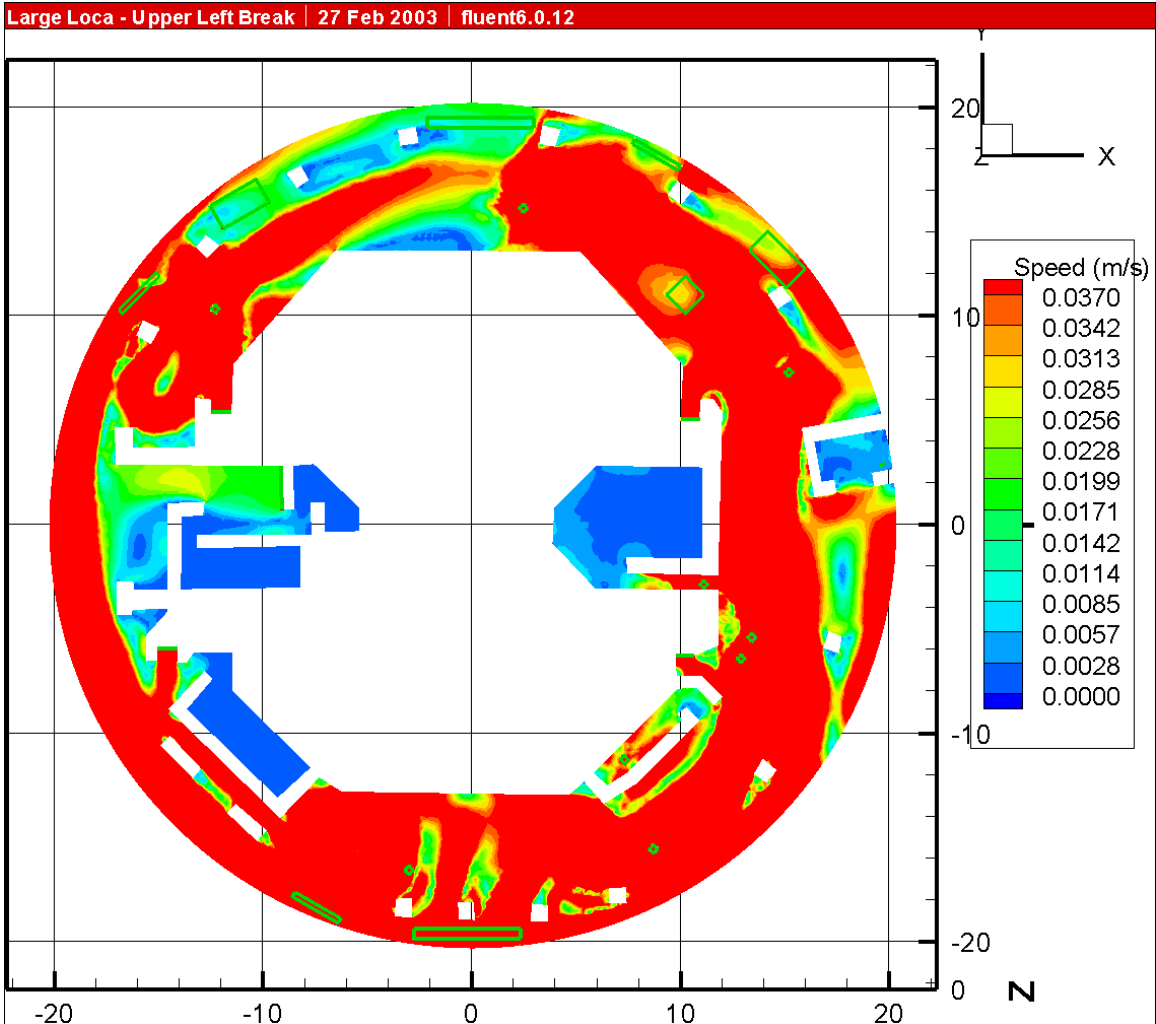


Figure III.2-28. Small LOCA Break Located in the Lower-Right Quadrant. Speeds Greater Than or Equal to the Fiber Threshold (0.037 m/s) Are Colored RED.



**Figure III.2-29. Small LOCA Break Located in the Lower-Right Quadrant. Speeds Greater Than or Equal to the RMI Threshold (0.085 m/s) Are Colored RED.**



**Figure III.2-30. Large LOCA Break Located in the Upper-Left Quadrant. Speeds Greater Than or Equal to the Fiber Threshold (0.037 m/s) Are Colored RED.**

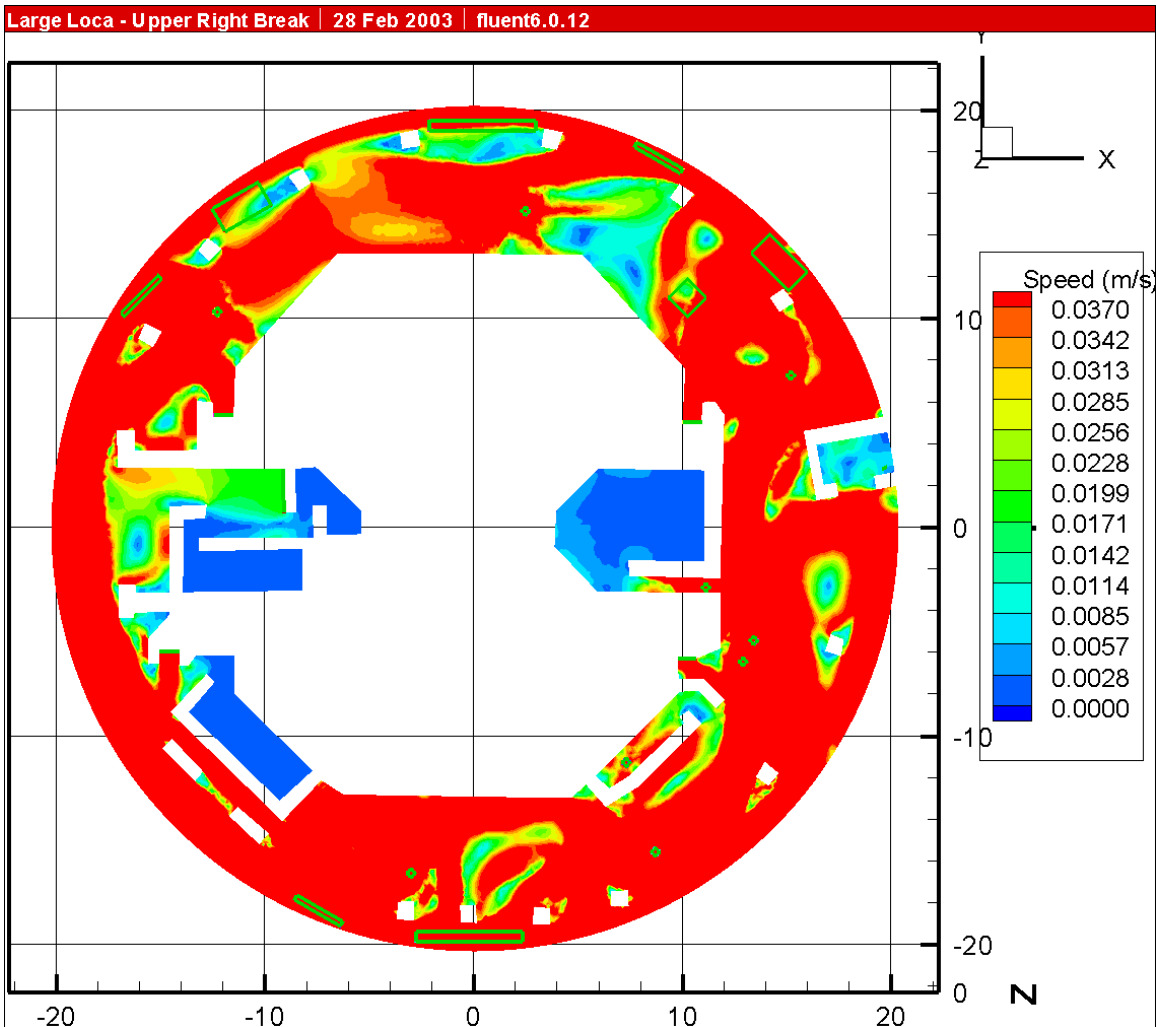


**Figure III.2-31. Large LOCA Break Located in the Upper-Right Quadrant. Speeds Greater Than or Equal to the Fiber Threshold (0.037 m/s) Are Colored RED.**

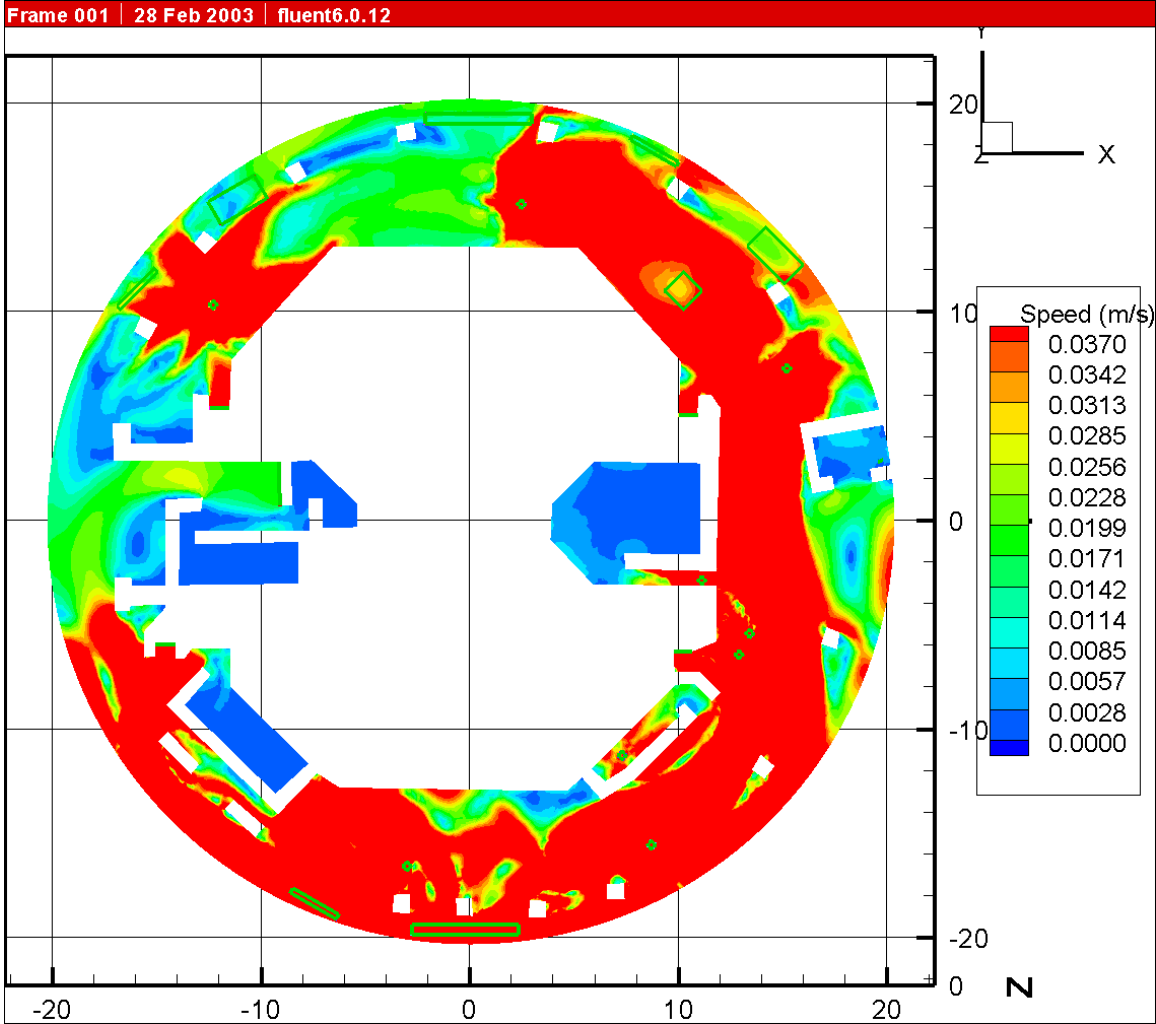


**Figure III.2-32. Large LOCA Break Located in the Lower-Left Quadrant. Speeds Greater Than or Equal to the Fiber Threshold (0.037 m/s) Are Colored RED.**

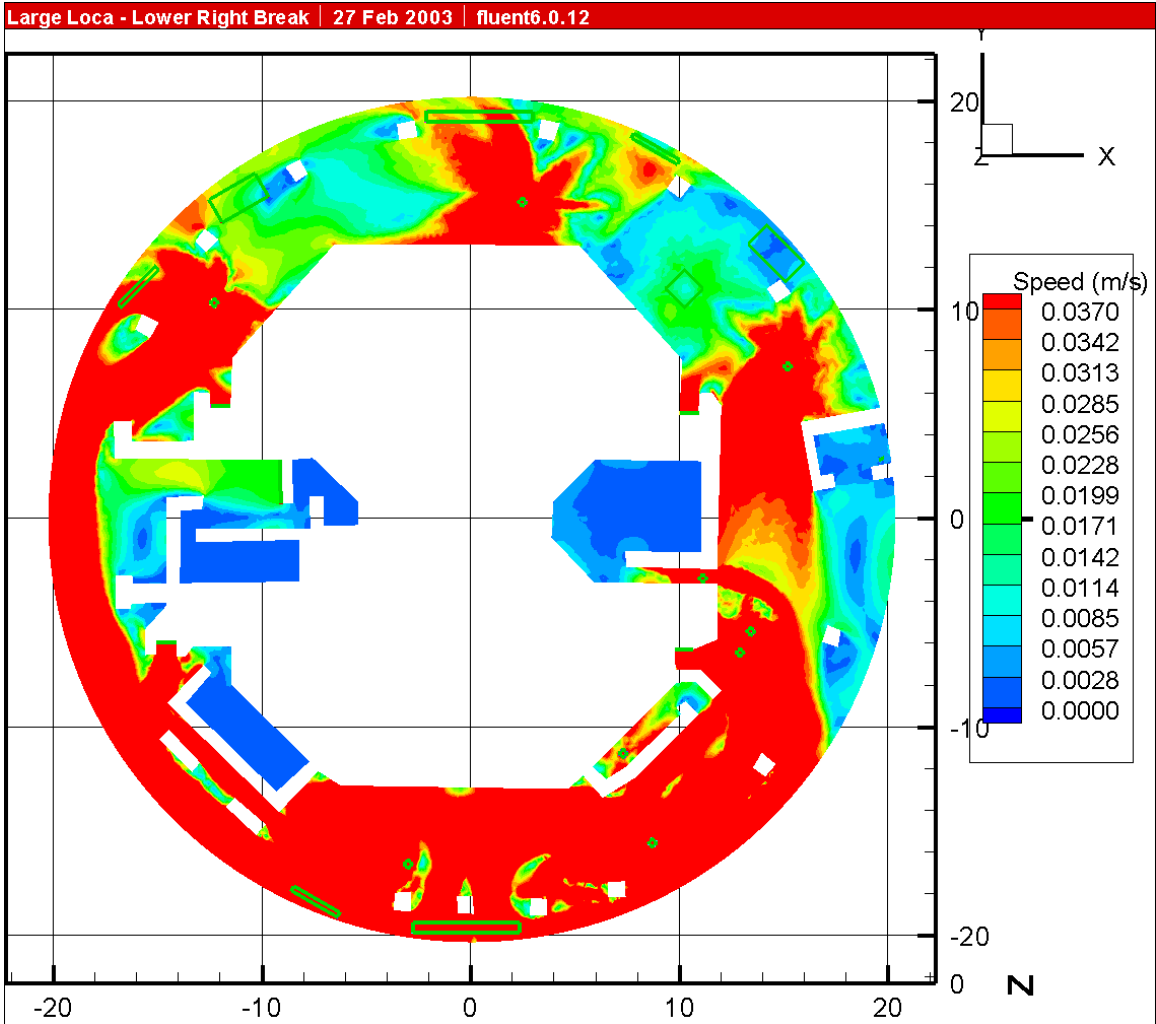


**Figure III.2-33. Large LOCA Break Located in the Lower-Right Quadrant. Speeds Greater Than or Equal to the Fiber Threshold (0.037 m/s) Are Colored RED.**

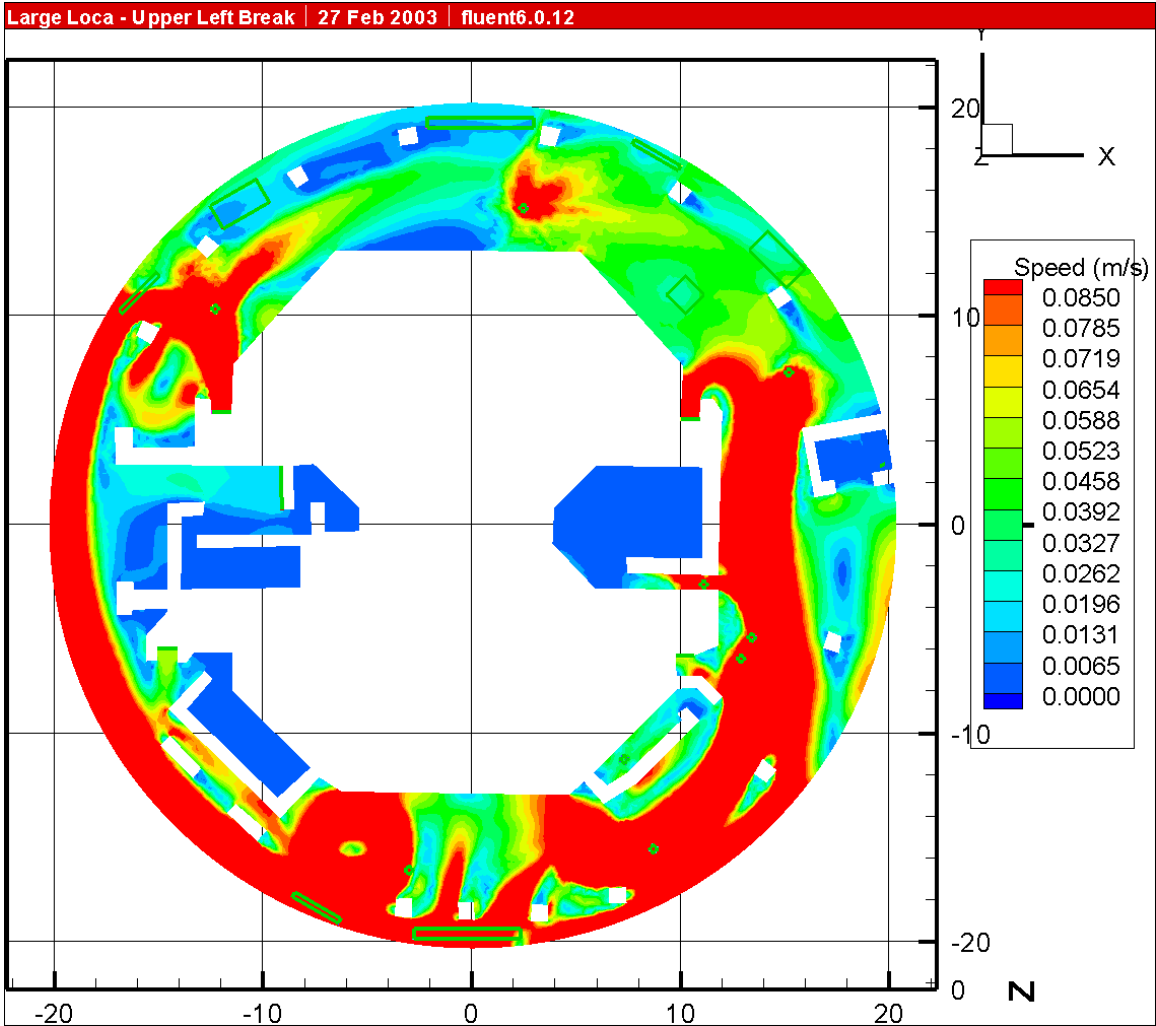


**Figure III.2-34. Large LOCA Break Located in the Upper-Left Quadrant. Speeds Greater Than or Equal to the RMI Threshold (0.085 m/s) Are Colored RED.**

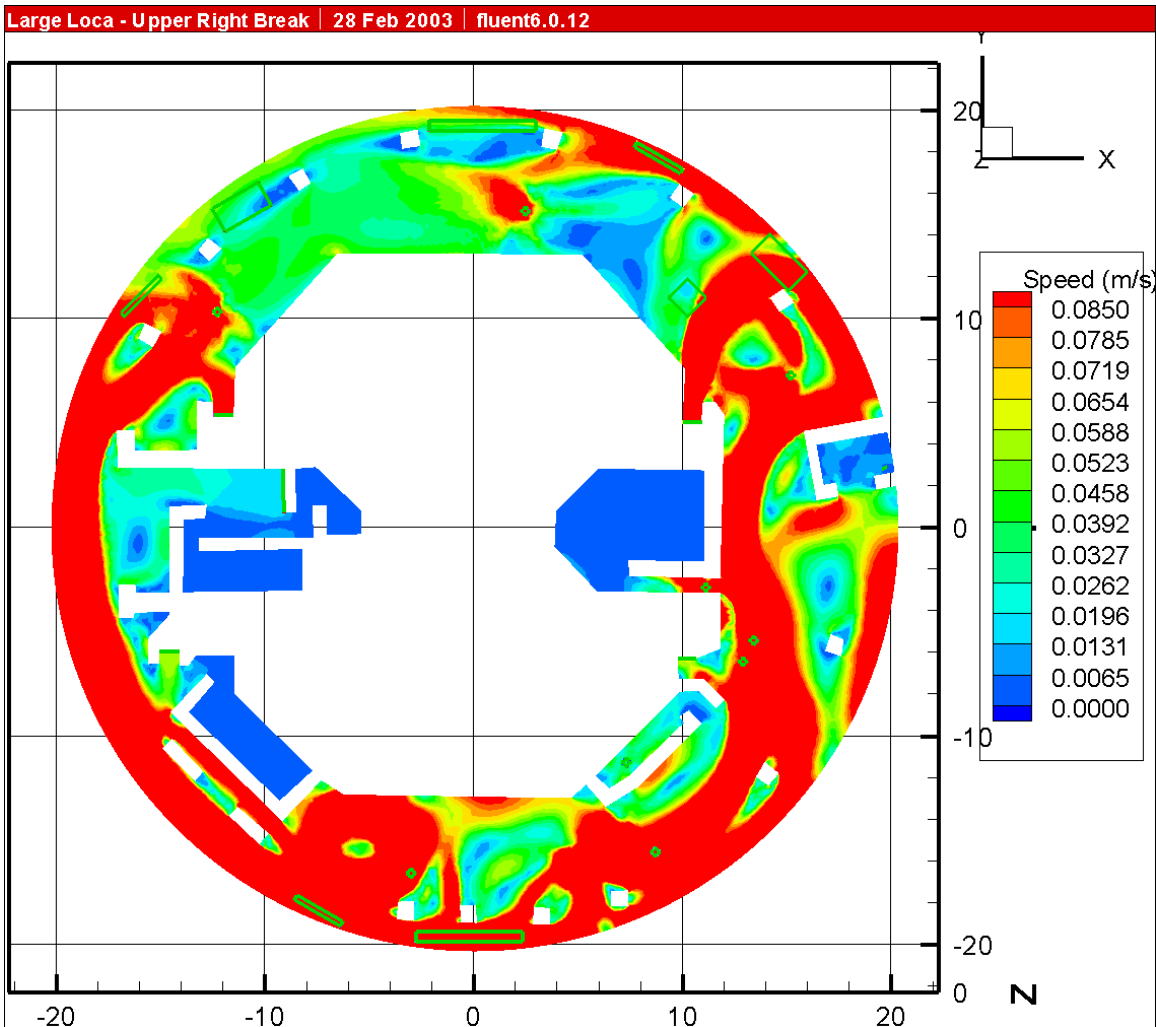


**Figure III.2-35. Large LOCA Break Located in the Upper-Right Quadrant. Speeds Greater Than or Equal to the RMI Threshold (0.085 m/s) Are Colored RED.**

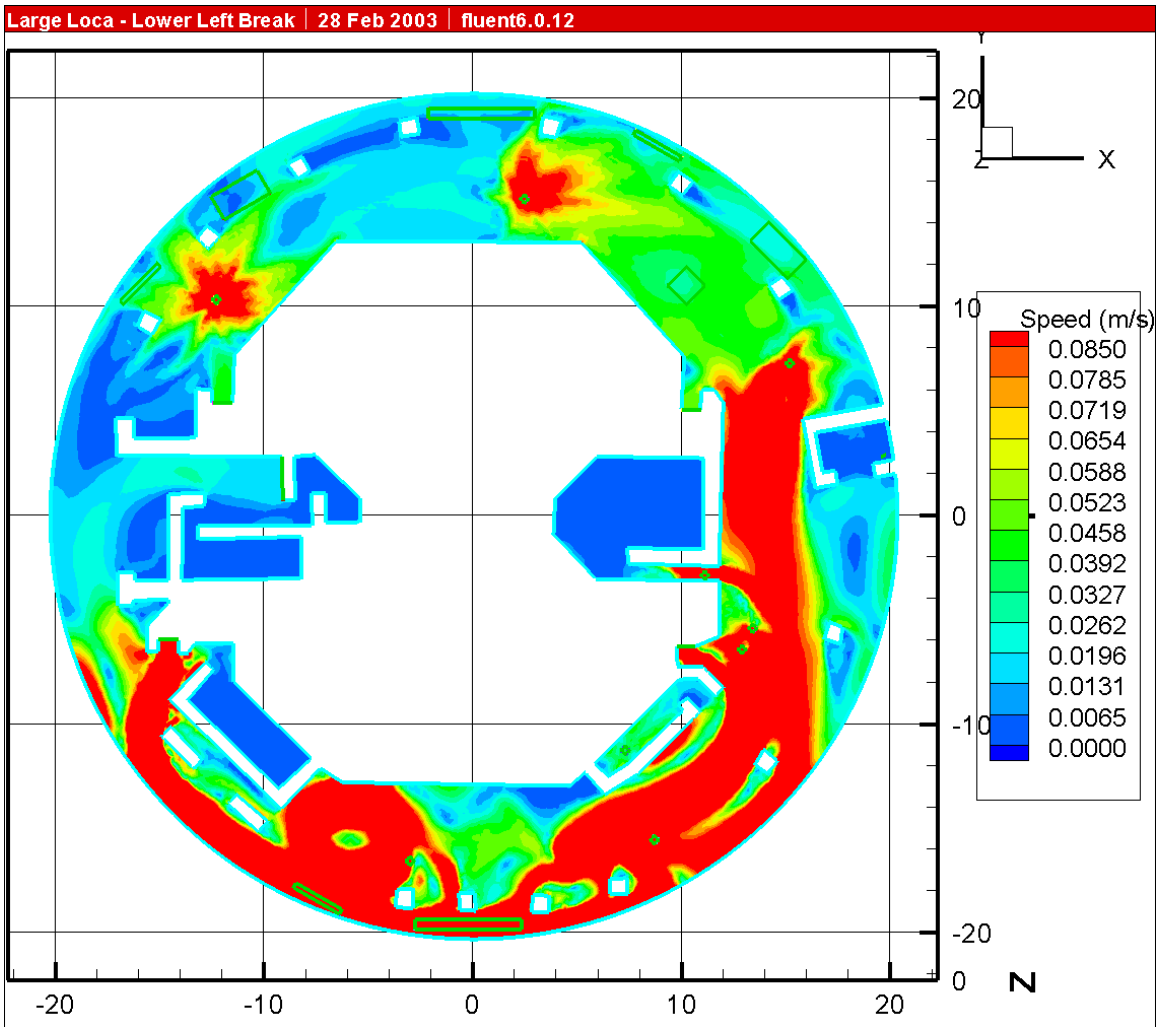


**Figure III.2-36. Large LOCA Break Located in the Lower-Left Quadrant. Speeds Greater Than or Equal to the RMI Threshold (0.085 m/s) Are Colored RED.**

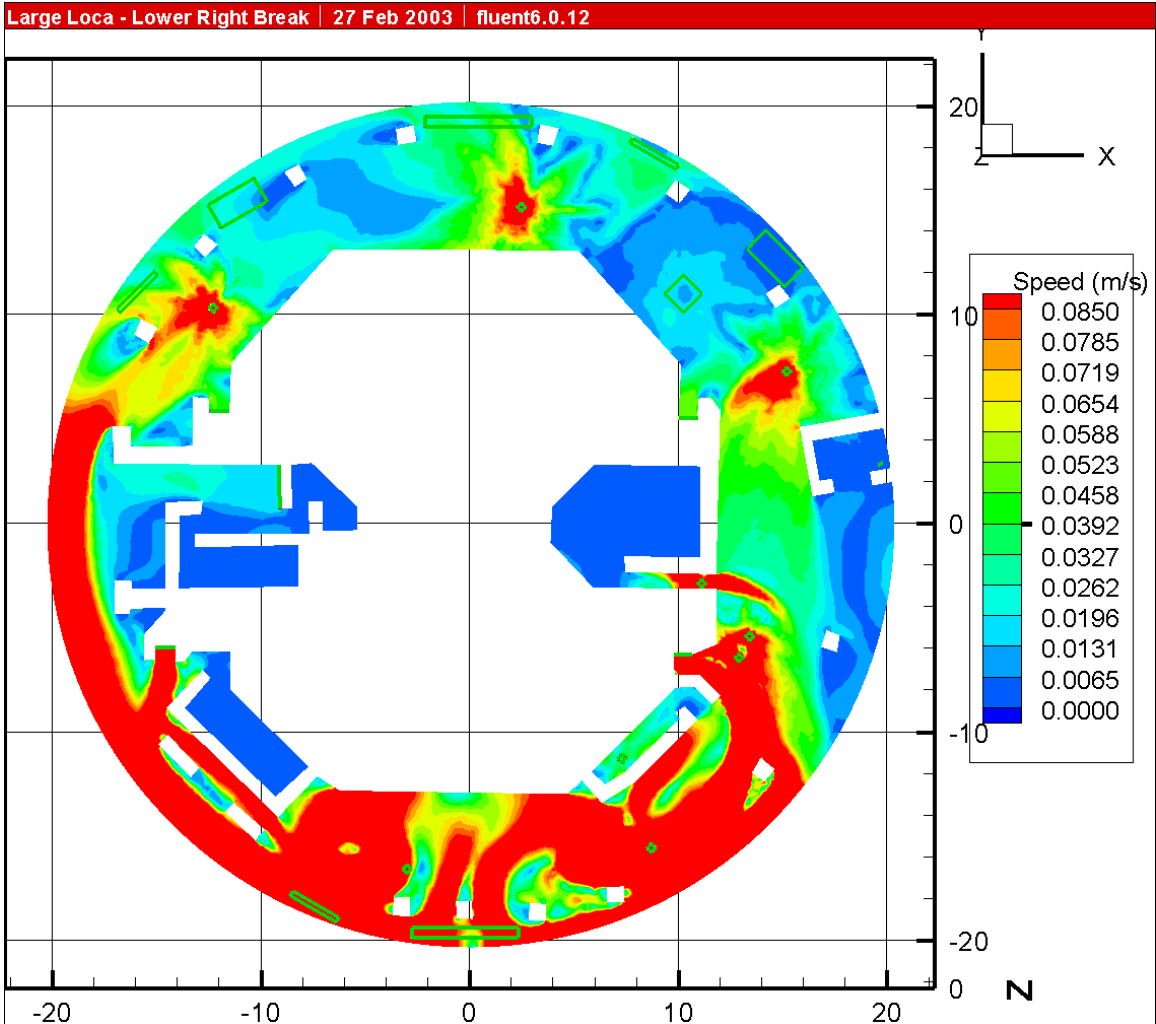


**Figure III.2-37. Large LOCA Break Located in the Lower-Right Quadrant. Speeds Greater Than or Equal to the RMI Threshold (0.085 m/s) Are Colored RED.**

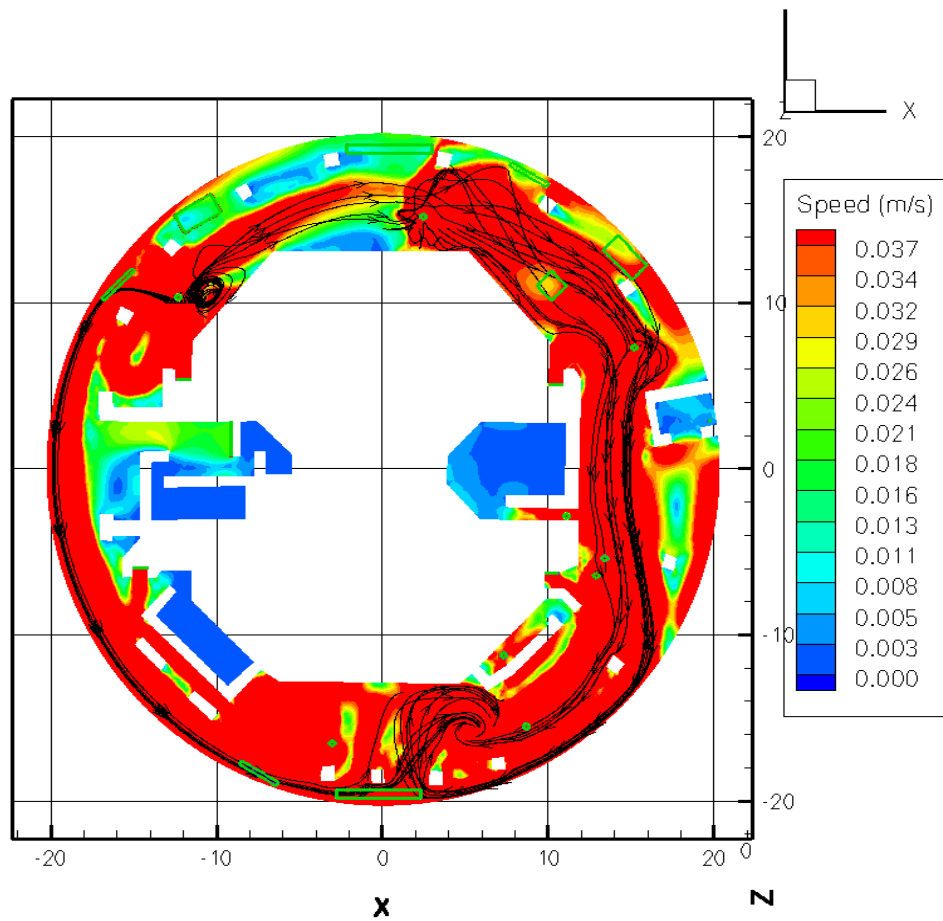


**Figure III.2-38. Streamtraces across Two Splash Locations, Coordinates (-12,10) and (5,15), as Shown in the Figure, for a Large LOCA Break Located in the Upper-Left Quadrant. Speeds Greater Than or Equal to the Fiber Threshold (0.037 m/s) Are Colored RED.**

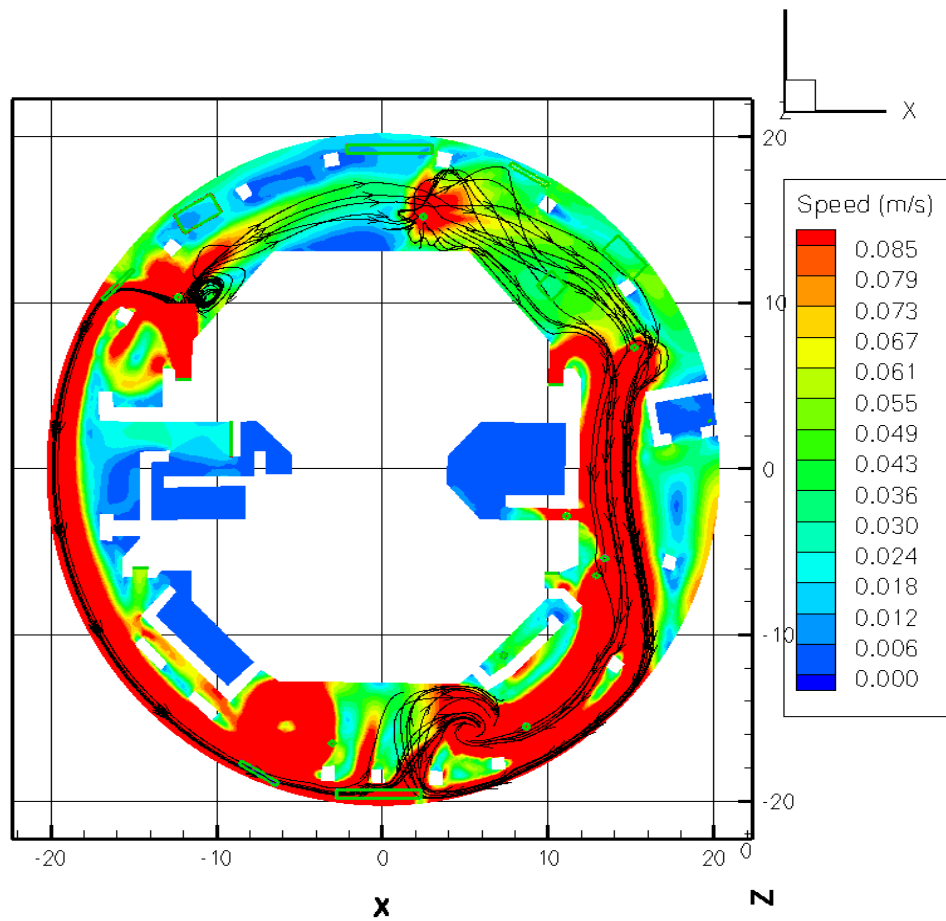


**Figure III.2-39. Streamtraces across Two Splash Locations, Coordinates (-12,10) and (5,15), as Shown in the Figure, for a Large LOCA Break Located in the Upper-Left Quadrant. Speeds Greater Than or Equal to the RMI Threshold (0.085 m/s) Are Colored RED.**

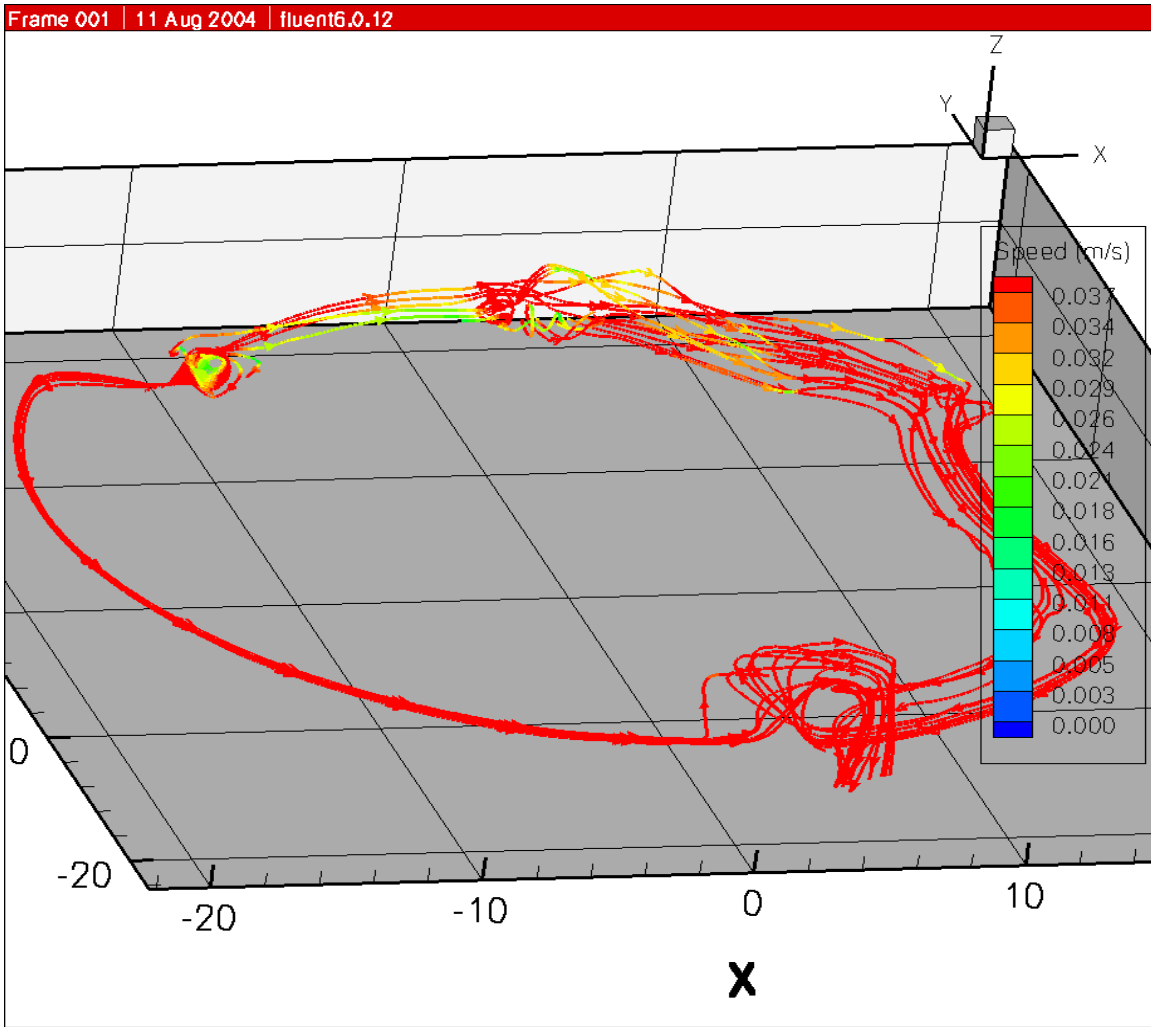


**Figure III.2-40. Oblique View of the Streamtraces, as Shown in Figure III.2-38 for the Fiber Threshold Velocity. Traces Are Color Coded to the Local Fluid Velocity. Speeds Greater Than or Equal to the Fiber Threshold (0.037 m/s) Are Colored RED.**

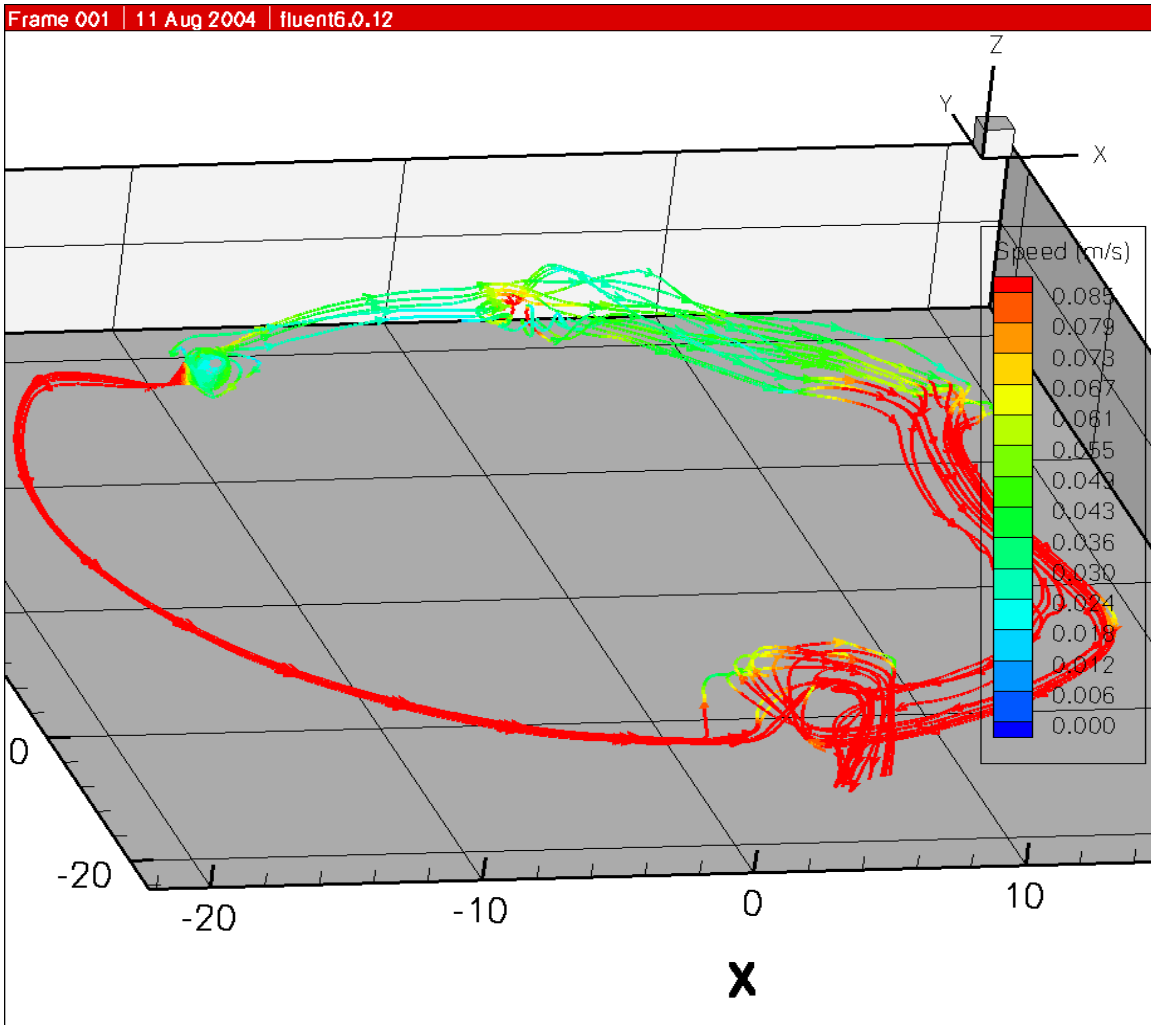


**Figure III.2-41. Oblique View of the Streamtraces Shown in Figure III.2-39 for the RMI Threshold Velocity. Traces are Color Coded to the Local Fluid Velocity. Speeds Greater Than or Equal to the RMI Threshold (0.085 m/s) Are Colored RED.**

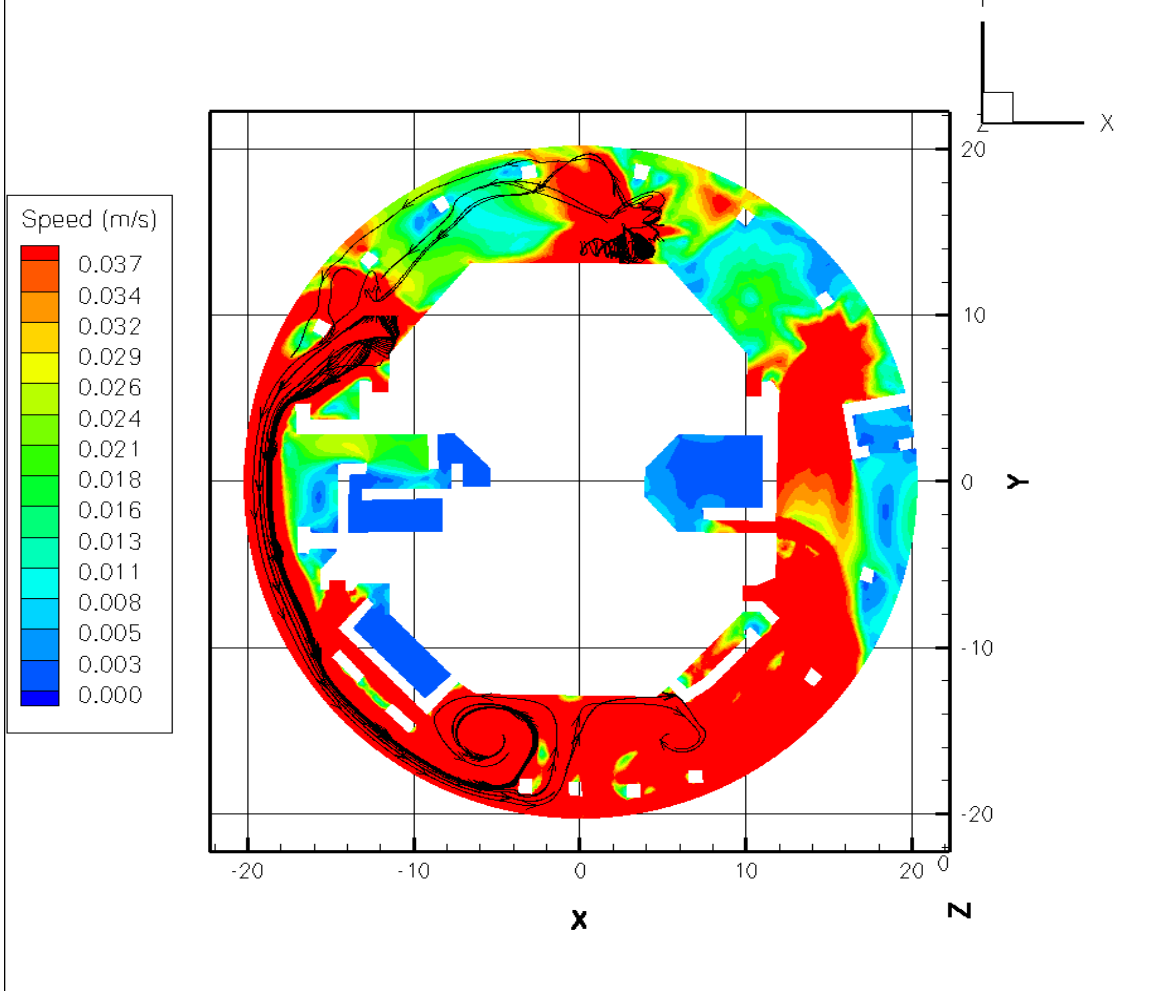


**Figure III.2-42. Streamtraces across Two Splash Locations, Coordinates (-12,10) and (5,15) as Shown in the Figure, for a Large LOCA Break Located in the Lower-Right Quadrant. Speeds Greater Than or Equal to the Fiber Threshold (0.037 m/s) Are Colored RED.**

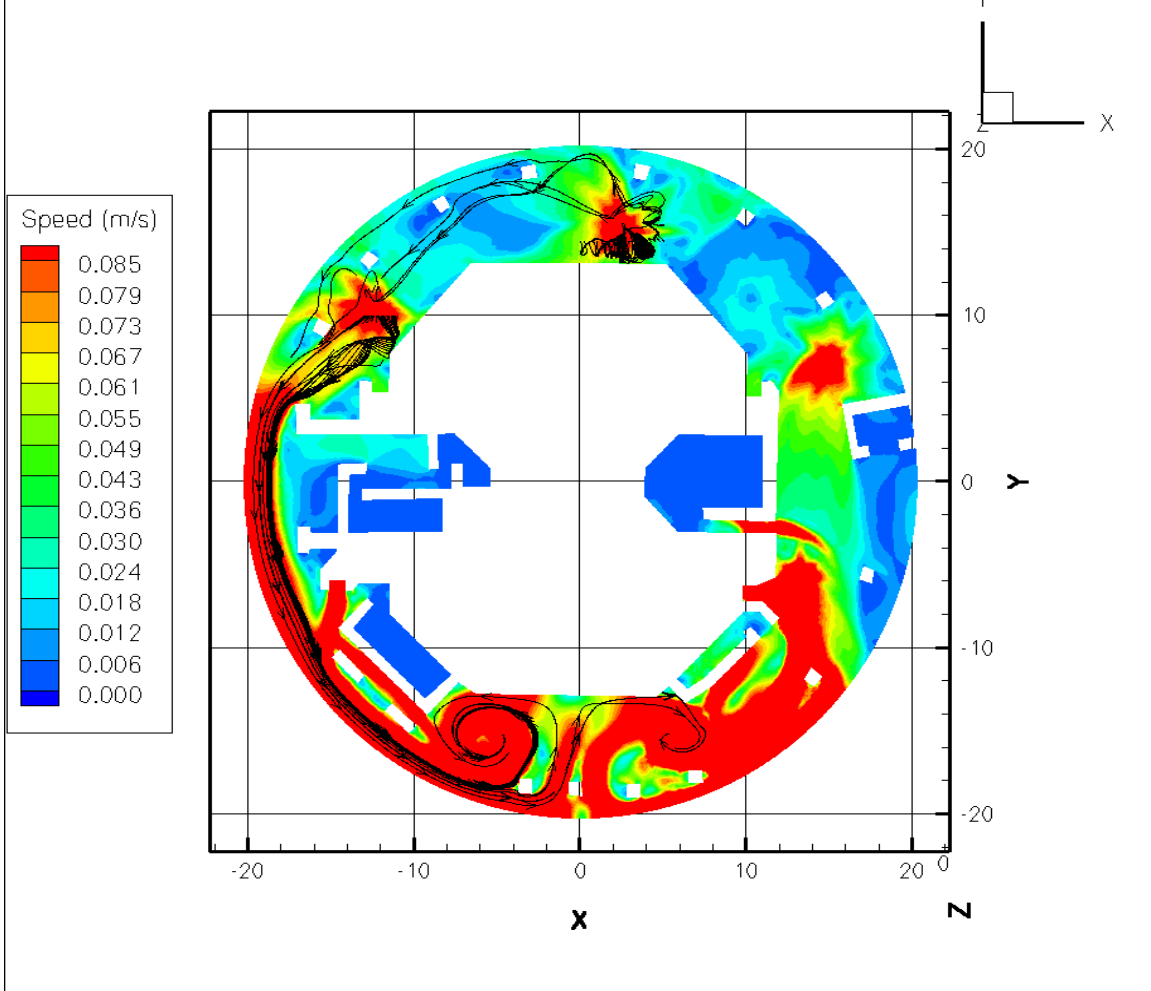


**Figure III.2-43. Streamtraces across Two Splash Locations, Coordinates (-12,10) and (5,15), as Shown in the Figure, for a Large LOCA Break Located in the Lower-Right Quadrant. Speeds Greater Than or Equal to the RMI Threshold (0.085 m/s) Are Colored RED.**

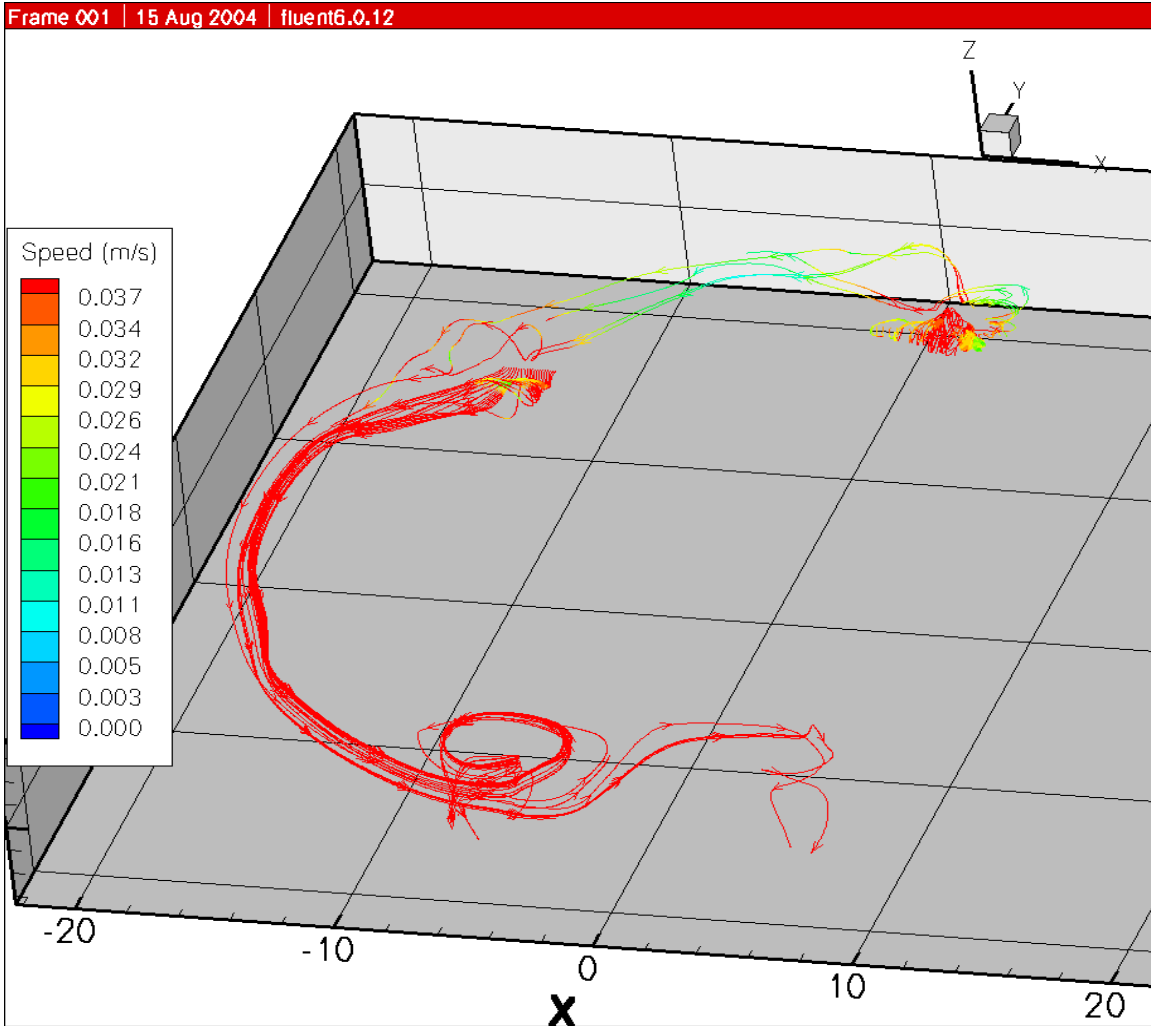


**Figure III.2-44. Oblique View of the Streamtraces Shown in Figure III.2-42 for the Fiber Threshold Velocity. Traces Are Color Coded to the Local Fluid Velocity. Speeds Greater Than or Equal to the Fiber Threshold (0.037 m/s) Are Colored RED.**

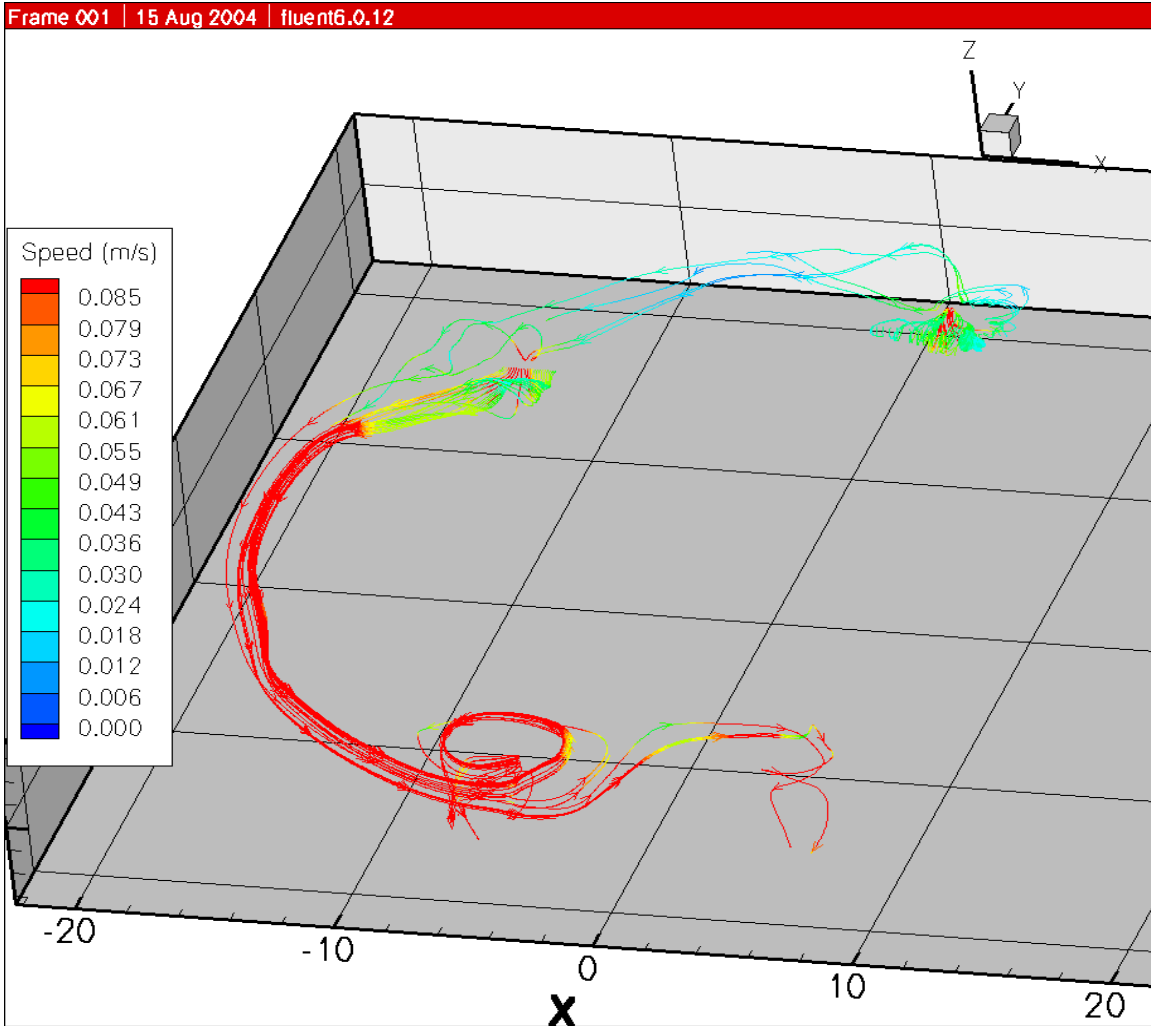


**Figure III.2-45. Oblique View of the Streamtraces Shown in Figure III.2-43 for the Fiber Threshold Velocity. Traces Are Color Coded to the Local Fluid Velocity. Speeds Greater Than or Equal to the RMI Threshold (0.085 m/s) Are Colored RED.**

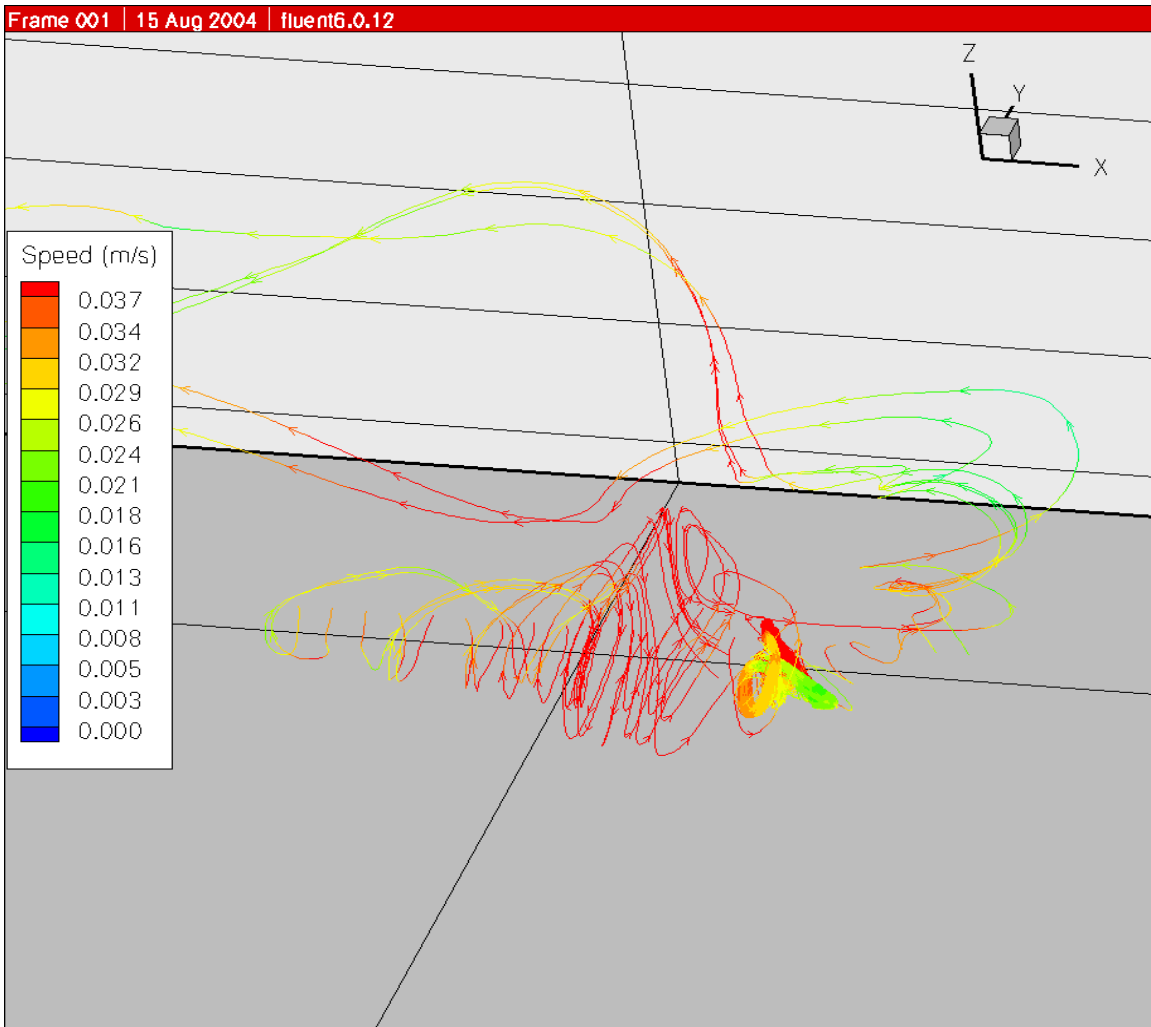


**Figure III.2-46. Large LOCA Lower-Right Break, Zoom in at Upper-Right Splash Location Shown in Figures III.2-42 and III.2-43. Traces Are Color Coded to the Local Fluid Velocity. Speeds Greater Than or Equal to the Fiber Threshold (0.037 m/s) Are Colored RED.**

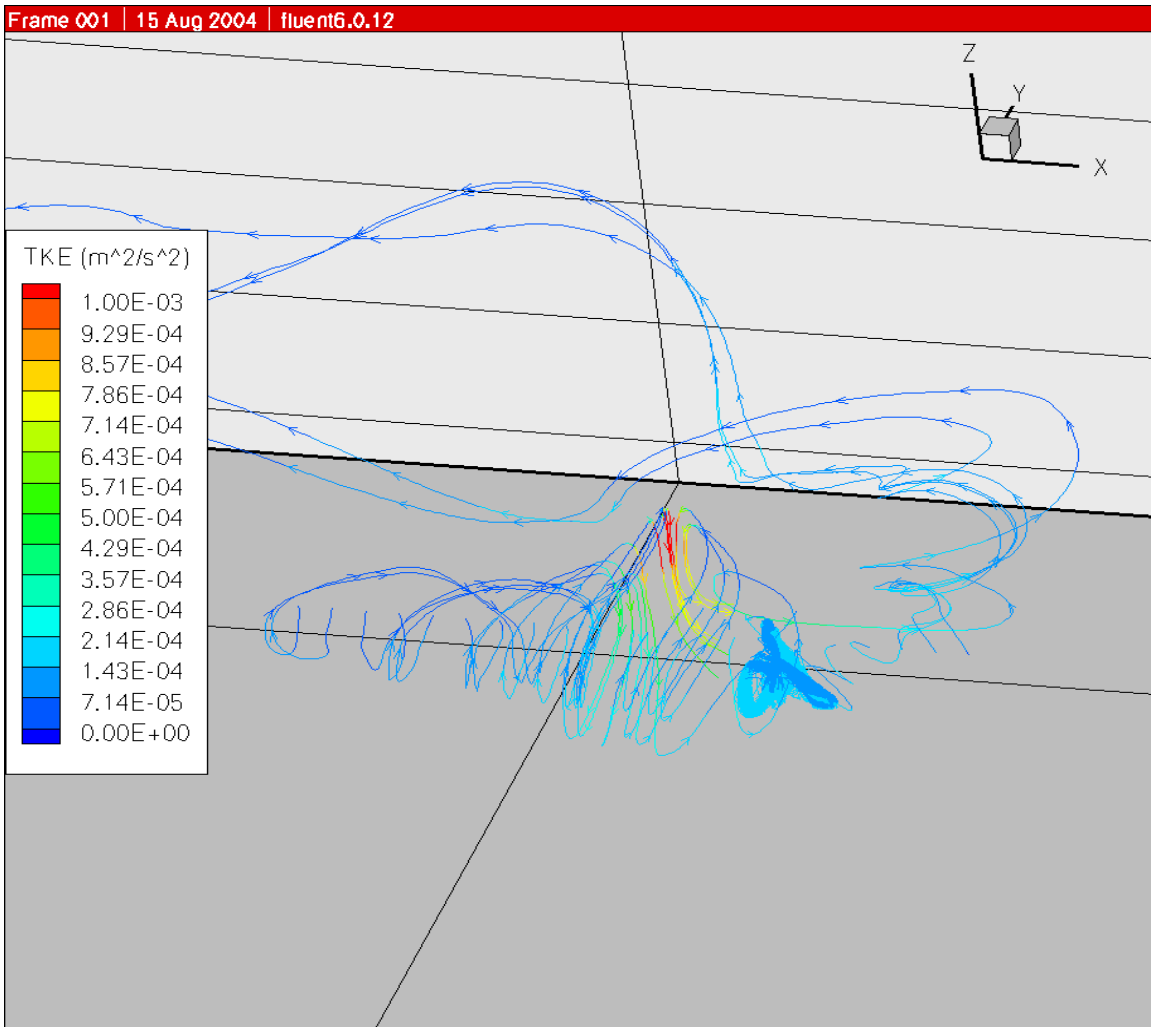


Figure III.2-47. Same as Figure III.2-46, with Streamlines Color Coded by TKE.

### III.3 SUMP POOL DEBRIS TRANSPORT

The CFD analyses characterized the flow conditions in the sump for a selection of LOCA accident scenarios. These conditions include flow velocity patterns, pool turbulence, and flow streamlines. The pool velocity and turbulence characteristics determine areas of the pool where debris entrapment may occur. The flow streamlines can be used to determine whether debris entering the pool at a discrete location would be likely to pass through one of the potential entrapment locations. The debris transport process was broken down using a logic chart approach to facilitate the individual transport steps—steps that could be determined analytically, experimentally, or simply judged. The subsequent quantification of the chart then provided an estimate of the overall sump pool debris transport.

### III.3.1 Debris Transport Logic Chart Methodology

Key to the evaluation of sump pool debris transport is “when” and “where” the debris enters the pool. The question of when debris enters the pool is basically separated into whether the debris was directly deposited onto the sump floor during the blowdown phase or entered the pool with the subsequent drainage of the containment sprays. To put the timing in perspective, the reactor cavity would likely fill in less than 12 minutes (e.g., a large LOCA break flow rate of 7400 GPM would fill the reactor cavity volume, estimated by the plant to be less than 12,000 ft<sup>3</sup>, in less than 12 minutes neglecting the contribution from the containment sprays), and the sump pool should reach a reasonable steady state in ~30 minutes. The entrance location for blowdown-deposited debris is a debris distribution on the floor that likely favors deposition nearer the location of the break. The question of where the debris enters the pool is decomposed into whether the debris is blown onto the break room floor (SG compartment housing the break) or the remainder of the sump floor, which is the lower-level annulus floor. Debris transport into the pool via the spray drainage would enter at the primary drainage locations. The debris transport analysis requires a distribution for where the washdown debris enters the sump pool. The spray drainage analysis in Appendix VI provides a distribution for drainage flows entering the sump pool. The assumption used in these analyses is that the distribution of washdown debris entering the pool mimics that of the spray water distribution for debris deposited outside the break compartment. Note that the blowdown deposition analyses determined substantial debris deposition within the break compartment that would subsequently wash directly to the break compartment floor; this deposition was considered in the debris introduction to the pool. The drainage from the containment sprays drained into the sump pool at many locations including floor drains, stairwells, an equipment hatch, the containment liner, overflow from upper levels into the annular gap, refueling pool drains, spray falling directly into the steam generator compartments and the containment spray trains location at the sump level. To simplify the analysis, the multiple drainage entrance locations into the sump pool were grouped into seven groups around the sump annulus. Figure III.3-1 shows this distribution in an event chart format. One of these charts is applied to each size category of each type of insulation. The distributions in the chart (moving from left to right) are the following:

1. the blowdown transport deposition distribution that splits the total debris among debris deposited in the upper level floors, the break compartment floor, and the remainder of the lower level (sump) floor;
2. the washdown transport distributions of whether the debris deposited in the upper levels would likely transport to the sump pool or remain in the upper levels;
3. the distribution of the locations where debris entrained in the containment spray drainage would enter the sump pool;
4. the distributions associated with sump pool formation debris transport;
5. the distributions associated with pool recirculation debris transport; and
6. the distributions associated with potential debris erosion.

Each transport path is assumed to transport debris to one of three destinations, which include (1) accumulation on the sump screens, (2) debris entrapped within the inactive

pools, and (3) debris otherwise entrapped at locations along the transport pathways. The fraction of the debris predicted to accumulate on the screens is then the transport fraction for the size and type of debris. The overall transport fraction by insulation type is obtained by applying the debris-size distributions to the size-specific transport fractions.

Debris Size	Blowdown Transport	Washdown Transport	Washdown Entry Location	Pool Fill Up Transport	Pool Recirculation Transport	Debris Erosion in Pool	Path	Fraction	Deposition Location					
POOL TRANSPORT LOGIC CHART FIBROUS DEBRIS	Deposited Above	Trapped Above					1		Not Transported					
							Sump Area	Stalled in Pool	Erosion Products	2		Sump Screen		
								Transport	Remainder	3		Sump Screen		
							SG #4	Stalled in Pool	Erosion Products	4		Sump Screen		
								Transport	Remainder	5		Sump Screen		
							Eq. Room	Stalled in Pool	Erosion Products	6		Sump Screen		
								Transport	Remainder	7		Sump Screen		
							SG #3 (Stairs)	Stalled in Pool	Erosion Products	8		Not Transported		
								Transport	Remainder	9		Sump Screen		
							Opposite Side	Stalled in Pool	Erosion Products	10		Sump Screen		
								Transport	Remainder	11		Not Transported		
							SG #2 (Elevator)	Stalled in Pool	Erosion Products	12		Sump Screen		
								Transport	Remainder	13		Sump Screen		
							SG #1 (RV Cavity)	Stalled in Pool	Erosion Products	14		Not Transported		
								Transport	Remainder	15		Sump Screen		
							Small Pieces	Break Room Floor	To Near Screen	Stalled in Pool	Erosion Products	16		Sump Screen
										Transport	Remainder	17		Not Transported
							Sump Floor	Away From Screen	To Near Screen	Stalled in Pool	Erosion Products	18		Sump Screen
										Transport	Remainder	19		Not Transported
							Sump Floor	Inactive	To Near Screen	Stalled in Pool	Erosion Products	20		Sump Screen
										Transport	Remainder	21		Not Transported
Sump Floor	Inactive	To Near Screen	Stalled in Pool	Erosion Products	22		Sump Screen							
			Transport	Remainder	23		Not Transported							
Sump Floor	Inactive	To Near Screen	Stalled in Pool	Erosion Products	24		Sump Screen							
			Transport	Remainder	25		Not Transported							
Sump Floor	Inactive	To Near Screen	Stalled in Pool	Erosion Products	26		Sump Screen							
			Transport	Remainder	27		Not Transported							
Sump Floor	Inactive	To Near Screen	Stalled in Pool	Erosion Products	28		Sump Screen							
			Transport	Remainder	29		Not Transported							
Sump Floor	Inactive	To Near Screen	Stalled in Pool	Erosion Products	30		Sump Screen							
			Transport	Remainder	31		Not Transported							

Figure III.3-1. Sump Pool Debris Transport Chart

### III.3.2 Blowdown/Washdown Debris Entry into the Sump Pool

The distributions for the blowdown and washdown phases of the transport analysis were obtained from the details of the volunteer blowdown/washdown debris transport analyses documented in Appendix VI; these distributions are shown in Table III.3-1.

The volunteer-plant fibrous debris was categorized as (1) fines, (2) small pieces, (3) large pieces, and (4) intact pieces. The fines and small pieces represent debris capable of passing through a typical grating during blowdown. The fines are generally the individual fibers that remain suspended in the sump pool, whereas the small-piece fibrous debris typically would readily sink to the pool floor in hot water. Thus, the fines and small pieces must be evaluated differently. The large-piece and intact-piece debris represents debris too large to pass through a grating, which is a process fundamental to blowdown debris transport evaluations. The difference between the large and intact piece debris is whether the fibrous insulation continues to be protected by covering material. With large-piece debris, the fibrous insulation is subject to erosion, whereas the intact-piece debris insulation is not. Another distinguishing difference is that the covering materials on the intact debris, which include nearly intact blankets, are more likely to snag onto structures, including gratings during blowdown transport such that it is less likely to fall back to a floor or wash off with the sprays. The guidance-report (GR) baseline small-fines category corresponds to the combination of the fines and small-piece debris in the volunteer-plant analyses, and the GR large-piece debris corresponds to the large- and intact-piece debris in the volunteer-plant analyses.

**Table III.3-1. Blowdown/Washdown Debris Transport Fractions**

Debris Size and Type	Debris Transport Fractions				
	Blowdown Transport			Washdown Transport	
	Deposited in Upper Levels	Deposited on Break Room Floor	Deposited on Sump Floor	Remains Trapped Above	Transports to Sump Pool
<b><i>Fibrous Debris</i></b>					
Fines	0.92	0.05	0.03	0.07	0.93
Small Pieces	0.92	0.05	0.03	0.37	0.63
Large Pieces	0.57	0.39	0.04	0.81	0.19
Intact Pieces	0.69	0.30	0.01	0.78	0.22
<b><i>RMI Debris</i></b>					
< 2-in.	0.47	0.50	0.03	0.38	0.62
2 to 6-in.	0.35	0.61	0.04	0.69	0.31
> 6-in.	0.22	0.77	0.01	0.68	0.32

The volunteer-plant RMI debris was categorized as (1) debris pieces less than 2-inches, (2) pieces between 2- and 6 -inch in size, and (3) pieces greater than 6 inches in size. The GR RMI size groups were subdivided at 4-inch rather than the 2- and 6-inch used for the volunteer plant analysis. However, the combination of the volunteer-plant analysis categories less than 6-inch is a reasonable representation of the GR small-fines category, leaving the pieces larger than 6-inch to represent the large-piece debris.

The debris washing down from the upper levels was assumed to enter the sump pool with the same distribution as the spray drainage. However, blowdown debris that was preferentially deposited in the steam generator (SG) compartment where the break (SG1) occurred and its adjacent SG compartment (SG4) would wash directly to the

floors of these compartments, regardless of the spray drainage fractions. For the volunteer plant, the spray drainage distribution, as shown in Table III.3-2, was obtained from the spray drainage analysis documented in Appendix VI. The location distributions for debris washing down from the upper levels are provided by debris size category in Table III.3.3 and III.3.4 for fibrous and RMI debris, respectively. Because the larger debris was preferentially trapped in SG1 and SG4, these washdown location fractions are larger.

**Table III.3-2. Spray Drainage Distribution into the Sump Pool**

No.	Location in Annular Sump	Spray Drainage Water Sources	Drainage Fraction
1	Annulus Section Containing Recirculation Sumps	Floor drains and annular gap sources	0.14
2	Vicinity of SG4 Access (Steam Generator Adjoining Break Room)	SG4 personnel access doorway and liner flow. Includes flow from a 6-in. refueling pool drain.	0.08
3	Vicinity of Interior Equipment Room Access (~90° from Sumps)	Refueling pool water drains into equipment room below refueling pools, then exits doorway into sump and liner flow.	0.06
4	Vicinity of SG3 Access	SG3 personnel access doorway, annular gap sources, and stairwell. Includes flow from a 6-in. refueling pool drain.	0.18
5	Annulus Section Directly Opposite Recirculation Sumps	Floor drains and annular gap sources.	0.09
6	Vicinity of SG2 Access	SG2 personnel access doorway, floor drains, upper-level equipment hatch, annular gap sources, and stairwell. Includes flow from a 6-in. refueling pool drain.	0.25
7	Vicinity of SG1 Access (Compartment with Break)	SG1 personnel access doorway, floor drains, and annular gap sources. Includes flow from a 6-in. refueling pool drain.	0.20

**Table III.3-3. Fibrous Debris Entrance Distributions to Sump Pool**

No.	Location in Annular Sump	Drainage Fraction	Fines Debris	Small-Piece Debris	Large-Piece Debris	Intact-Piece Debris
1	Sumps	0.14	0.09	0.09	0.01	0.01
2	SG4	0.08	0.17	0.17	0.28	0.22
3	Eq. Room	0.06	0.04	0.04	0	0
4	SG3	0.18	0.12	0.12	0.07	0.07
5	Opposite	0.09	0.06	0.06	0.01	0.01
6	SG2	0.25	0.16	0.16	0.07	0.07
7	SG1	0.20	0.36	0.36	0.56	0.62

**Table III.3-4. RMI Debris Entrance Distributions to Sump Pool**

No.	Location in Annular Sump	Drainage Fraction	<2-in. Debris	2- to 6-in. Debris	>6-in. Debris
1	Sumps	0.14	0.06	0.01	0.01
2	SG4	0.08	0.24	0.28	0.22
3	Eq. Room	0.06	0.02	0	0
4	SG3	0.18	0.06	0.07	0.07
5	Opposite	0.09	0.04	0.01	0.01
6	SG2	0.25	0.09	0.07	0.07
7	SG1	0.20	0.49	0.56	0.62

### III.3.3 Sump Pool Debris Transport Estimates

Debris transport in the sump pool was separated into the following three phases: (1) transport of floor deposited debris during the formation (fill-up) of the sump pool, (2) debris transport in an established sump during recirculation mode, and (3) long-term erosion of exposed fibrous debris in the sump pool.

#### III.3.3.1 Pool Formation Debris Transport

Based on observations taken during the integrated debris transport tests [NUREG/CR-6773], the primary driver for moving debris during pool formation, especially for the large debris, is the sheeting flow as the initial water from the break spreads across the sump floor. Debris initially deposited on the floor is pushed along with the wave front. As such, the movement of the debris has significant momentum that can carry the debris past the openings into interior spaces. Once the water depth becomes significant, further transport occurs due to the drag forces of the flow of water, and for larger debris that transport becomes substantially less dynamic than the sheeting flow transport. Individual fibers will move as suspended debris following the water flow.

In the volunteer plant, a majority of the debris initially deposited on the floor of the compartment containing the break (SG compartment 1 in this evaluation) would likely transport from that compartment onto the annular sump floor through either of the personnel access door for SG 1 or the door for SG 4. Because the break is in SG 1, considerably more flow would exit the door to SG 1 than to SG 4. In the scenario evaluated herein, the larger portion of the break room flow and therefore the debris (perhaps 75%) would flow through the personnel access door into the annulus on the side nearer the access for the reactor cavity (the flow distribution assumption was discussed in Section III.2.1). A smaller portion of the debris would exit the SG compartment through the access door into SG compartment 2. In the volunteer plant, nearly all of the essentially inactive pool is the water below the sump floor in the reactor cavity. All other quiescent regions would have sufficient water circulation that suspended fibers over time would circulate from those regions. When debris exits a SG compartment through a personnel access door due to the initial sheeting flow, the flow splits, with part going toward the recirculation sumps and part going in the opposite

direction. In the scenario analyzed, the part going away from the sump screens flowed past the narrow passageway into the room leading to the reactor cavity access hatch. For debris to follow water into this passageway, it must essentially make a 90° bend in a short distance. Therefore, it must be concluded that only a small fraction of debris moving with the dynamic wave front, especially larger debris, will make the 90° turn into the reactor cavity passageway.

With these concepts in mind, the pool transport distributions were judged as shown in Table III.3-4. Starting with the fines, it is assumed that 75% of the flow exits the SG1 compartment on the reactor cavity side, then that 60% of that flows in the direction of the reactor cavity, then that 50% of the flow makes the turn into reactor cavity passageway, which indicates that perhaps 25% of the fines initially on the break room floor goes into the reactor cavity on initial formation of the pool. Because these fibers are suspended, the remaining pool formation could increase this number to, for example, a conservative 40%. Then, the remaining amount is split 50%–50%, as toward the recirculation sump and away from the sump. With each fibrous debris category of increasing size, the fraction into the reactor cavity is decreased somewhat, with the even split maintained between the “toward” and “away” from the screen. With the heavier metallic debris, even the smaller pieces would transport less readily than the fiber pieces.

For debris initially deposited on the annular sump floor, a significant fraction of this debris could be located such that it would not be greatly affected by flow from the break compartment to the reactor cavity because the exit from the break compartment is near the entrance to the reactor cavity. However, larger debris deposition would also likely be preferential near the break compartment door. For lack of better justifications, the same distributions judged for debris initially deposited on the break room floor are assumed for debris initially deposited on the annular sump floor. In any case, only a few percent of the total debris is estimated to be deposited on the annular sump floor due to the relatively small doorway areas as compared with the upward area of the SG compartments.

**Table III.3-4. Pool Formation Debris Transport Distributions**

Debris Size and Type	Pool Formation Debris Transport Distributions					
	Floor of Break Room			Floor of Sump Pool		
	Toward Screen	Away from Screen	Into Inactive Pools	Toward Screen	Away from Screen	Into Inactive Pools
<b><i>Fibrous Debris</i></b>						
Fines	0.30	0.30	0.40	0.30	0.30	0.40
Small Pieces	0.35	0.35	0.30	0.35	0.35	0.30
Large Pieces	0.40	0.40	0.20	0.40	0.40	0.20
Intact Pieces	0.40	0.40	0.20	0.40	0.40	0.20
<b><i>RMI Debris</i></b>						
<2 in.	0.35	0.35	0.30	0.35	0.35	0.30
2 to 6 in.	0.40	0.40	0.20	0.40	0.40	0.20
>6 in.	0.50	0.50	0.00	0.50	0.50	0.00

### III.3.3.2 Recirculation Pool Debris Transport

Important aspects of sump pool debris transport were observed during the integrated debris transport tests [NUREG/CR-6773]. For low-density fiberglass debris, the fines (e.g., individual fibers) remain suspended and move with the flow of water, whereas the debris pieces of significant size readily saturate with water at the water temperatures typical of LOCA accidents and then sink to the pool floor, where further transport depends on the flow velocity and turbulence near the floor. For RMI debris, all debris sinks to the floor of the pool, with the occasional exception of a piece of debris that encapsulates an air pocket, keeping that piece buoyant.

The CFD analyses provide realistic descriptions of the floor-level flow conditions, which were described in Section III.2 as contours established so that the velocities higher than the experimental measured threshold are clearly indicated. The velocity contours illustrate the portion of the pool where debris would most likely readily move with the flow. In addition to velocity contours, the streamline plots provide a reasonable connecting pathway whereby a piece of debris would likely travel from its original location in the pool to the recirculation sumps. If a transport pathway passes through a slower portion of the pool, then debris moving along that pathway could stall and not transport to the recirculation sump. Otherwise, the transport is very likely.

The effects of pool turbulence are more difficult to quantify. Test observations have shown the occasional reentrainment of debris once stalled in relatively quiescent water. Water within quiescent regions typically tends to rotate, sending debris into the center of the vortex, where it becomes semi-trapped. However, that occasional pulsation can kick a piece of debris out of the vortex and back into the main stream. Although this behavior cannot be reasonably quantified, transport estimates should be enhanced to consider these effects.

A detailed transport analysis using the CFD predicted flow contours and flow streamlines would subdivide the sump pool floor into relatively fine subdivisions, where each subdivision would have a source term for debris depositing onto the pool floor at that location. Then the transport of the debris from each specific subdivision would be independently evaluated using a streamline generated from that subdivision to the recirculation sumps to illustrate where that debris would likely reside after movement ceases. Quantification of all the subdivision transport results would provide an overall sump pool transport fraction for each debris category. The transport results should then be adjusted to account for pool turbulence effects on debris, i.e., the threshold transport tumbling velocities reported in NUREG/CR-6772 were measured in very uniform and turbulence-dampened flows but turbulence is capable of moving debris where bulk flow will not. One method of accounting for turbulence effects would be to decrease the threshold velocities for transport.

In this analysis, the above detailed model description was simplified to only seven subdivisions for the sump floor. Even then, the available CFD streamlines did not form a complete set. Therefore, the individual pool transport fractions used to populate the transport charts were basically engineering judgments made while viewing the velocity profiles. The individual transport estimates are provided in Table III.3-5. The CFD flow velocity contours maps used to make these judgments are shown in Figures III.2-33 and III.2-37 for fibrous and RMI debris, respectively. A sampling of corresponding flow streamline plots are shown in Figures III.2-42 and III.2-43, for fibrous and RMI debris,

respectively. The transport fractions range from 100% transport for the suspended fibers and debris located nearer the recirculation sumps to 0% transport for the largest debris located on the opposite side of the containment.

### III.3.3.3 Sump Pool Debris Erosion

The only source of data for the erosion of fibrous debris in a sump pool was the integrated debris transport tests documented in NUREG/CR-6773. Four longer-term tests (3- to 5-hour durations) were conducted in this test program where debris accumulation on the simulated sump screen was collected after every 30 minutes.

Three sources of fibrous debris contributed to this accumulation: (1) small-piece debris tumbling or sliding along the floor, (2) suspended fibers initially introduced into the tank, and (3) fibers that had eroded from the small-piece debris residing on the floor of the tank. Late into these tests, most of the small-piece debris had already either transported to the screen or had come to relative rest in some quiescent location on the tank floor; therefore, its contribution should have been minimal near the end of the tests. Also, late in the tests, water recirculation should have substantially reduced the initially suspended fibers so that continued accumulation would fall off quite noticeably. Note that sufficient time had elapsed in each test for the water in the tank to be replaced (tank water volume divided by the simulated break flow) from 19 to 46 times during the course of the test. Because the continued accumulation tended to hold at a somewhat sustainable rate, it is likely that continued erosion was supporting the continued debris accumulation.

**Table III.3-5. Recirculation Pool (Steady-State) Debris Transport Fractions**

Location Where Debris Enters Sump Pool	Fraction of Debris Transported to Sump Screen							
	Fibrous Debris				RMI Debris			
	Fines	Small Pieces	Large Pieces	Intact Pieces	<2 in.	2 to 6 in.	>6 in.	
<i>Debris Entering with Annular Sump Pool by Containment Spray Drainage (Debris Assumed to Enter Established Sump Pool)</i>								
Annulus Section Containing Recirculation Sumps	1	1	1	1	1	1	1	
Vicinity of SG4 Access (SG Adjoining Break Room)	1	1	1	1	1	1	1	
Vicinity of Interior Equipment Room Access (~90° from Sumps)	1	1	1	1	1	1	1	
Vicinity of SG3 Access (Includes Inter-Level Stairwell)	1	0.5	0.4	0.3	0.3	0.2	0.1	
Annulus Section Directly Opposite Recirculation Sumps	1	0.2	0.1	0	0.1	0	0	

Vicinity of SG2 Access (Includes Inter-Level Stairwell and Hatch)	1	0.5	0.4	0.3	0.3	0.2	0.1
Vicinity of SG1 Access (Compartment with Break, Includes Multiple Floor Drains)	1	0.7	0.6	0.5	0.5	0.4	0.3
<i>Debris Directly Blowdown Deposited onto Sump Floor but Subsequently Relocated Away from Recirculation Sumps during Pool Formation (Section III.3.3.1)</i>							
Initially on Break Room Floor, Relocated Away from Recirculation Sumps	1	0.3	0.2	0.1	0.2	0.1	0
Initially Spread Around Annular Sump Floor, Relocated Away from Recirculation Sumps	1	0.3	0.2	0.1	0.2	0.1	0

Table III.3-6 shows the end of test debris accumulation rates for these longer-term tests. Although these tests were run several hours, as indicated in the table, the tests were of short duration compared with LOCA long-term recirculation times. One of the four tests was conducted with a shallower pool of 9-in. depth compared with the usual depth of 16 in. Note that the accumulation was about eight times more rapid for the shallow pool test than for the deeper tests. Also note that during the shallow pool test, the water recirculation in terms of water replacements (46) was significantly more frequent for the 9-in. test than for the 16-in. tests; thus, the initial suspended debris would have been more readily filtered from the tank. Therefore, most of the longer-term debris accumulation should have been due to the continued erosion of fibrous debris in the tank. Further, the erosion rate was greater in the shallow depth pool, which can most likely be attributed to the greater turbulence in the shallow pool relative to the deeper pools.

**Table III.3-6. Late-Term Debris Accumulation in Integrated Debris Transport Tests**

Test ID	Pool Depth (in.)	Test Duration (Hours)	Accumulation Rate near the End of the Test (Percent of Debris in Tank/hr)	Approximate Number of Water Replacements During the Test
LT1	16	4	0.4	26
LT2	9	4	2	46
LT3	16	3	0.3	19
LT4	16	5	0.3	32

In conclusion, the only applicable test data for long-term debris erosion in a sump pool strongly indicate a sustainable rate of erosion that is affected by the relative turbulence in the pool. It should also be noted that the small-piece debris residing on the floor of the pool, late term, was generally found in quiescent locations, not necessarily directly under the simulated break flow. It might also be noted that the turbulence associated with the

spray drainage was not simulated. Because the 16-in. depth more closely resembles the fully established volunteer-plant pool, the erosion rate of 0.3 percent of the current tank debris/hour is adapted for this analysis.

In the debris transport charts, the overall fraction of debris on the sump floor that erodes into fines is required. Using the long-term recirculation mission time of 30 days, analysis indicates that nearly 90% of the initial debris mass would become eroded if this erosion rate remained constant throughout the 30 days. This calculation took into account the steadily decreasing mass of debris the pool using the following equation.

$$f_{eroded} = 1 - (1 - rate)^{\text{Number of Hours}}$$

Therefore, in the debris transport charts, 90% of the small- and large-piece debris predicted to reside on the sump floor is assumed to erode into suspended fibers unless the debris is still enclosed in a protective cover.

There are substantial sources of uncertainty with this calculation:

1. The durations of the integral debris transport tests were 3 to 5 hours. This leaves the question “Does the erosion rate taper off with time?” In addition, it is not certain that all of the end-of-test debris accumulation was due to erosion products.
2. The test results include the usual variances in test data, such as flow and depth control, and debris collection.
3. Although the test series was designed to approximate the flow and turbulence characteristics of the volunteer plant sump pool, the tank characteristics may have been significantly different than what might occur at the plant. The difference in the erosion rates between the 9 and 16-inch pool depths in the integrated tests clearly illustrate the effect of pool turbulence on fibrous debris erosion.
4. The geometry of the volunteer plant sump pool is larger and more complex than the test tank used in the integrated tests.
5. Large piece debris was not tested in the long term tests.

The 90% debris eroded value is used for both the small and large piece debris, despite the uncertainties. With such limited data, the use of 90% is necessary to ensure conservatism in the overall transport results. It may be that this number can be relaxed once better erosion data is available.

### III.3.4 Quantification Results

The blowdown/washdown/pool transport estimates presented in Sections III.3.2 and III.3.3 were entered into debris transport charts shown generically in Figure III.3-1 and quantified to obtain overall transport fractions. A separate chart was created for each size category and for each type of debris. Figures III.3-2, III.3-3, III.3-4, and III.3-5 illustrate the transport processes for fibrous debris categories of fines, small pieces,

large pieces, and intact pieces, respectively. Figures III.3-6, III.3-7, and III.3-8 illustrate the transport processes for RMI debris categories of pieces <2 in., 2 to 6 in., and >6 in., respectively.

Debris Size	Blowdown Transport	Washdown Transport	Washdown Entry Location	Pool Fill Up Transport	Pool Recirculation Transport	Debris Erosion in Pool	Path	Fraction	Deposition Location					
POOL TRANSPORT LOGIC CHART  FIBROUS DEBRIS	Deposited Above 0.92	Trapped Above 0.07	Sump Area 0.09	SG #4 0.17	Eq. Room 0.04	SG #3 (Stairs) 0.12	Opposite Side 0.06	SG #2 (Elevator) 0.16	SG #1 (RV Cavity) 0.36	Stalled in Pool	1.00	1	6.440E-02	Not Transported
										Erosion Products	1.00	2	0.000E+00	Sump Screen
										Remainder	0.00	3	0.000E+00	Not Transported
										Transport	0.00		7.700E-02	Sump Screen
										Stalled in Pool	1.00	4	0.000E+00	Sump Screen
										Erosion Products	1.00	5	0.000E+00	Not Transported
										Remainder	0.00	6	1.455E-01	Sump Screen
										Transport	0.00		1.00	Sump Screen
										Stalled in Pool	1.00	7	0.000E+00	Sump Screen
										Erosion Products	1.00	8	0.000E+00	Not Transported
										Remainder	0.00	9	3.422E-02	Sump Screen
										Transport	0.00		1.00	Sump Screen
										Stalled in Pool	1.00	10	0.000E+00	Sump Screen
										Erosion Products	1.00	11	0.000E+00	Not Transported
										Remainder	0.00	12	1.027E-01	Sump Screen
										Transport	0.00		1.00	Sump Screen
										Stalled in Pool	1.00	13	0.000E+00	Sump Screen
										Erosion Products	1.00	14	0.000E+00	Not Transported
										Remainder	0.00	15	5.134E-02	Sump Screen
										Transport	0.00		1.00	Sump Screen
										Stalled in Pool	1.00	16	0.000E+00	Sump Screen
										Erosion Products	1.00	17	0.000E+00	Not Transported
										Remainder	0.00	18	1.369E-01	Sump Screen
										Transport	0.00		1.00	Sump Screen
										Stalled in Pool	1.00	19	0.000E+00	Sump Screen
										Erosion Products	1.00	20	0.000E+00	Not Transported
										Remainder	0.00	21	3.080E-01	Sump Screen
										Transport	0.00		1.00	Sump Screen
										To Near Screen		22	1.500E-02	Sump Screen
										Stalled in Pool	1.00	23	0.000E+00	Sump Screen
										Erosion Products	1.00	24	0.000E+00	Not Transported
										Remainder	0.00		0.00	
										Transports	1.00	25	1.500E-02	Sump Screen
Inactive		26	2.000E-02	Inactive Pools										
To Near Screen		27	9.000E-03	Sump Screen										
Stalled in Pool	1.00	28	0.000E+00	Sump Screen										
Erosion Products	1.00	29	0.000E+00	Not Transported										
Remainder	0.00		0.00											
Transports	1.00	30	9.000E-03	Sump Screen										
Inactive		31	1.200E-02	Inactive Pools										
			1.0000000											
			0.06440	Not Transported										
			0.03200	Inactive Pools										
			0.90360	Sump Screen										

Figure III.3-2. Sump Pool Debris Transport Chart for Fine Fibrous Debris.

Debris Size	Blowdown Transport	Washdown Transport	Washdown Entry Location	Pool Fill Up Transport	Pool Recirculation Transport	Debris Erosion in Pool	Path	Fraction	Deposition Location					
POOL TRANSPORT LOGIC CHART  FIBROUS DEBRIS	Deposited Above 0.92	Trapped Above 0.37					1	3.404E-01	Not Transported					
							2	0.000E+00	Sump Screen					
							3	0.000E+00	Not Transported					
							Sump Area 0.09	Stalled in Pool	0.10	Erosion Products	4	0.000E+00	Sump Screen	
								Transport	0.90	Remainder	5	0.000E+00	Not Transported	
							SG #4 0.17	Stalled in Pool	0.10	Erosion Products	6	9.853E-02	Sump Screen	
								Transport	0.90	Remainder	7	0.000E+00	Not Transported	
							Eq. Room 0.04	Stalled in Pool	0.10	Erosion Products	8	0.000E+00	Not Transported	
								Transport	0.90	Remainder	9	2.318E-02	Sump Screen	
							Transports to Pool 0.63	SG #3 (Stairs) 0.12	Stalled in Pool	0.10	Erosion Products	10	3.478E-03	Sump Screen
									Transport	0.90	Remainder	11	3.130E-02	Not Transported
							Opposite Side 0.06	SG #2 (Elevator) 0.16	Stalled in Pool	0.10	Erosion Products	12	3.478E-02	Sump Screen
									Transport	0.90	Remainder	13	2.782E-03	Sump Screen
							SG #1 (RV Cavity) 0.36	0.50	Stalled in Pool	0.10	Erosion Products	14	2.504E-02	Not Transported
									Transport	0.90	Remainder	15	6.955E-03	Sump Screen
							To Near Screen 0.35	0.20	Stalled in Pool	0.10	Erosion Products	16	4.637E-03	Sump Screen
									Transport	0.90	Remainder	17	4.173E-02	Not Transported
							To Near Screen 0.35	0.50	Stalled in Pool	0.10	Erosion Products	18	4.637E-02	Sump Screen
									Transport	0.90	Remainder	19	6.260E-03	Sump Screen
							To Near Screen 0.35	0.30	Stalled in Pool	0.10	Erosion Products	20	5.634E-02	Not Transported
									Transport	0.90	Remainder	21	1.461E-01	Sump Screen
							To Near Screen 0.35	0.70	Stalled in Pool	0.10	Erosion Products	22	1.750E-02	Sump Screen
									Transport	0.90	Remainder	23	1.225E-03	Sump Screen
							Away From Screen 0.35	0.30	Stalled in Pool	0.10	Erosion Products	24	1.103E-02	Not Transported
									Transport	0.90	Remainder	25	5.250E-03	Sump Screen
							Inactive 0.30	0.30	Inactive			26	1.500E-02	Inactive Pools
									Inactive			27	1.050E-02	Sump Screen
							To Near Screen 0.35	0.30	Stalled in Pool	0.10	Erosion Products	28	7.350E-04	Sump Screen
									Transport	0.90	Remainder	29	6.615E-03	Not Transported
							Away From Screen 0.35	0.30	Stalled in Pool	0.10	Erosion Products	30	3.150E-03	Sump Screen
									Transport	0.90	Remainder	31	9.000E-03	Inactive Pools
Inactive 0.30	0.30	Inactive				1.0000000								
		Inactive				0.51245	Not Transported							
						0.02400	Inactive Pools							
						0.46355	Sump Screen							

Figure III.3-3. Sump Pool Debris Transport Chart for Small-Piece Fibrous Debris.



Debris Size	Blowdown Transport	Washdown Transport	Washdown Entry Location	Pool Fill Up Transport	Pool Recirculation Transport	Debris Erosion in Pool	Path	Fraction	Deposition Location																																						
FIBROUS DEBRIS	0.69	0.78	Trapped Above	Sump Area	0.01	Stalled in Pool	0.00	Erosion Products	2	5.382E-01	Not Transported																																				
						Remainder	1.00	3	0.000E+00	Sump Screen																																					
						Transport	1.00	4	0.000E+00	Sump Screen																																					
						0.69	0.22	SG #4	0.01	Stalled in Pool	0.00	Erosion Products	4	0.000E+00	Sump Screen																																
										Remainder	1.00	5	0.000E+00	Not Transported																																	
										Transport	1.00	6	3.340E-02	Sump Screen																																	
										0.69	0.22	Eq. Room	0.00	Stalled in Pool	0.00	Erosion Products	7	0.000E+00	Sump Screen																												
														Remainder	1.00	8	0.000E+00	Not Transported																													
														Transport	1.00	9	0.000E+00	Sump Screen																													
														0.69	0.22	SG #3 (Stairs)	0.07	Stalled in Pool	0.00	Erosion Products	10	0.000E+00	Sump Screen																								
																		Remainder	1.00	11	7.438E-03	Not Transported																									
																		Transport	1.00	12	3.188E-03	Sump Screen																									
																		0.69	0.22	Opposite Side	0.01	Stalled in Pool	0.00	Erosion Products	13	0.000E+00	Sump Screen																				
																						Remainder	1.00	14	1.518E-03	Not Transported																					
																						Transport	1.00	15	0.000E+00	Sump Screen																					
																						0.69	0.22	SG #2 (Elevator)	0.07	Stalled in Pool	0.00	Erosion Products	16	0.000E+00	Sump Screen																
																										Remainder	1.00	17	7.438E-03	Not Transported																	
																										Transport	1.00	18	3.188E-03	Sump Screen																	
																										0.69	0.22	SG #1 (RV Cavity)	0.62	Stalled in Pool	0.00	Erosion Products	19	0.000E+00	Sump Screen												
																														Remainder	1.00	20	4.706E-02	Not Transported													
																														Transport	1.00	21	4.706E-02	Sump Screen													
																														0.69	0.22	Intact Pieces	0.40	To Near Screen	0.50	22	1.200E-01	Sump Screen									
																																		Stalled in Pool	0.00	Erosion Products	23	0.000E+00	Sump Screen								
																																		Remainder	1.00	24	1.080E-01	Not Transported									
																																		0.69	0.22	Break Room Floor	0.30	Away From Screen	0.40	25	1.200E-02	Sump Screen					
																																						Transports	0.10	26	6.000E-02	Inactive Pools					
																																						Inactive	0.20	27	4.000E-03	Sump Screen					
																																						0.69	0.22	Sump Floor	0.01	To Near Screen	0.40	28	0.000E+00	Sump Screen	
																																										Stalled in Pool	0.00	Erosion Products	29	3.600E-03	Not Transported
																																										Remainder	1.00	30	4.000E-04	Sump Screen	
																																										0.69	0.22	Sump Floor	0.01	Away From Screen	0.40
Transports	0.10	32	1.0000000																																												
Inactive	0.20	33	0.71325	Not Transported																																											
0.69	0.22	Sump Floor	0.01	Inactive	0.20																																									34	0.06200
				Inactive	0.20	35	0.22475	Sump Screen																																							

Figure III.3-5. Sump-Pool-Debris Transport Chart for Intact-Piece Fibrous Debris.



Debris Size	Blowdown Transport	Washdown Transport	Washdown Entry Location	Pool Fill Up Transport	Pool Recirculation Transport	Debris Erosion in Pool	Path	Fraction	Deposition Location						
POOL TRANSPORT LOGIC CHART  RMI DEBRIS	Deposited Above 0.35	Trapped Above 0.69					1	2.415E-01	Not Transported						
							Erosion Products	2	0.000E+00	Sump Screen					
								Stalled in Pool	0.00	3	0.000E+00	Not Transported			
							Remainder		1.00		1.085E-03	Sump Screen			
							Sump Area	0.01	0.00	1.00	0.00	Erosion Products	4	0.000E+00	Sump Screen
							SG #4	0.28	0.00	1.00	0.00	Erosion Products	6	3.038E-02	Sump Screen
							Eq. Room	0.00	0.00	1.00	0.00	Erosion Products	8	0.000E+00	Not Transported
							Tranports to Pool	0.31	0.00	1.00	0.00	Erosion Products	10	0.000E+00	Sump Screen
							SG #3 (Stairs)	0.07	0.80	1.00	0.00	Erosion Products	12	1.519E-03	Sump Screen
							Opposite Side	0.01	1.00	1.00	0.00	Erosion Products	14	1.085E-03	Not Transported
							SG #2 (Elevator)	0.07	0.80	1.00	0.00	Erosion Products	16	0.000E+00	Sump Screen
							SG #1 (RV Cavity)	0.56	0.60	1.00	0.00	Erosion Products	18	1.519E-03	Sump Screen
							To Near Screen	0.40	0.40	1.00	0.00	Erosion Products	20	3.646E-02	Not Transported
							Pieces 2-6"	1.00	0.40	0.40	0.40	Erosion Products	22	2.440E-01	Sump Screen
							Break Room Floor	0.61	0.90	1.00	0.00	Erosion Products	24	2.196E-01	Not Transported
							Sump Floor	0.04	0.40	0.10	0.20	Inactive	26	1.220E-01	Inactive Pools
							To Near Screen	0.40	0.40	1.00	0.00	Erosion Products	27	0.000E+00	Sump Screen
							Away From Screen	0.40	0.90	1.00	0.00	Erosion Products	29	1.440E-02	Not Transported
Remainder	1.00	30	1.600E-03	Sump Screen											
Inactive	0.20				0.40	0.10	0.20	Inactive	31	8.000E-03	Inactive Pools				
		0.20	1.0000000	0.52519								Not Transported			
0.13000	Inactive Pools														
		0.34481	Sump Screen												

Figure III.3-7. Sump-Pool-Debris Transport Chart for 2- to 6-in. RMI Debris.



The RMI debris transport fractions were dominated by the large (> 6-inches) debris since 98.4% of the RMI was predicted to be in this category. It should be pointed out that this category includes quite large pieces including intact or nearly intact cassettes, which would required a faster flow to move the debris than 0.28 ft/s implemented into the CFD analyses.

**Table III.3-7. Quantified Category-Specific Sump-Pool-Debris Transport Results**

Debris Category	Category-Specific Debris Transport Fractions				
	Size Distribution	Entering Pool	Into Inactive Pools	Sump Pool Transport	Overall Transport
<b><i>Fibrous Debris</i></b>					
Fines	0.133	0.90	0.032	1	0.90
Small Pieces	0.397	0.64	0.024	0.97	0.62
Large Pieces	0.235	0.45	0.086	0.96	0.44
Intact Pieces	0.235	0.40	0.062	0.56	0.23
<b><i>RMI Debris</i></b>					
<2 in.	0.011	0.66	0.15	0.61	0.40
2 to 6 in.	0.005	0.63	0.13	0.55	0.35
>6 in.	0.984	0.85	0	0.49	0.42

**Table III.3-8. Quantified Insulation-Specific Sump-Pool-Debris Transport Results**

Debris Category	Insulation Specific Debris Transport Fractions			
	Entering Pool	Into Inactive Pools	Sump Pool Transport	Overall Transport
Fibrous	0.57	0.05	0.88	0.52
RMI	0.85	0.0024	0.50	0.42

The fractions of the sump pool floor where the floor level flow velocity was slower than the threshold velocities for debris (0.12 and 0.28 ft/s for fibrous and RMI debris, respectively) were calculated from the CFD results presented in Section III.2. The floor fractions corresponding to a large break in SG1 (lower-right quadrant in the CFD results) are 0.41 and 0.22 for fibrous and RMI debris, respectively. These floor area fractions are compared in Figure III.3-9 with the sump pool transport fractions by insulation type and size categories. In this scenario, if the debris was uniformly introduced into the pool across the pool cross sectional area and erosion was not significant, then the area fractions might be a reasonable indicator of the pool debris transport fractions. However, as shown, the area fractions are a poor indicator of debris transport when the debris is introduced into the pool in a more realistic and nonuniform manner and erosion is substantial. A uniform area fraction model can easily underpredict the pool debris transport by a factor of two or more.

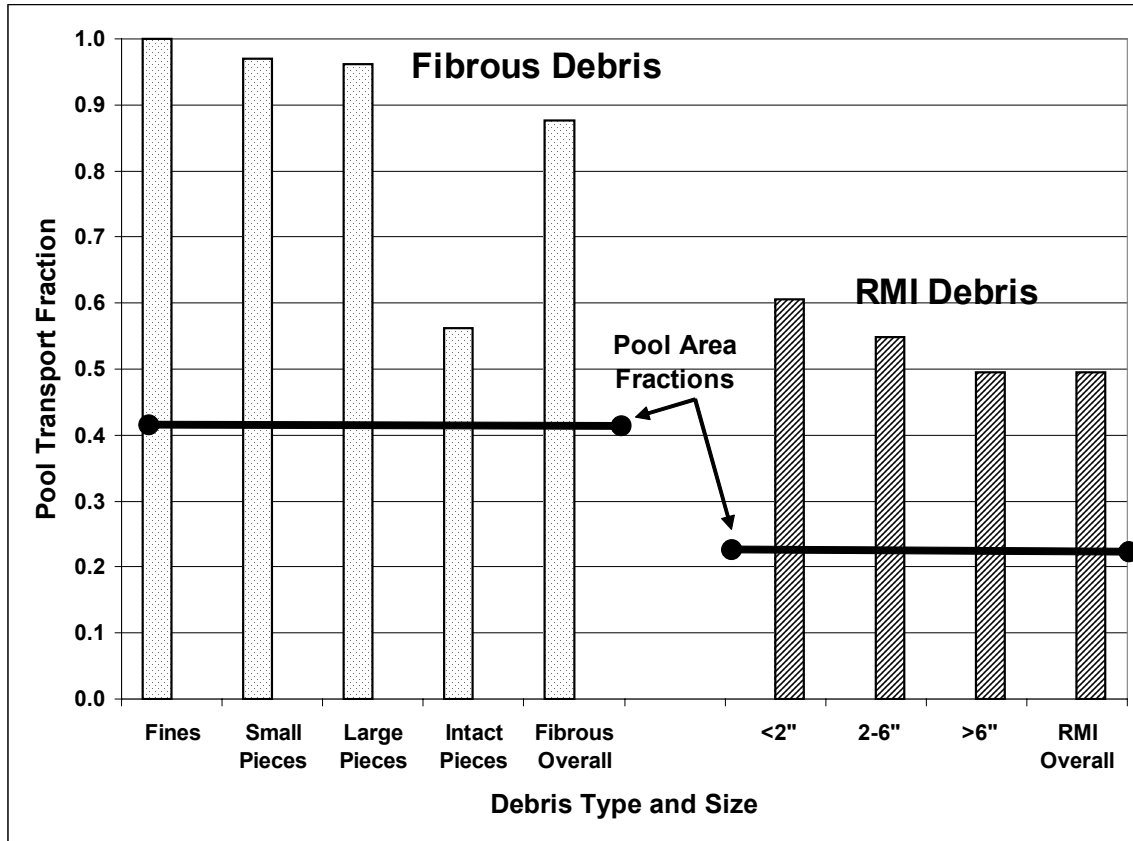


**Figure III.3-9. Comparison of Sump Pool Transport Fraction with Velocity Area Fractions.**

The transport of debris from its generation in the ZOI throughout the containment during the RCS depressurization phase, then the washdown transport by the containment sprays, and then its transport through the sump pool to the recirculation sump screens is a rather intractable problem. A logic chart method was used to decompose the overall transport problem into many smaller problems that were subsequently evaluated by either analysis or simply conservatively judged. As such, the results of the volunteer analyses contain many sources of uncertainties; however, these uncertain results are plausible results and show insight into the many aspects of debris transport that should be useful to subsequent evaluations. These sources of uncertainty regarding sump pool transport include (1) the timing and locations where debris enters the pool; (2) concerns regarding the effects of local pool turbulence that can move debris even when the bulk flow does not; (3) lack of data regarding erosion rates for debris that can decompose within the pool (e.g., fibrous debris); (4) the simplification of the analysis; and (5) the limited scenario space that can be realistically evaluated.

The debris transport results in this section pertain to a large LOCA in SG1. The same LOCA in another compartment could easily result in different transport results, which could be higher or lower than the scenario evaluated herein. In addition, the sump pool debris transport was evaluated herein using simplified nodalization, as discussed above.

A more detailed evaluation would likely refine these transport results significantly; however, the transport methodology has been demonstrated.

### **III.4 CONCLUSIONS AND RECOMMENDATIONS**

Section III.2 outlined a method for performing reactor containment pool flow dynamic analysis. A commercial CFD code was used to perform the simulations and assess the flow properties relevant to debris transport. From the simulations, flow area fractions in excess of debris transport threshold velocities were obtained. Transient containment pool fill-up simulations were performed that could potentially be used to design debris diversion systems to sequester debris into zones that do not participate in the flow when sump pumps are engaged.

Recommendations for future simulations include performing grid-mesh convergence studies, further analysis of debris degradation mechanisms, and flow diversion. The grid-mesh convergence studies are required to have a defensible CFD analysis. Additional constraints on the grid mesh, not used or presented in this document, should include clustering grid points near the mass flow injection locations (break and splash locations) and development of a proper boundary layer grid near the no-slip walls, particularly on the containment floor. With additional grid points near the floor, a near-wall velocity profile will be established. This near-wall velocity gradient and drag forces could have an impact on debris transport and should be thoroughly investigated as part of the grid refinement study. The debris degradation mechanisms should also be the subject of further study. Examples of degradation have been shown in this document, but no attempt to quantify the dynamics has been made at this time.

The transport of debris from its generation in the ZOI throughout the containment during the RCS depressurization phase, then the washdown transport by the containment sprays, and then its transport through the sump pool to the recirculation sump screens is a rather intractable problem. A logic chart method was used to separate the overall transport problem into many smaller problems that were subsequently evaluated by either analysis or engineering judgment. As such, the results of the volunteer analyses contain many source of uncertainties; however, these uncertain results are plausible results and show insight into the many aspects of debris transport that should be useful to subsequent evaluations. These sources of uncertainty regarding sump pool transport include (1) the timing and locations where debris enters the pool; (2) concerns regarding the effects of local pool turbulence that can move debris even when the bulk flow does not; (3) lack of data regarding erosion rates for debris that can decompose within the pool (e.g., fibrous debris); (4) the simplification of the analysis; and (5) the limited scenario space that can be realistically evaluated.

The debris transport results in this appendix pertain to one LOCA scenario: a large LOCA in SG1. The same LOCA in another compartment could easily result in different transport results that could be higher or lower than the scenario evaluated herein. In addition, the sump pool debris transport was evaluated herein using simplified nodalization, as discussed above. A more detailed evaluation would likely refine these transport results significantly; however, the transport methodology has been demonstrated.

### **III.5 REFERENCES**

[NUREG/CR-6772, 2001] D. V. Rao, B. C. Letellier, A. K. Maji, and B. Marshall, 2002, "GSI-191: Separate-Effects Characterization of Debris Transport in Water." NUREG/CR-6772, LA-UR-01-6882.

[NUREG/CR-6773, 2002] D. V. Rao, C. Shaffer, B. C. Letellier, A. K. Maji, and L. Bartlein, "GSI-191: Integrated Debris-Transport Tests in Water Using Simulated Containment Floor Geometries," NUREG/CR-6773, LA-UR-02-6786, December 2002.